NONCANONICAL NF-κB SIGNALING IN GLIOMA IS ACTIVATED BY TWEAK AND PROMOTES INVASION

A Dissertation

by

EVAN MICHAEL CHERRY

Submitted to the Office of Graduate and Professional Studies of
Texas A&M University
in partial fulfillment of the requirements for the degree of

DOCTOR OF PHILOSOPHY

Chair of Committee,	Raquel Sitcheran
Committee Members,	Kayla Bayless
	Farida Sohrabji
	Emily Wilson
Head of Program,	Warren Zimmer

May 2017

Major Subject: Medical Sciences

ABSTRACT

High-grade gliomas are an invasive and deadly brain cancer. We have shown that noncanonical NF-κB/RelB signaling can drive invasion in the aggressive mesenchymal subtype of glioma. TNF-like weak inducer of apoptosis (TWEAK) can activate canonical/RelA and noncanonical/RelB NF-κB signaling, but its role in glioma invasion is unclear. Moreover, the relevance of expression of TWEAK and NF-κB-inducing Kinase (NIK) in patient gliomas is unknown.

TWEAK-regulated NF-κB signaling and cell invasion were investigated in both established and primary high-grade glioma tumor lines using a three-dimensional (3-D) collagen invasion assay. NF-κB proteins regulating both glioma cell invasion and expression of Matrix Metalloproteinase 9 (MMP9) in response to TWEAK were evaluated using shRNA-mediated loss-of-function. NIK-promoted glioma growth *in vivo* was investigated using an orthotopic xenograft mouse model. Expression of TWEAK, its receptor, NIK, and a negative regulator of NIK (altogether termed the TWEAK Axis) in glioma tumors was evaluated using microarray data from the NCI-curated TCGA and REMBRANDT databases. TWEAK Axis expression was stratified by prognostic factor and glioma subtype as well as correlated with expression of both NF-κB genes and glioma subtype markers. Patient survival by TWEAK Axis gene expression was determined using Kaplan-Meier survival analysis.

Protein levels of RelB correlate positively with glioma cell invasiveness. Loss of RelB attenuates invasion without altering RelA expression or phosphorylation. RelB promotes invasion independent of RelA. TWEAK selectively activates noncanonical NF-κB signaling through p100-p52 processing and nuclear accumulation of RelB and p52. TWEAK, but not TNFα, significantly increases NIK mRNA expression and sustains MMP9 mRNA expression. TWEAK-increased invasion is reversible by loss of NIK. NIK overexpression increases invasiveness *in vitro* and gliomagenesis *in vivo.* TWEAK, its receptor, and NIK are expressed primarily in mesenchymal gliomas and correlate negatively with survival.

Our data establish a key role for NIK and TWEAK in noncanonical NF-κB signaling and MMP9-dependent invasion in glioma cells. Meta-analysis of patient glioma tumors indicates poorer prognosis with increased TWEAK Axis expression in the aggressive mesenchymal subtype. Together, these studies reveal the importance of TWEAK and noncanonical NF-κB signaling in glioma cell invasion and rationalize therapeutic targeting of TWEAK and NIK in glioma.

DEDICATION

This work is dedicated to all who helped it and to all it will help.

ACKNOWLEDGMENTS

Chapter II material has been published in Molecular Cancer, 2015 Jan 27;14:9. doi: 10.1186/s12943-014-0273-1. Authors for this work are EM Cherry, DW Lee, JU Jung, and R Sitcheran. This work is included within my thesis with acknowledgment to BioMed Central in compliance with their open-access license policies.

I would like to thank my committee chair, Dr. Sitcheran, and my committee members, Dr. Bayless, Dr. Sohrabji, and Dr. Wilson, for their mentorship, understanding, and encouragement in my medical and graduate training. For their continued mentorship through difficult periods and their confidence in my ability to complete this study, I am eternally grateful.

I would like to thank M.D./Ph.D. Program Director Dr. Leibowitz, Vice Dean of Research Dr. Van Wilson, and MCMD Department Head Dr. Geoffrey Kapler for their dedication to the M.D./Ph.D. and graduate programs as well as their support of student development.

I would like to thank Dr. Dong Lee and Jiung Jung and recognize their data contributions to Chapter II and its publication.

I would like to thank Dr. Threadgill, Dr. Hillhouse, and Kranti Konganti from the Texas A&M Institute for Genome Sciences and Society for their guidance in analyzing the gene expression data. Special thanks to the Agilent GeneSpring science and technical support teams for their guidance in utilizing the GeneSpring GX software.

Thanks also to my colleagues in the Sitcheran lab, friends in the program, and the department faculty and staff for making my time in the College of Medicine graduate studies program an enjoyable and enriching experience. I want to extend my gratitude especially to Amanda Watkins-Borths and Peggy Brigman for their dedication to coordinating and assisting students every step of the way.

Finally, thanks be to God, family, and friends for their encouragement and love.

[†]Data contributed by Dong Lee. [‡]Data contributed by Jiung Jung.

NOMENCLATURE

2-D	Two-dimensional
3-D	Three-dimensional
AAALAC	Association for Assessment and Accreditation of Laboratory Animal Care
ANCOVA	Analysis of Covariance
ANOVA	Analysis of Variance
ATCC	American Type Culture Collection
BAFFR	B-cell-Activating Factor receptor
BT	Brain Tumor
CHI3L1	Chitanse-3-Like Protein 1
CHUK	Conserved Helix-loop-helix Ubiquituous Kinase
cIAP	cytoplasmic Inhibitor of Apoptosis Protein
CNS	Central Nervous System
COL1A1	Collagen Type 1 α1
CRISPR	Clustered Regularly Interspaced Short Palindromic Repeat
DMEM/F12	Dulbecco's Modified Eagle Medium/Ham's F12
EGF	Epidermal Growth Factor
EGFR	Epidermal Growth Factor Receptor
FBS	Fetal Bovine Serum
FGF	Fibroblast Growth Factor
FN14	FGF-inducible immediate-early response gene Number 14
GBM	Glioblastoma
GF	Growth Factor
GSEA	Gene Set Enrichment Analysis
HCC	Hepatocellular Carcinoma
HER	Human EGF Receptor
HSD	Honest Significant Difference

IACUC	Institutional Animal Care and Use Committee
IDH1	Isocyanate Dehydrogenase 1
IκBα	Inhibitor of Kappa-Beta alpha
IKK	Inhibitor of nuclear factor Kappa-B Kinase
IVIS	*In Vivo* Imaging System
LGG	Lower Grade Glioma
LOWESS	Locally-Weighted Scatterpoint Smoothing
MAP3K	Mitogen-activated Protein Kinase Kinase Kinase
MBP	Myelin Basic Protein
MGMT	O6-Methylguanine DNA Methyltransferase
MMP	Matrix Metalloproteinase
NCI	National Cancer Institute
NF-κB	Nuclear Factor kappa-light-chain enhancer of activated B cells
NIK	NF-κB-Inducing Kinase
NLS	Nuclear Localization Signal
NSC	Neural Stem Cell
OLIG2	Oligodendrocyte Transcription Factor 2
PBS	Phosphate-Buffered Saline
REMBRANDT	Repository of Molecular Brain Neoplasia Data
RFP	Red Fluorescent Protein
RHD	Rel Homology Domain
RMA	Robust Multichip Analysis
RPLP0	Ribosomal Protein Large Phosphoprotein 0
SD	Standard Deviation
SEM	Standard Error of the Mean
SMAC	Second Mitochondrial Activator of Caspases
SOX2	Sex-determining-region Y-Box 2
TBK1	TANK-Binding Kinase 1
TCGA	The Cancer Genome Atlas

TNFα	Tumor Necrosis Factor alpha
TNFSF12	TNF Superfamily member 12
TNFRSF12A	TNF Receptor Superfamily member 12A
TRAF3	TNF Receptor-Associated Factor 3
TWEAK	TNF-like Weak Inducer of Apoptosis
TWEAK Axis	TWEAK, FN14, NIK, TRAF3

TABLE OF CONTENTS

Page

ABSTRACT ii

DEDICATION iv

ACKNOWLEDGMENTS v

NOMENCLATURE vi

TABLE OF CONTENTS ix

LIST OF FIGURES x

LIST OF TABLES xii

CHAPTER I INTRODUCTION AND LITERATURE REVIEW 1

CHAPTER II TWEAK PROMOTES GLIOMA CELL INVASION THROUGH INDUCTION OF NIK AND NONCANONICAL NF-KB SIGNALING 11

- Background 11
- Results 13
- Discussion 27
- Conclusion 31
- Methods 32

CHAPTER III META-ANALYSIS OF NCI PATIENT DATA INDICATES TWEAK AXIS EXPRESSION IS A NEGATIVE PROGNOSTIC INDICATOR 36

- Background 36
- Results 39
- Discussion 54
- Conclusion 58
- Methods 59

CHAPTER IV CONCLUSIONS AND RECOMMENDATIONS 61

REFERENCES 70

APPENDIX A SUPPLEMENTAL FIGURES 90

APPENDIX B SUPPLEMENTAL TABLES 95

LIST OF FIGURES

Page

Figure 1 Schematic representation of canonical and noncanonical NF-κB pathways 5

Figure 2 Glioma cells have diverse invasion phenotypes that correlate positively with RelB expression 14

Figure 3 RelB poteniates glioma invasion independently of RelA 17

Figure 4 TWEAK induces invasion, NIK mRNA expression, and noncanonical NF-κB nuclear translocation 19

Figure 5 MMPs are required for glioma invasion and TWEAK-induced MMP9 expression is p52-dependent 22

Figure 6 NIK mRNA is up-regulated by TWEAK and NIK protein overexpression promotes tumorigenesis 25

Figure 7 NIK overexpression increases invasion and NIK knockdown inhibits TWEAK-induced invasion 29

Figure 8 The TWEAK Axis 37

Figure 9 TCGA and REMBRANDT samples' clinical data are representative of glioma patients 41

Figure 10 Expression of TWEAK Axis genes stratified by age range 44

Figure 11 Expression of TWEAK Axis genes stratified by tumor grade 46

Figure 12 Expression of TWEAK Axis genes stratified by histologic type 47

Figure 13 Expression of TWEAK Axis genes stratified by glioblastoma subtype 50

Figure 14 Overall survivals within quartiles of TWEAK Axis gene expression 55

Figure 15 Proposed model for TWEAK/FN14 activation of noncanonical NF-κB in glioma invasion. 66

Figure A1 Efficiency of RelA knockdown among multiple shRNA constructs and quantification of RelB overexpression 90

Figure A2 TWEAK specifically induces noncanonical NF-κB activation in glioma cells via NIK protein accumulation 91

Figure A3 TWEAK-enhanced invasion is attenuated by broad-spectrum MMP and MMP9-selective inhibition 92

Figure A4 NIK overexpression specifically induces p100 processing in glioma cells 93

Figure A5 Expression of subtype marker genes stratified by glioblastoma subtype 94

LIST OF TABLES

Page

Table 1 Spearman's ρ-values for TWEAK Axis and NF-κB gene expression 51

Table 2 Spearman's ρ-values for TWEAK Axis and subtype expression 53

Table B1 GSEA genes correlated with Verhaak *et al.* subtypes.....95

Table B2 NCI Dataset Summaries 104

Table B3 Entrez Gene IDs for probesets.....105

CHAPTER I

INTRODUCTION AND LITERATURE REVIEW

High-grade gliomas, including Grade III Anaplastic Astrocytoma and Grade IV Glioblastoma (GBM), are aggressive tumors of the brain and central nervous system. High-grade gliomas are the most common primary brain tumor, with an annual United States incidence of 0.37 and 3.19 per 100,000 person-years for anaplastic astrocytomas and glioblastomas, respectively [1]. High-grade gliomas can occur *de novo* or progress from low-grade gliomas [2]. First-line therapy includes maximal surgical resection and a combination of neoadjuvant as well as post-operative chemotherapy and radiation [3-5]. Despite multiple advances in surgical techniques, chemotherapy, and radiotherapy, current median survival is 2-7 years for anaplastic astrocytomas and an abysmal 15-months for glioblastoma [6, 7]. Non-modifiable good prognostic factors include young age, female gender, frontal and cortical tumor location, and low tumor grade [8-10]. Unlike certain hematological cancers with definitive genetic or chromosomal aberrations, high-grade gliomas can be initiated and propagated by diverse networks of signaling events [11]. Instead, multiple genetic prognostic factors such as Isocitrate Dehydrogenase 1 (IDH1) mutation, O6-methylguanine DNA methyltransferase (MGMT) promoter methylation status, and 1p/19q chromosomal deletions have been identified in high-grade gliomas [12]. These independent genetic factors have shown to be clinically relevant in predicting outcome, but the complexity and relation of these genetic factors to other genetic and clinical factors is a major area of ongoing research [13, 14]. The extent of surgical resection is the foremost treatment prognostic factor [15, 16], but resection is difficult due to the inherently invasive nature of glioma cells into the stroma surrounding the bulk tumor. Chemotherapy and target-specific therapy are complicated due to marked heterogeneity of glioma cell populations within the tumor [11]. Regardless, tumor relapse is inevitable and poorly amenable to additional resection or therapy [17, 18]. Altogether, high-grade gliomas are an incurable and devastating

disease with considerable challenges to the advancement of basic science and clinical outcome.

Promising basic science approaches have been developed to understand initiation, development, and genetic diversity of high-grade gliomas. Early murine *in vivo* glioma models utilized amplification or ectopic expression of members of the Epidermal Growth Factor Receptor (EGFR) pathway to form tumors histologically comparable to patient tumors [19]. Although aberrant expression of the EGFR was well-studied and occurs frequently in glioma, anti-EGFR therapeutic efforts failed and highlighted additional genetic complexity mandating a bioinformatical approach [20, 21]. To that end, the National Cancer Institute (NCI) has founded curated repositories such as The Cancer Genome Atlas (TCGA) and Repository of Molecular Brain Neoplasia Data (REMBRANDT) to catalog tumor data and the corresponding patient data for meta-analysis [22, 23]. Analysis of TCGA data for high-grade gliomas has further illuminated increased complexity between glioma samples. Three subtypes were described by Phillips *et al.* in 2008 [11], which were further developed into four distinct subtypes proposed by Verhaak *et al.* in 2010 [24]: Classical, Mesenchymal, Neural, and Proneural. A published Gene Set Enrichment Analysis set of the gene signatures for each Veerhak subtype is available in Appendix B: Table B1 [24]. The Classical subtype is named and characterized by increased expression of EGFR and other Growth Factor (GF) family genes. The Mesenchymal subtype is named and characterized by increased expression of genes categorically attributed to migratory mesenchymal cells. The Neural subtype is named and characterized by increased expression of genes associated with terminally-differentiated cells such as neurons and astrocytes. The Proneural subtype is named and characterized by increased expression of genes associated with less-differentiated cells such as neural progenitors and neural stem cells. Theses subtype names were designated mostly categorically by gene sets, and considerable efforts are being made to understand functional differences between these groups [11, 13, 22, 24]. Response to therapy and overall prognosis have been shown to vary between subtypes, with the best prognosis in the Proneural subtype and the worst prognosis in the

Mesenchymal subtype, though the Mesenchymal subtype is initially amenable to conventional therapy [11, 24]. Therefore, therapeutic approaches for glioma must be considered in the context of the genetic complexity within and across multiple glioma tumors.

The Mesenchymal subtype is particularly enriched in genes associated with cellular invasion, which is a complex cell behavior including interaction with the extracellular environment, dynamic cell-shape changes, and cellular locomotion. Cellular invasion has been studied as a necessary cell behavior underlying fibroblast migration in wound healing [25], neural migration in brain development [26], and endothelial invasion in angiogenesis [27, 28]. The initial step in cellular invasion is the formation of invadopodia, which are extensions of the cell membrane generated by actin polymerization [29]. Invadopodia regularly include coordinated attachment to the extracellular matrix, focused proteolysis, and generation of mechanical forces to propel the cell [30-32]. Dysregulation of invasion signaling pathways is the defining feature in progression of many cancers from carcinoma *in situ* to invasive carcinoma [33]. Protease-dependent invasion is termed "mesenchymal" in light of the necessity of mesenchyme-derived cells such as fibroblasts and endothelial cells to infiltrate tissue stroma [25, 27]. Protease-independent invasion has been reported in some cell types and is termed "amoeboid" [34, 35]. Distinction between the two types is therefore determined by activity of matrix-degrading proteolytic enzymes such as Matrix Metalloproteinase (MMPs). MMPs are a family of zinc-dependent endopeptidases with varying specificities to degrade collagens, laminin, fibronectin, aggrecan, and elastin [36]. MMPs can also cleave cell-surface proteins and have been shown to regulate cell proliferation, differentiation, and cytokine signaling [37]. MMP9 in particular has been shown as an indicator of poor prognosis in many invasive types of cancer, including high-grade gliomas [38-42]. Anti-MMP9 antisense RNA has been shown to inhibit proliferation of glioma cells *in vitro* and *in vivo*, indicating a complex role for MMP9 in regulating invasion and proliferation [43]. In addition to aberrant MMP expression, upregulation of matrix-adhesion proteins and synthesis of extracellular matrix allow

invading cells to preferentially adhere to matrix components and promote invasion [44, 45]. Pathological deposition of type I collagen and upregulation of collagen-binding receptors facilitate the invasive nature of high-grade gliomas [46-48]. Our lab has shown that high-grade glioma cells are capable of adhering and invading into 3-dimensional collagen matrices [49, 50]. Overall, invasion is a complex cell behavior that requires cell-signaling events to coordinate expression and activity of a diverse network of cellular events [33]. As such, it is imperative to advance comprehensive understanding of the role and capabilities of cell-signaling pathways underlying cellular invasion to identify promising targets for therapy.

Also implicated in Mesenchymal subtype tumors is the increased expression of Nuclear Factor kappa-light-chain enhancer of activated B cells (NF-κB) [24], a family of transcription factors including RelA, RelB, c-Rel, p105/p50, and p100/p52. NF-κB transcription factor dimers recognize a wide variety of DNA 11-mers that make up the κB consensus sequence RGGRNNHHYYB [51] to mediate a wide variety of cellular functions including immunity, survival, and cytokine response [52]. Dysregulated NF-κB signaling has been implicated in a wide variety of cancers, including glioma [53, 54]. In glioma, NF-κB has been shown to contribute to cell survival, cell differentiation, invasion, and radiotherapy resistance [55, 56]. The two major NF-κB pathways are the canonical NF-κB pathway and the noncanonical NF-κB pathway (Figure 1).

Activation of the canonical pathway involves phosphorylation of a hetero-trimeric Inhibitor of nuclear factor Kappa-B Kinase (IKK) complex (α, β, γ) by cellular kinases or cell-surface receptors [57]. IKKβ of the IKK complex phosphorylates Inhibitor of Kappa-Beta alpha (IκBα) [58], which sequesters the canonical transcription factor heterodimer of RelA and p50 by protein-protein interactions that block the RelA & p50 nuclear localization signals (NLS) [59, 60]. Phosphorylation of IκBα allows for proteasome-dependent IκBα degradation and translocation of RelA/p50 dimers to the nucleus for gene transcription [61]. Dissociation from IκBα and transcriptional activity can be altered by phosphorylation of RelA at Serine 536 [62]. Canonical NF-κB signaling is terminated by RelA-dependent transcription of IκBα [63, 64]. The

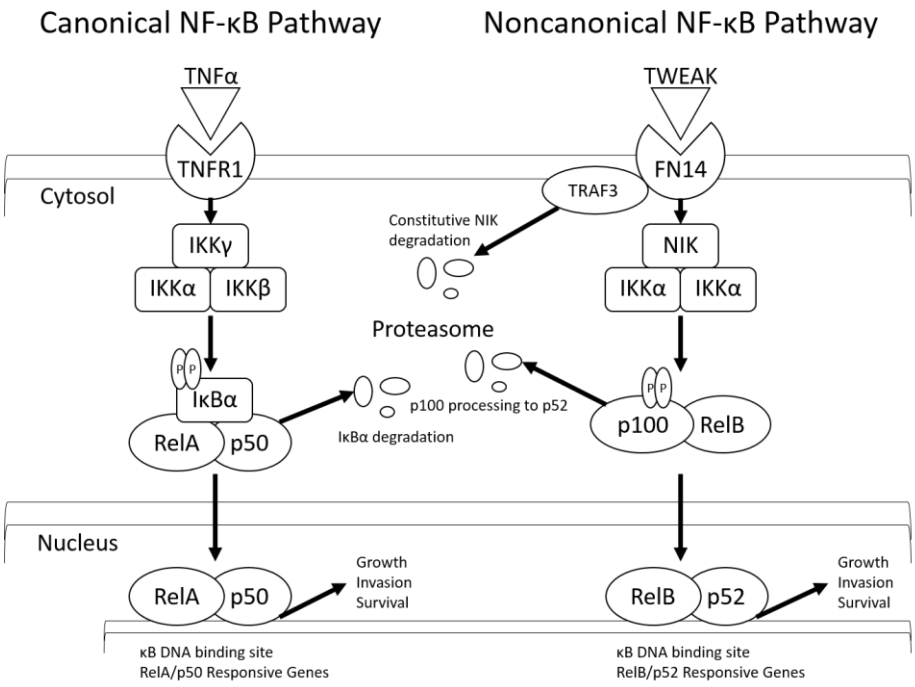

Figure 1 Schematic representation of canonical and noncanonical NF-κB pathways.

noncanonical NF-κB pathway requires constitutively active NF-κB-Inducing Kinase (NIK) [65, 66]. NIK protein levels in basal conditions are low due to constant negative regulation by TNF Receptor-Associated Factor 3 (TRAF3) resulting in degradation of NIK [67]. Extracellular signals can inhibit TRAF3 negative regulation and induce accumulation of NIK protein [67, 68]. NIK phosphorylates and forms a complex with IKKα that phosphorylates the C-terminus of p100 [69, 70]. p100 sequesters RelB in the cytoplasm by protein-protein interactions obscuring the RelB NLS [71]. Phosphorylated p100 is partially degraded to p52 by the proteasome, allowing RelB/p52 dimers to translocate to the nucleus and activate gene transcription [72, 73]. Noncanonical NF-κB signaling is terminated by negative feedback through IKKα-dependent phosphorylation and destabilization of NIK [74] as well as NF-κB-dependent transcription of p100 [64].

While the canonical NF-κB pathway is ubiquitous in all cells and exists as highly-regulated proteins constitutively expressed, the noncanonical NF-κB pathway is

differentially expressed and has been shown to control maturation of B cells and activation of dendritic cells [75-77]. Knockout of RelA is embryonic lethal [78], whereas knockout of noncanonical NF-κB constituents RelB, p100, and NIK result in mice with dysregulated B cell maturation and absent peripheral lymph nodes [79-82]. Considerable interplay exists within the pathways, including stabilized NIK activating the IKK complex [83], RelA-dependent RelB transcription [84], and RelA/p52 and RelB/p50 heterodimers [85]. Furthermore, RelB DNA binding activity has been shown to be repressed by RelA when both pathways are active [86], further indicating specific roles for each pathway. Aberrant canonical NF-κB signaling has been well-studied in gliomagenesis. RelA protein overexpression and increased phosphorylation at Serine 536 has been observed in glioma versus normal brain tissue and correlates positively with grade [87]. Increased canonical NF-κB signaling has been shown to promote cell survival, invasion, and therapy resistance in glioma [55]. Although noncanonical NF-κB has been recently implicated in gliomagensis [24], its role in glioma invasion and gliomagenesis is not well-understood. Our lab has shown that expression and activity of the noncanonical NF-κB pathway protein RelB promotes glioma cell survival, proliferation, and invasion *in vitro* and *in vivo* [49]. Additionally, our lab has shown that RelB regulates expression of genes associated with the aggressive mesenchymal glioblastoma subtype [49] and that activation and overexpression of the noncanonical NF-κB pathway increases invasion *in vitro* and tumor formation *in vivo* [50]. Therefore, further understanding of tumorigenic functions of the noncanonical NF-κB pathway is necessary.

Canonical and noncanonical NF-κB pathways can be activated by extracellular cytokines with varying specificity for canonical or noncanonical NF-κB signaling. Induction of canonical NF-κB signaling is rapid and transient, while noncanonical NF-κB signaling has slower onset and longer duration [88]. The most-studied ligands for activation of NF-κB pathways are members of the TNF superfamily of ligands and receptors. TNF-like Weak Inducer of Apoptosis (TWEAK) is a member of the TNF superfamily of ligands encoded by the *TNFSF12* gene [89]. TWEAK expression is

induced in response to inflammation and has cell-specific effects in promoting inflammation, proliferation, and angiogenesis [90-93]. TWEAK is active in either membrane-bound or soluble forms [89]. Membrane-bound TWEAK and pathologically high concentrations of soluble TWEAK predominately activate the canonical NF-κB pathway [94, 95]. At low physiological concentrations, soluble TWEAK is capable of activating the noncanonical NF-κB pathway through its receptor Fibroblast Growth Factor (FGF)-inducible immediate-early response gene Number 14 (FN14), induction of TRAF3 degradation, and accumulation of NIK [94, 96, 97]. TWEAK is expressed in the brain [89] and stimulates astrocyte proliferation in concert with EGF signaling [92, 98]. TWEAK induces neuronal cell death and increased blood-brain barrier permeability through activation of NF-κB [99, 100]. The pro-inflammatory and pro-astrocytic functions of TWEAK are an open area of research in neurologic diseases [92, 101, 102]. Pro-invasive MMP9 expression and secretion is induced by high-dose TWEAK through IκBα degradation, RelA phosphorylation, NIK stabilization, and p100 processing [95]. TWEAK-stimulated IκBα degradation and RelA translocation has been observed to increase migration and synthesis of pro-angiogenic Vascular Endothelial Growth Factor in ovarian carcinoma, a highly invasive and metastatic form of cancer [103]. In neuroblastoma cells, TWEAK is overexpressed under basal conditions and further induced by TNFα [104]. TWEAK stimulates phosphorylation of NF-κB and activates MMP9 [104].TWEAK has been shown to stimulate migration in glioma cells through FN14 in a canonical NF-κB-dependent manner and correlate with poor prognosis [105, 106]. Thus, TWEAK is a relevant inflammatory and pro-tumorigenic cytokine in glioma, though its roles in development or progression of glioma are not known.

The TWEAK receptor FN14, encoded by the *TNFRSF12A* gene, is a GF-inducible member of the TNF superfamily of receptors [107]. Prior to its classification as the TWEAK receptor, FN14 was an orphan receptor induced by FGF [108, 109]. FN14 was shown to increase migration in mesenchymal cells [109] and induce proliferation and inhibit terminal differentiation of mesenchymal progenitors in muscle repair [110]. Like other members of the TNFR superfamily, the FN14 cytoplasmic tail

binds TNF-receptor associated factors (TRAFs) including TRAF1, TRAF2, TRAF3, and TRAF5 [107, 111]. Similar to other receptors that activate noncanonical NF-κB signaling, engagement of FN14 with its ligand TWEAK recruits TRAF3 for degradation and results in stabilization of NIK [96, 97]. Activation of FN14 has been shown to result in transcription and secretion of MMP9 in glioma, neuroblastoma, and prostate cancers [95, 104, 112]. FN14 overexpression has been identified in invasive cancers of the liver, lung, breast, and prostate in addition to CNS malignancies such as neuroblastoma, and glioma [103-105, 108, 112-114]. FN14 expression is induced by activation of the Human EGF Receptors (HERs) in HER2 and HER3-positive breast cancers [113]. RNA silencing of FN14 decreases MMP9 mRNA expression and migration of HER-positive breast cancer cells [113]. Overexpression of human FN14 in non-small cell lung carcinoma cells increases cell migration as well as the frequency of metastases in mouse xenografts [114]. FN14 is highly expressed in hepatocytes during liver regeneration as well as in hepatocellular carcinoma (HCC) cells [108, 115]. Blockade of FN14-TWEAK signaling using a decoy FN14 fusion protein induces HCC cell procaspases and apoptosis *in vitro* as well as reduces HCC xenografts *in vivo* [115]. RNA silencing of TWEAK and FN14 decrease NF-kB phosphorylation and viability of neuroblastoma cells [104]. In glioma cells, overexpression of FN14 and its activate by TWEAK has been shown to promote glioma cell motility and survival through activation of IKKβ and the canonical NF-κB pathway [105, 116]. Initial reports indicated that FN14 is expressed at low levels in the brain [109], while more recent research has shown that FN14 is overexpressed in glioma and correlates with poor prognosis [105, 108]. The functional importance of FN14 signaling in the transformation and progression of glioma is not understood.

NIK was originally described as an activator of the canonical NF-κB pathway [117], but was discovered as essential for transmitting extracellular signals from cell-membrane receptors for all ligands known to activate the noncanonical NF-κB pathway [74, 81, 118], including TWEAK [97]. NIK is a Mitogen-Activated Protein Kinase Kinase Kinase (MAP3K) and its designated gene symbol is *MAP3K14*. A loss-of-

function mutation in NIK results in a B-cell-mediated alymphoplasia and immunodeficiency [82]. Conversely, elevated NIK activity has been recently implicated in hematological and ovarian cancers [119-122]. Loss of TRAF3 negative regulation of NIK can induce proliferation and malignancy of B cells [123]. NIK was identified in a differential gene expression study to promote resistance to ionized radiation when treated with a radioprotective compound [124]. shRNA-mediated knockdown of NIK abrogated the elongation, migration, and invasion of glioblastoma cells treated with a Second Mitochondrial Activator of Caspases (SMAC) mimetic [125]. Although understandings of NIK structure, regulation, and contribution to hematological malignancies have improved considerably in the last decade, tumorigenic functions of NIK in progression or maintenance of glioma are poorly understood.

Recent studies discussed here have advanced the fundamental understanding of glioma progression, NF-κB signaling, and TWEAK/FN14 signaling. The interrelation of these observations is still unclear and merits investigation. A combination of reports demonstrate NF-κB genes implicated in the aggressive Mesenchymal glioblastoma subtype [24], a pro-invasive function of noncanonical NF-κB transcription factor RelB [49], and TWEAK/FN14 overexpression inducing glioma invasion and correlating with poor outcome [105, 106]. Altogether, this implicates TWEAK/FN14 extracellular activation of NIK by preventing TRAF3 negative regulation as a glioma-relevant signaling axis yet to be specifically evaluated in glioma invasion. We designate TWEAK, FN14, NIK, and TRAF3 as the TWEAK Axis. In this work, we investigate how TWEAK promotes invasion through noncanonical NF-κB signaling and the significance of gene expression of the TWEAK Axis in clinical gliomas. Our specific questions for this dissertation are:

- How does upstream and extracellular activation of the noncanonical NF-κB pathway affect glioma invasion and tumorigenesis?
- What is the clinical context for expression of TWEAK-Axis genes?

In this thesis, we demonstrate a role for TWEAK and NIK in RelB-dependent noncanonical NF-κB signaling and high-grade glioma invasion. We utilized an *in vitro*

collagen I invasion model for understanding functional significance of cell-signaling events through the TWEAK Axis and noncanonical NF-κB pathway. We used an *in vivo* mouse orthotopic xenograft model to demonstrate that overexpressing NIK is pro-tumorigenic in glioma. Furthermore, we investigated gene expression and clinical data from NCI-curated databases for clinical correlations of the TWEAK Axis in glioma pathogenesis and patient outcome. Our results indicate that TWEAK, FN14, and NIK have a relevant biological and clinical role in high-grade gliomas, particularly the Mesenchymal subtype. These findings support previous reports and advance the field of TWEAK-FN14-noncanonical NF-κB signaling in high-grade gliomas.

CHAPTER II

TWEAK PROMOTES GLIOMA CELL INVASION THROUGH INDUCTION OF NIK AND NONCANONICAL NF-κB SIGNALING*

Background

The aggressive, infiltrative growth of gliomas renders them highly refractory to surgery, radiation and chemotherapy. Thus, understanding the biochemical and molecular pathways that control glioma cell invasion is critical for identifying more effective therapeutic targets. Aberrant activation of the canonical NF-κB pathway is well-documented in a variety of malignancies [126, 127] and plays important roles in regulating glioma invasion and tumor progression [55, 56, 128]. However, specific roles for the noncanonical NF-κB pathway in tumor pathogenesis, particularly in solid tumors of the central nervous system (CNS), are poorly understood.

NF-κB proteins are evolutionarily-conserved transcription factors that play central roles as coordinators of key biological processes including immunity, inflammation, cell death and survival. The five mammalian family members RelA (p65), RelB, c-Rel, NFKB1 (p105/p50), and NFKB2 (p100/p52) share an evolutionarily-conserved Rel homology domain that mediates DNA binding and dimerization with other NF-κB subunits. NF-κB complexes are held in the cytoplasm in an inactive state, bound to members of the NF-κB inhibitor (IκB) family, which includes IκBα. In response to specific extracellular signals such as the cytokine tumor necrosis factor-α (TNFα), activation of canonical NF-κB signaling is triggered by signal-induced phosphorylation and degradation of IκBα, followed by nuclear translocation of the active, liberated RelA-p50 complexes. IκBa phosphorylation-induced degradation and

---

*Reprinted with permission from "Tumor necrosis factor-like weak inducer of apoptosis (TWEAK) promotes glioma cell invasion through induction of NF-κB-inducing kinase (NIK) and noncanonical NF-κB signaling" by EM Cherry, DW Lee, JU Jung, R Sitcheran 2015. *Molecular Cancer*, Volume 14, Pages 1-13, Copyright [2015] by BioMed Central.

activation of the canonical NF-κB pathway is dependent on IκB kinase-β (IKKβ).

Noncanonical NF-κB signaling is mediated by RelB-p52 heterodimers whose activation is dependent on NF-κB-inducing kinase (NIK). NIK, a Mitogen-Activated Protein Kinase Kinase Kinase (MAP3K14), is regulated primarily through protein stabilization [129]. In unstimulated cells, NIK interacts with TNF Receptor-Associated Factor 3 (TRAF3) in a multi-subunit E3 ubiquitin ligase complex which leads to NIK polyubiquitination and proteasomal degradation [130]. Consequently, NIK protein levels are maintained at low levels. A critical step in activation of noncanonical NF-κB signaling is the ubiquitination-mediated proteasomal degradation of TRAF3, which stabilizes NIK protein, leading to IKKα activation and phosphorylation of p100, an inhibitory IκB-like protein that retains RelB in the cytoplasm. Phosphorylation of p100 leads to its proteolytic processing to form p52, culminating in nuclear translocation of transcriptionally active RelB-p52 heterodimers [66, 120]. Notably, unlike other NF-κB proteins, RelB is inherently unstable and its protein levels are stabilized by interaction with p100/p52 in the cytoplasm [131] and DNA binding in the nucleus [132].

The noncanonical NF-κB pathway can be specifically activated by signals such as B-cell-activating factor receptor (BAFFR) [129]. However, some signals, such as TNF-like weak inducer of apoptosis (TWEAK) have been shown to regulate both the canonical and noncanonical NF-κB pathways for sustained NF-κB activation [97]. TWEAK and its receptor, Fibroblast Growth Factor (FGF)-inducible immediate-early response gene Number 14 (FN14), have recently been implicated in tumor cell pathogenesis [104, 133] and upregulation of MMP9 [95], which is generally associated with poor disease prognosis due to its ability to promote tumor growth, migration, invasion, and metastasis [39]. However, the functional outcomes of TWEAK signaling in glioma with regard to specific downstream NF-κB signaling events are not clear. We have previously demonstrated that the noncanonical NF-κB protein, RelB, is highly expressed in a subset of aggressive, mesenchymal glioma, where it is a potent driver of oncogenesis and a predictor of survival in human patients [49]. In this study, we investigate the effects of TWEAK on noncanonical NF-κB/RelB signaling, MMP9

expression, and glioma invasion.

Results

The invasive potential of glioma tumor lines positively correlates with RelB expression

Because aggressive invasion of high-grade gliomas into normal health tissue is a significant barrier to treatment, we sought to further evaluate the relationship between NF-κB signaling pathways and glioma cell invasion. First, we analyzed the invasive potential of both established high-grade glioma tumor lines (U87 & U373) and primary brain tumor-derived lines (BT25, BT114, BT116, BT132) using a three-dimensional (3-D) collagen matrix assay [28]. Compared with two-dimensional (2-D) assays, modeling tumor cell invasion in 3-D collagen matrices better reflects both the *in vivo* cell-cell and cell-extracellular matrix interactions within a tumor [134], as well as the significantly elevated levels of collagen in the adult brain tumor microenvironment [47]. Analysis of side-view images of cells invading the collagen matrix and quantification of invading cells demonstrated that BT25, BT116, and U87 cells were the most invasive tumor lines, while BT132, BT114 and U373 were significantly less invasive (Figure 2A). Quantification of invasion density confirmed these observations (Figure 2B).

Next, we analyzed expression of canonical and noncanonical NF-κB proteins in the different glioma tumor lines. Western blot analysis demonstrated that, compared with BT25 and BT114 cells, BT116, BT132, U87 and U373 cells exhibited higher levels of phosphorylated RelA at serine 536 (RelA-P536), a marker of enhanced NF-κB transcriptional activation potential [135, 136], while total RelA levels were comparable in all cell lines (Figure 2C). We noted that neither total RelA, nor RelA-P536 levels correlated with invasiveness. For example, low RelA-P536 is seen in both invasive BT25 cells,as well as low-invasive BT114 cells. Likewise, high RelA-P536 expression was observed in both high-invasive BT116 and low-invasive BT132 (see Figure 2A, B). In contrast to RelA, RelB protein levels were more varied in the different glioma lines, and high RelB-expressing cells (U87, BT25, and BT116) invaded much more efficiently than low RelB-expressing cells (BT132, BT114 and U373). These results demonstrate

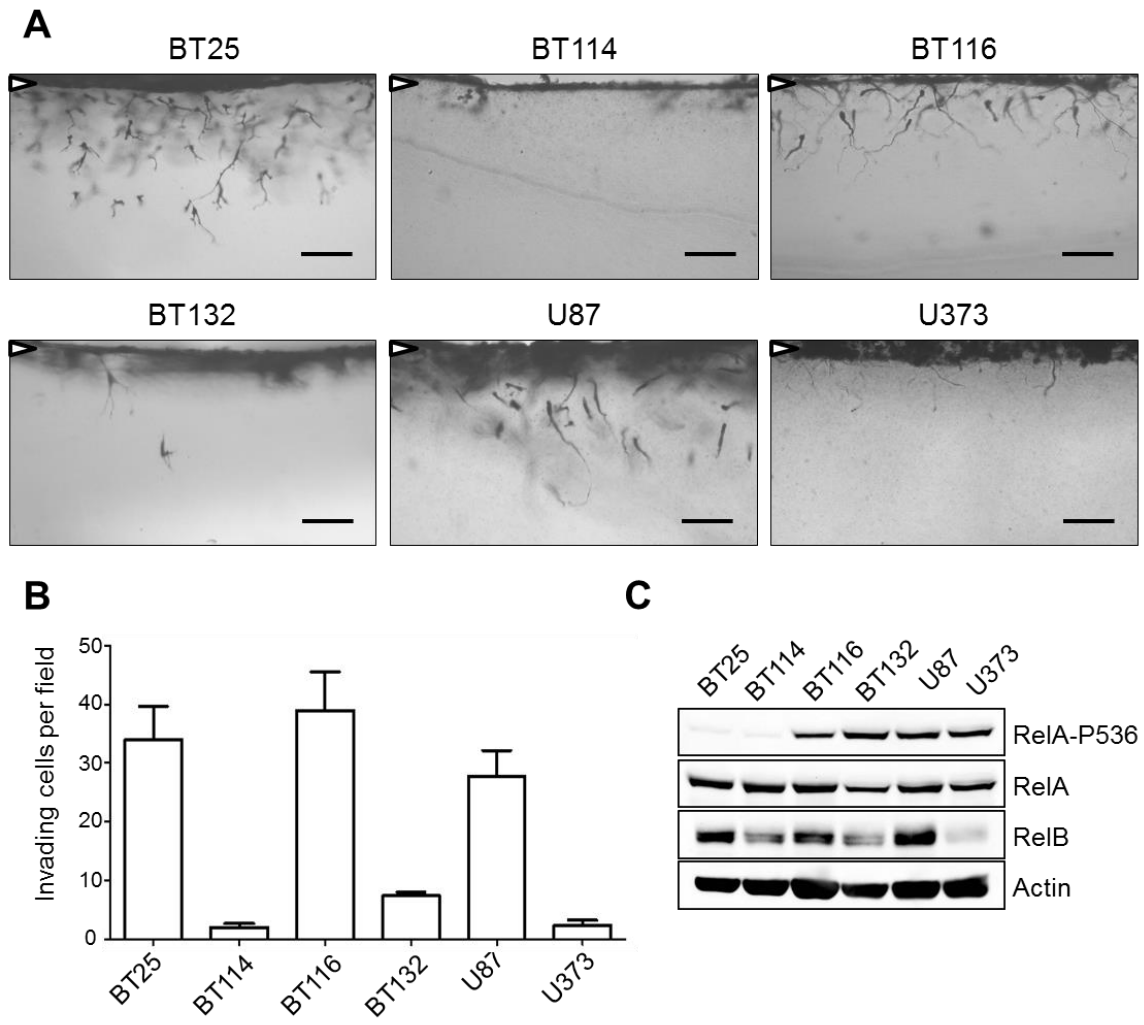

Figure 2 Glioma cells have diverse invasion phenotypes that correlate positively with RelB expression. Equal numbers of glioma cells from indicated cell lines were seeded on 3-D collagen matrices and allowed to invade for 48 h, fixed with 3% glutaraldehyde, and stained with 0.1% toluidine blue. **(A)** Side-view light microscopy images were taken from thin slices of the collagen matrices at 10x magnification. White arrowheads indicate cell monolayer. Scale bars = 100 μm. **(B)** Quantification of invasion density for cell lines in Figure 2A. Data represent average numbers of invading cells per 1-mm^2 field (n = 3 wells) ± SEM. **(C)** Western blot of whole-cell lysates from glioma lines using the indicated antibodies.

that levels of RelB, but not RelA or RelA-P536, strongly correlate with the invasive potential of glioma cells.

RelB poteniates glioma invasion independently of RelA

We have previously reported that loss of RelB in glioma significantly reduces the number and depth of invading tumor cells [49]. To further characterize and compare the roles of RelA and RelB in invasion, we used lentivirally-delivered shRNA to inhibit expression of these proteins in the highly invasive BT25 and U87 cells (Figure 3A). Side-view images of 3-D collagen invasion matrices and quantification of invading cells demonstrated that loss of either RelA or RelB each resulted in a significant decrease of glioma invasive potential (Figure 3B, C and Appendix A: Figure A1A, B). In shRelA cells, a significant loss of RelB was observed (Figure 3A), consistent with the known ability of RelA to regulate expression of RelB [84]. In contrast, RelA protein levels were not significantly affected by loss of RelB (Figure 3A), demonstrating that the loss of invasive potential of in shRelB cells was mediated by RelB and was not due to loss of signaling through the canonical RelA-dependent NF-κB pathway.

Next, we tested whether ectopic expression of RelB could restore the invasive potential of RelA knockdown cells. U87 shRelA cells were transduced with lentivirus to express either a control vector or RelB. We observed that ectopic expression of RelB in the RelA knockdown cells was approximately 5-fold higher than endogenous RelB expression in shControl cells (Figure 3D and Appendix A: Figure A1C). Notably, overexpression of RelB did not affect shRNA-mediated knockdown of RelA and also did not alter the levels of either total or phosphorylated RelA (Figure 3D). RelB was nevertheless able to restore the loss of invasion observed in RelA knockdown cells (Figure 3E). These results demonstrate that in glioma cells with attenuated levels of RelA protein, RelB can rescue invasion without increasing the expression or activity of RelA and canonical NF-κB signaling.

Figure 3 RelB potentiates glioma invasion independently of RelA. (A) Western blot of whole-cell lysates from NSC-cultured BT25 and U87 cells transduced with lentiviral vectors expressing shRNA targeting RelA (shRelA), RelB (shRelB), or a scrambled control (shCon). **(B)** Representative images of invading shRNA-transduced glioma cells at 48 h. White arrowheads indicate monolayer. Scale bars = 100 μm. **(C)** Quantification of invasion density at 48 h for BT25 and U87 knockdown cell lines. Data represent average numbers of invading cells per 1-mm^2 field (n = 3 wells) ± SEM. ***$p < 0.001$ relative to shCon using One-way ANOVA with Tukey's HSD. post-test. **(D)** Western blot of whole-cell lysates from U87 shRelA cells transduced with lentiviral vectors containing RFP cDNA (+Vector) or RelB cDNA (+RelB). **(E)** Quantification of invasion density at 48 h for U87 shRelA cells in Figure 3D. ***$p < 0.001$ relative to shCon using One-way ANOVA with Tukey's HSD post-test. †Data contributed by DW Lee.

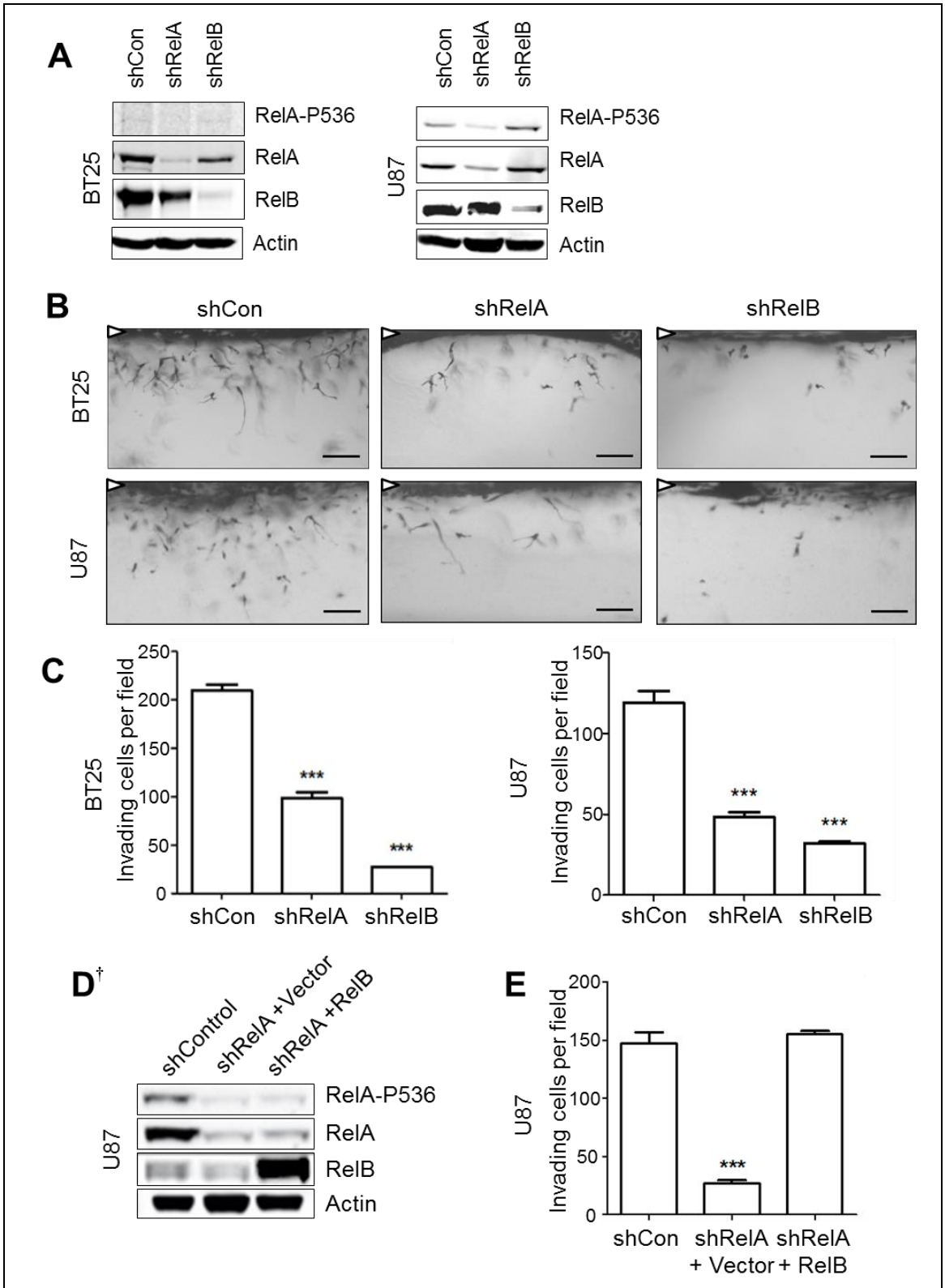

Figure 3. RelB potentiates glioma invasion independently of RelA.

TWEAK promotes glioma cell invasion and predominantly activates noncanonical NF-κB signaling

TWEAK has been reported to be an activator of both canonical and noncanonical NF-κB pathways [97, 137, 138]. However, very high concentrations of TWEAK (100 ng/ml) are required for activation of RelA [95, 137]. We observed that treatment with a low, physiological concentration of TWEAK (10 ng/ml) was sufficient to increase glioma invasion in the 3-D collagen matrices (Figure 4A). Thus, we next examined the effect of TWEAK on NF-κB signaling. Glioma cells were treated with TWEAK (10 ng/ml) and western blot analysis was performed with cytoplasmic and nuclear protein lysates. We observed that TWEAK robustly induced noncanonical NF-κB activity, as evidenced by increased p100 processing to p52, as well as nuclear accumulation of both RelB and p52 (Figure 4B). Increased nuclear accumulation of RelB was observed as early as 15 minutes after treatment with TWEAK and reached peak levels at 4 hours, with a concurrent increase in p100 processing and nuclear p52 and sustained levels of both proteins after 48 hours (Figure 4B). Notably, nuclear translocation of RelA, RelA-P536, p105, p50, or c-Rel was not induced by TWEAK stimulation (Figure 4B and Appendix A: Figure A2A). Moreover, no degradation of IκBα was observed in response to TWEAK (Figure 4B). In contrast, treatment with TNFα, a potent inducer of canonical NF-κB activity, led to rapid degradation of IκBα, and phosphorylation and nuclear translocation of RelA (Figure 4C), demonstrating that these cells have fully-functional canonical NF-κB signaling. TNFα also induced RelB nuclear accumulation and p100 processing, albeit more transiently compared with TWEAK treatment (Figure 4C). As with TWEAK, TNFα induced RelB nuclear localization starting at 15 minutes, reaching maximal levels at 4 hours. However, levels of nuclear RelB returned to basal by 24–48 hours (Figure 4C). Similar results were observed in TNFα- and TWEAK-treated BT25 and U87 cells (data not shown). Finally, consistent with predominant activation of the noncanonical NF-κB pathway by TWEAK, we observed a robust increase in NIK mRNA levels as early as one hour after TWEAK treatment (Figure 4D). TNFα, on the other hand, did not significantly alter NIK expression (Figure 4D). Induction of elevated

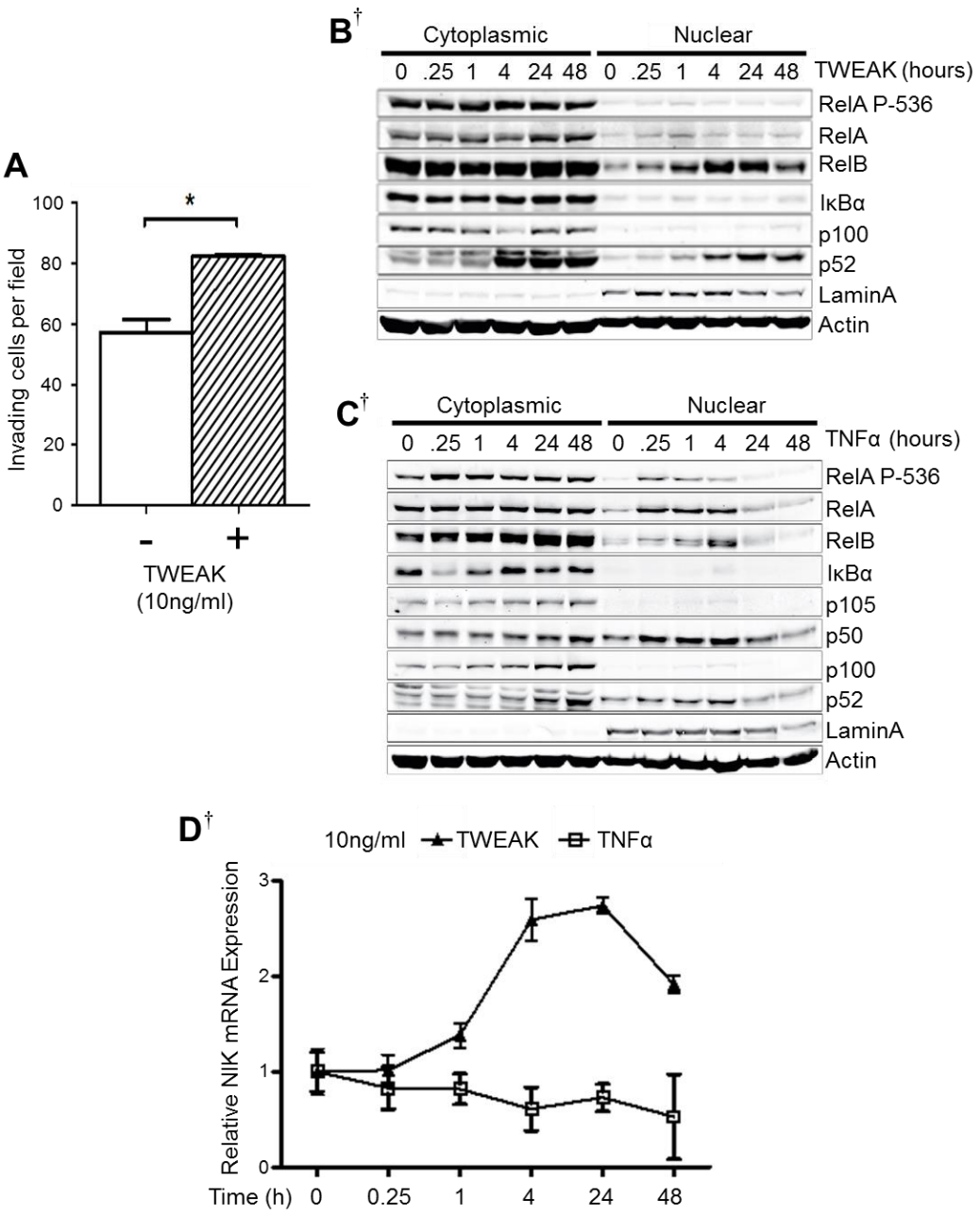

Figure 4 TWEAK induces invasion, NIK mRNA expression, and noncanonical NF-κB nuclear translocation. (A) Quantification of BT116 invasion density at 48 h with or without 10 ng/ml TWEAK in the collagen matrix. Data represent average numbers of invading cells per 1-mm^2 field (n = 3 wells) ± SEM. *p < 0.05 relative to vehicle control using unpaired Student's t-test. **(B)** Western blot analysis of proteins from cytoplasmic and nuclear fractions of BT116 cells stimulated with 10 ng/ml TWEAK for the indicated times using the indicated antibodies. **(C)** Western blot analysis of cytoplasmic and nuclear fractions as in Figure 4B post-stimulation with 10 ng/ml TNFα for the indicated times. **(D)** qRT-PCR analysis of NIK mRNA expression from BT116 cells. mRNA was collected at indicated time points after stimulation with TWEAK (10 ng/ml) or TNFα (10 ng/ml). Data represent average mRNA expression relative to RPLP0 mRNA (n = 3 replicates) ± SD. †Data contributed by DW Lee.

NIK mRNA synthesis at 4 hours post-TWEAK also correlated with increased protein levels (Appendix A: Figure A2B). Together, these data provide strong evidence supporting the ability of TWEAK to predominantly promote activation of the noncanonical NF-κB pathway in glioma.

TWEAK-dependent regulation of MMP9 expression is mediated by the noncanonical NF-κB pathway

Matrix Metalloproteinases (MMPs) play key roles in many aspects of cancer pathogenesis, including regulation of extracellular matrix remodeling during invasion [39]. To investigate the role of MMPs in glioma cells invasion, we tested the effects of a pan MMP inhibitor, GM6001, in our 3-D invasion assays. We observed that GM6001 blocked invasiveness of untreated cells in a dose-dependent manner, with almost complete inhibition of invasion with 1μM (Figure 5A, Appendix A: Figure A3A). The ability of TWEAK to promote invasion was also proportionately reduced with GM6001 treatment (Figure 5A). To examine the effect of TWEAK on expression of MMPs, we performed qRT-PCR on BT116 glioma cells treated with TWEAK (10 ng/ml) for 24 hours. Results from these experiments demonstrate that TWEAK robustly induced expression of MMP9 and negligibly affected expression of MMP2 and MMP14 (Figure 5B). Increased MMP9 expression was first discernable at 4 hours and peaking at 24–48 hours after TWEAK stimulation, concurrent with induction of RelB and p52 nuclear localization (see Figure 4C). TNFα also increased expression of MMP9 with more rapid kinetics but overall lower levels of induction compared to TWEAK (Figure 5B).

Given these findings, we surmised that the lower efficacy of GM6001 towards MMP9 activity (see Methods) might account for its inability to attenuate TWEAK-induced invasion. Therefore, to test the role of MMP9 in TWEAK-induced invasion we performed the 3-D invasion assay in the presence of a selective MMP9 inhibitor. MMP9Inhibitor I did not have a significant effect on untreated U87 cells, however, the ability of TWEAK to promote invasion was significantly attenuated (Appendix A: Figure A3B). Similar results were observed with BT116 cells (data not shown).

Figure 5 MMPs are required for glioma invasion and TWEAK-induced MMP9 expression is p52-dependent. (A) Quantification of invasion density at 48 h for BT116 cells with or without 10 ng/ml TWEAK in the collagen matrix. Cells were treated during the 48 h invasion assay with broad-spectrum MMP inhibitor GM6001 at indicated concentrations. Data represent average numbers of invading cells per 1-mm^2 field (n = 3 wells) ± SEM. **p < 0.01 ***p < 0.001 between indicated groups using unpaired Student's t-test. **(B)** qRT-PCR analysis of MMP mRNA expression in cultured BT116 cells. mRNA was collected at indicated time points after stimulation with TWEAK (10 ng/ml) or TNFα (10 ng/ml). Data represent average mRNA expression relative to GAPDH mRNA and normalized to untreated cells at t = 0 (n = 3 replicates) ± SD. **(C)** Western blot of whole-cell lysates from cultured BT25, BT116, and U87 cells transduced with shRNA targeting p100/p52 (NFKB2) or a scrambled control (Control). Lysates were collected at 48 h after stimulation with 10 ng/ml TWEAK or vehicle control. White arrowhead indicates p52 band. Black arrowhead indicates non-specific band. **(D)** qRT-PCR analysis of MMP9 mRNA expression from cell lines in Figure 5C. mRNA was collected at 48 h after stimulation with 10 ng/ml TWEAK or vehicle control. Data represent average MMP9 mRNA expression relative to RPLP0 mRNA and normalized to untreated control (n = 3 replicates) ± SD. ***p < 0.001 between indicated groups determined by unpaired Student's t-test for each cell line. †Data contributed by DW Lee.

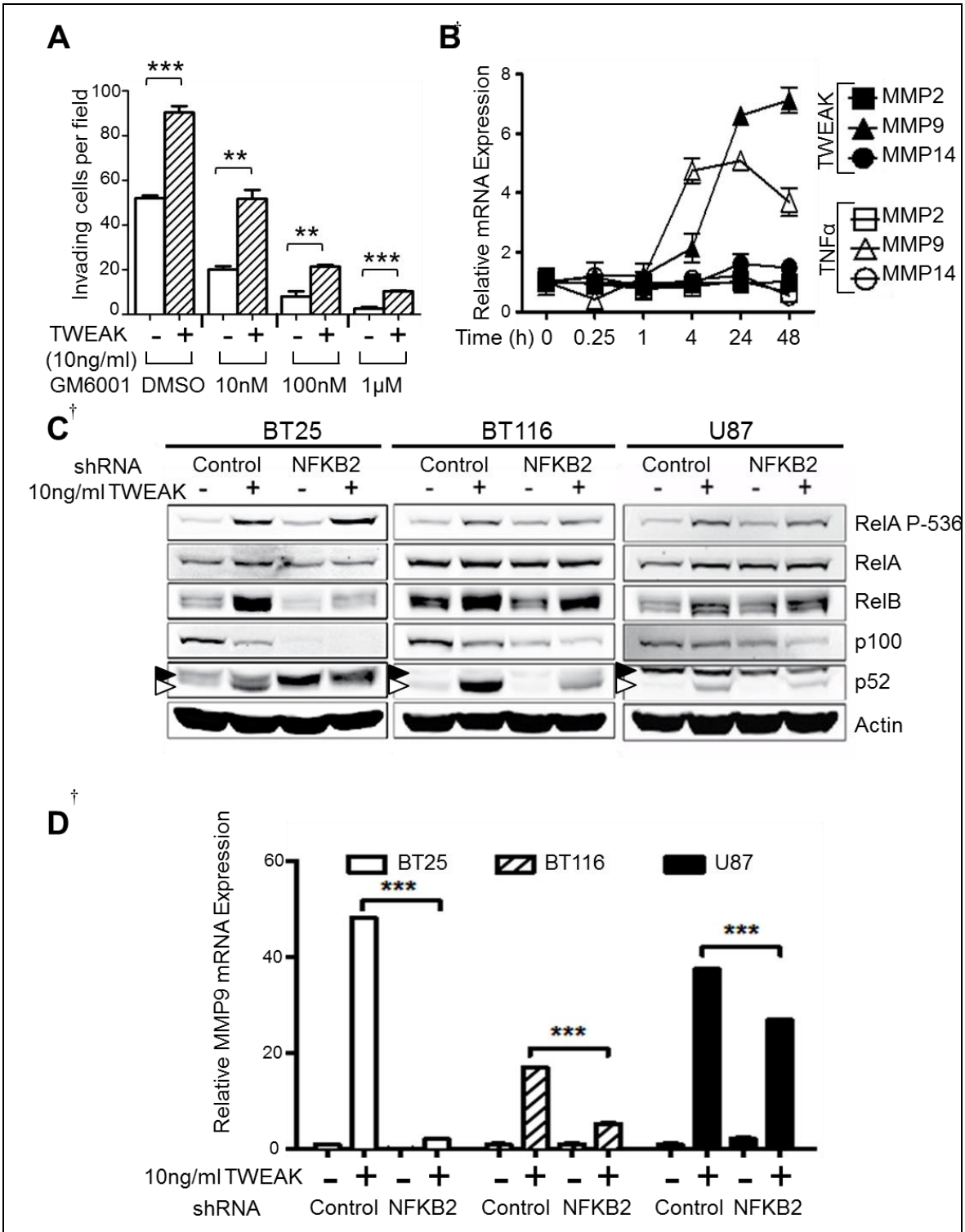

Figure 5 MMPs are required for glioma invasion and TWEAK-induced MMP9 expression is p52-dependent.

To determine whether noncanonical NF-κB activity is required for TWEAK-induced MMP9 expression, we transduced BT25, BT116, and U87 cells with shRNAs targeting NFKB2 (p100) or a scrambled shRNA. Western blot analysis demonstrated that loss of NFKB2 resulted in a decrease in p100 protein levels and TWEAK-dependent processing to p52 (Figure 5C). TWEAK induction of RelB protein was also attenuated in NFKB2 knockdown cells (Figure 5C). qRT-PCR analyses demonstrated that although basal MMP9 mRNA levels were comparable between shNFKB2 and shControl lines, the ability of TWEAK to induce MMP9 expression was significantly impaired in NFKB2 knockdown cells (Figure 5D). These results demonstrate that TWEAK-mediated induction of NIK and noncanonical NF-κB pathway are critical for increasing expression of MMP9 and glioma cell invasion.

Expression of NIK promotes gliomagenesis in vivo

Our data thus far demonstrate that a low concentration of TWEAK promotes invasion and predominantly activates noncanonical NF-κB signaling in glioma tumor lines with high RelB expression. Notably, we observed that similar to BT116 cells, TWEAK was also able to promote invasion in BT114 glioma cells, which are minimally invasive and express low levels of RelB (Figure 6A; also see Figure 2). TWEAK also significantly increased levels of NIK mRNA in these cells (Figure 6B). Therefore, we investigated whether NIK could potentiate noncanonical NF-κB signaling and enhance gliomagenesis *in vivo* using an orthotopic mouse xenograft model. Ectopic expression of NIK in BT114 cells increased p100 processing to p52 compared with BT114 cells expressing vector control, indicating that the ectopically expressed NIK was functional (Figure 6C). RelA-P536, IκBα, p50, and c-Rel levels were unaffected by NIK overexpression, indicating that NIK did not significantly affect the canonical NF-κB pathway (Appendix A: Figure A4A). BT114-control and BT114-NIK cells were fluorescently labeled and injected into the right cortex of CD-1 nude mice. 3-D tomographic reconstruction of fluorescent images taken *in vivo* revealed that BT114-NIK cells formed larger and more-dispersed tumors compared with BT114-control cells (Figure 6D). Quantification of

Figure 6 NIK mRNA is up-regulated by TWEAK and NIK protein overexpression promotes tumorigenesis. (A) Quantification of BT114 invasion density at 48 h with or without 10 ng/ml TWEAK in the collagen matrix. Data represent average numbers of invading cells per 1-mm^2 field (n = 3 wells) ± SEM. ***p < 0.001 relative to vehicle control using unpaired Student's t-test. **(B)** qRT-PCR analysis of NIK mRNA expression from BT114 cells. mRNA was collected at 48 h after stimulation with 10 ng/ml TWEAK or vehicle control. Data represent average NIK mRNA expression relative to RPLP0 mRNA and normalized to untreated control (n = 3 replicates) ± SD. ***p < 0.001 relative to vehicle control using unpaired Student's t-test. **(C)** Western blot analysis of BT114 glioma cells transduced with lentivirus containing NIK cDNA or luciferase cDNA (Con) using the indicated antibodies. **(D)** Representative IVIS images of 3-D rendering of tumors derived from DiD-stained intracranial-injected BT114-control (n = 7 mice) or BT114-NIK (n = 9 mice) cells at 14 and 24 days post-injection (n = 3 mice per group). Numbers indicate scale of Signal Intensity for each image. **(E)** Quantification of BT114 brain tumors in Figure 6D at 30 days. Data represent average tumor volume ± SEM. *p < 0.05 relative to BT114 control using unpaired Student's t-test. **(F)** Representative IVIS *ex-vivo* images of DiD-stained BT114 brain tumors in Figure 6D at 58 days post-injection. †Data contributed by DW Lee, ‡ Data contributed by J Jung.

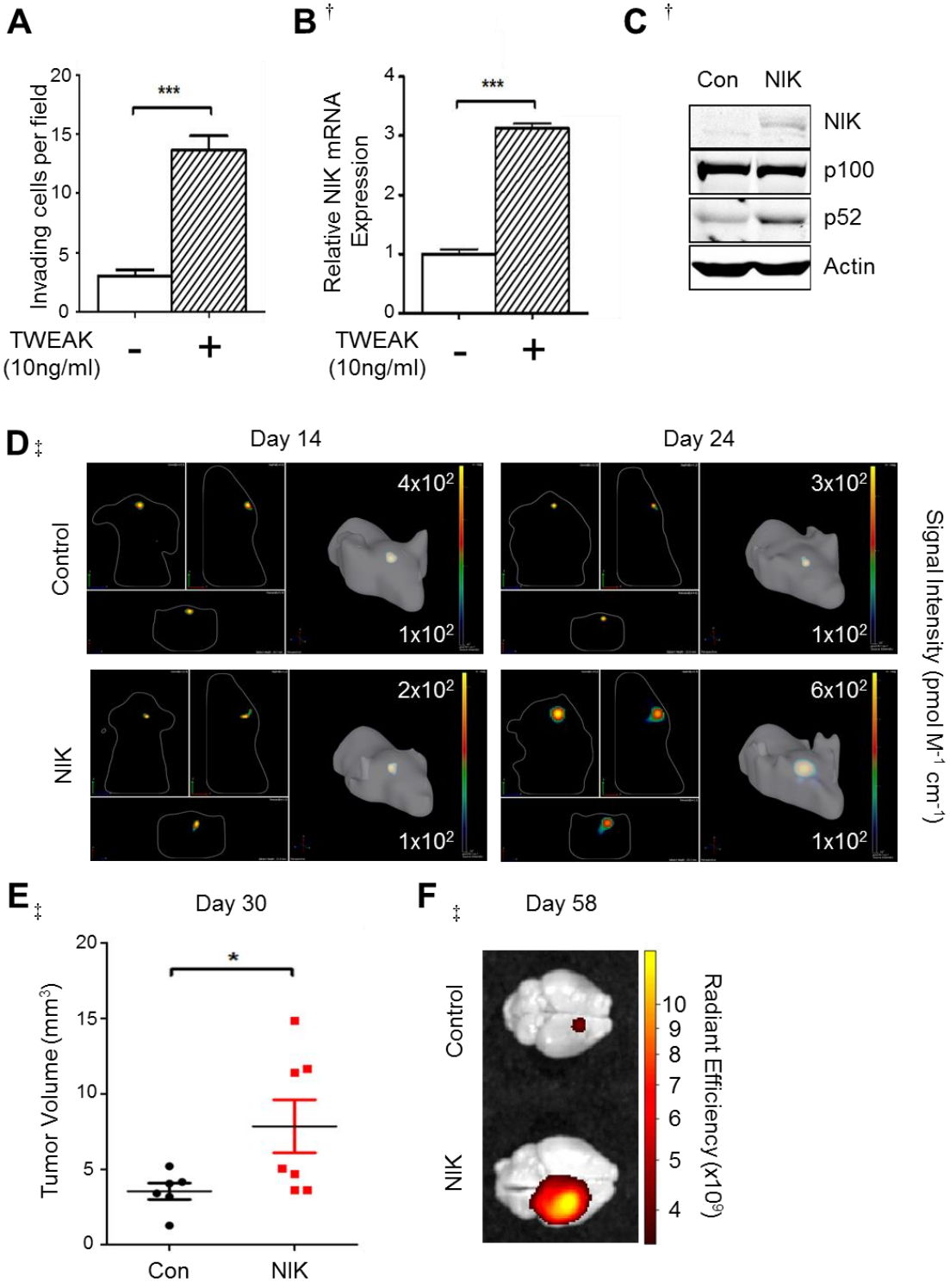

Figure 6 NIK mRNA is up-regulated by TWEAK and NIK protein overexpression promotes tumorigenesis.

tumor volume demonstrated that BT114-NIK cells formed significantly larger tumors (Figure 6E). Finally, *ex vivo* images taken 58 days after intracranial injection confirmed that BT114-NIK cells formed significantly larger tumors compared with BT114-control (Figure 6E,F). Taken together, these data reveal a key role for NIK and noncanonical NF-κB signaling in glioma pathogenesis.

NIK promotes invasion and mediates TWEAK-induced invasion in vitro

Constitutive activity of endogenous NIK is negatively regulated by polyubiqutinylation and proteasome-mediated degradation. TRAF3 is the most well-studied recruiter of a TRAF2/cIAP2/cIAP3 E3 ligase complex, but inhibition of this process is complex due to multiple ubiquitinylation sites and a large TRAF3-binding domain in the NIK protein. Multiple point mutations or a large domain deletion in the NIK protein could introduce considerable variability in the stability and activity of the NIK protein. We sought to artificially increase NIK activity by creating a mutant NIK construct with an alanine substitution at serine 867 (NIK-S867A) identified as the site for phosphorylation by TANK-Binding Kinase 1 (TBK1) in an alternate degradation pathway [139]. Transduction of BT114 and U87 cells with wild-type NIK (BT114-NIK and U87-NIK) and mutant NIK (BT114-NIK S867A and U87-NIK S867A) resulted in comparable levels of NIK protein under basal conditions (Figure 7A). Increased p100 processing to p52 was observed in BT114-NIK, U87-NIK, and U87-NIK S867A cells compared to control-transduced cells. BT114-NIK S867A did not significantly increase p52 production versus detectable p52 levels seen in unstimulated BT114 control-transduced cells (see Figure 6C). Side-view images of cells invading the collagen matrix demonstrated that BT114-NIK and U87-NIK cells were slightly more invasive than BT114-control and U87-control, while BT114-NIK S867A and U87-NIK S867A cells were significantly more invasive than BT114-control and U87-control lines (Figure 7B). Quantification of invasion density confirmed these observations (Figure 7C).

NIK acts as the receptor-activated MAP3K for all known ligands that specifically activate noncanonical NF-κB signaling [81, 118, 123]. We performed a NIK loss-of-function study to determine whether NIK acts as an intermediary in the observed TWEAK-induced induction of noncanonical NF-κB signaling and TWEAK-stimulated invasion. BT114 cells were transduced with shRNA targeting NIK (shNIK) or a scrambled shRNA control (shCon). Detection of endogenous NIK expression in transduced BT114 lines required treatment with proteasome inhibitor MG132 and could be increased with TWEAK treatment (Figure 7D). Functionality of the shNIK construct was verified by undetectable NIK protein in BT114-shNIK cells even with both MG132 and TWEAK treatment. TWEAK treatment induced p100 processing in BT114 lines, consistent with previous induction in other lines (see Figure 5C). Some p52 production was observed in TWEAK-stimulated BT114-shNIK cells, indicating incomplete knockdown and consistent with constitutive activity. As expected, MG132 treatment inhibited p100 processing to p52. TWEAK significantly increased invasion in BT114-control cells, consistent with the response seen in wild-type BT114 cells (Figure 7E, see Figure 6A). The significant increase in invasion with TWEAK treatment was lost in the BT114-shNIK line (Figure 7E). A slight increase in invasion in the BT114-shNIK cells is consistent with detectable NIK activity from incomplete knockdown (see Figure 7D). Together these results indicate that increased NIK activity is sufficient to increase glioma invasion and that NIK is a significant intermediary in TWEAK-induced invasion.

Discussion

Aberrant activation of the canonical NF-κB pathway has been correlated with the promotion of brain cancer cell survival and invasion. However, roles for the noncanonical NF-κB pathway in CNS pathologies are less clear. RelB expression was previously described to be elevated in the aggressive mesenchymal glioma subtype [24] and we have recently identified a functional role for RelB as a key driver of mesenchymal gene expression and tumorigenesis [49]. A critical feature of the noncanonical NF-κB signaling pathway is its dependence on the regulation of NIK

Figure 7 NIK overexpression increases invasion and NIK knockdown inhibits TWEAK-induced invasion. (A) Western blot analysis of whole-cell lysates from BT114 and U87 glioma cells transduced with lentiviral vectors containing NIK cDNA, NIK S867A cDNA, or luciferase cDNA (Con) using the indicated antibodies. **(B)** Representative images of invading NIK-transduced glioma cells at 48 h. White arrowheads indicate monolayer. Scale bars = 100 µm. **(C)** Quantification of invasion density at 48 h for BT114 and U87 ectopic NIK expression cell lines. Data represent average numbers of invading cells per 1-mm^2 field (n = 3 wells) ± SEM. **p<0.01 ***p < 0.001 relative to Con using One-way ANOVA with Tukey's HSD. post-test. **(D)** Western blot of whole-cell lysates from cultured BT114 cells transduced with shRNA targeting NIK (shNIK) or a scrambled control (shCon). Cells were pre-treated for 1 h with 5 µM proteasome inhibitor MG132 or vehicle control prior to stimulation with or without 10 ng/ml TWEAK for 6 h as indicated. **(E)** Quantification of invasion density in BT114 knockdown cell lines at 48h with or without 10 ng/ml TWEAK in the collagen matrix. Data represent average numbers of invading cells per 1-mm^2 field (n = 3 wells) ± SEM. ***p < 0.001 relative to vehicle control using unpaired Student's t-test. †Data contributed by DW Lee

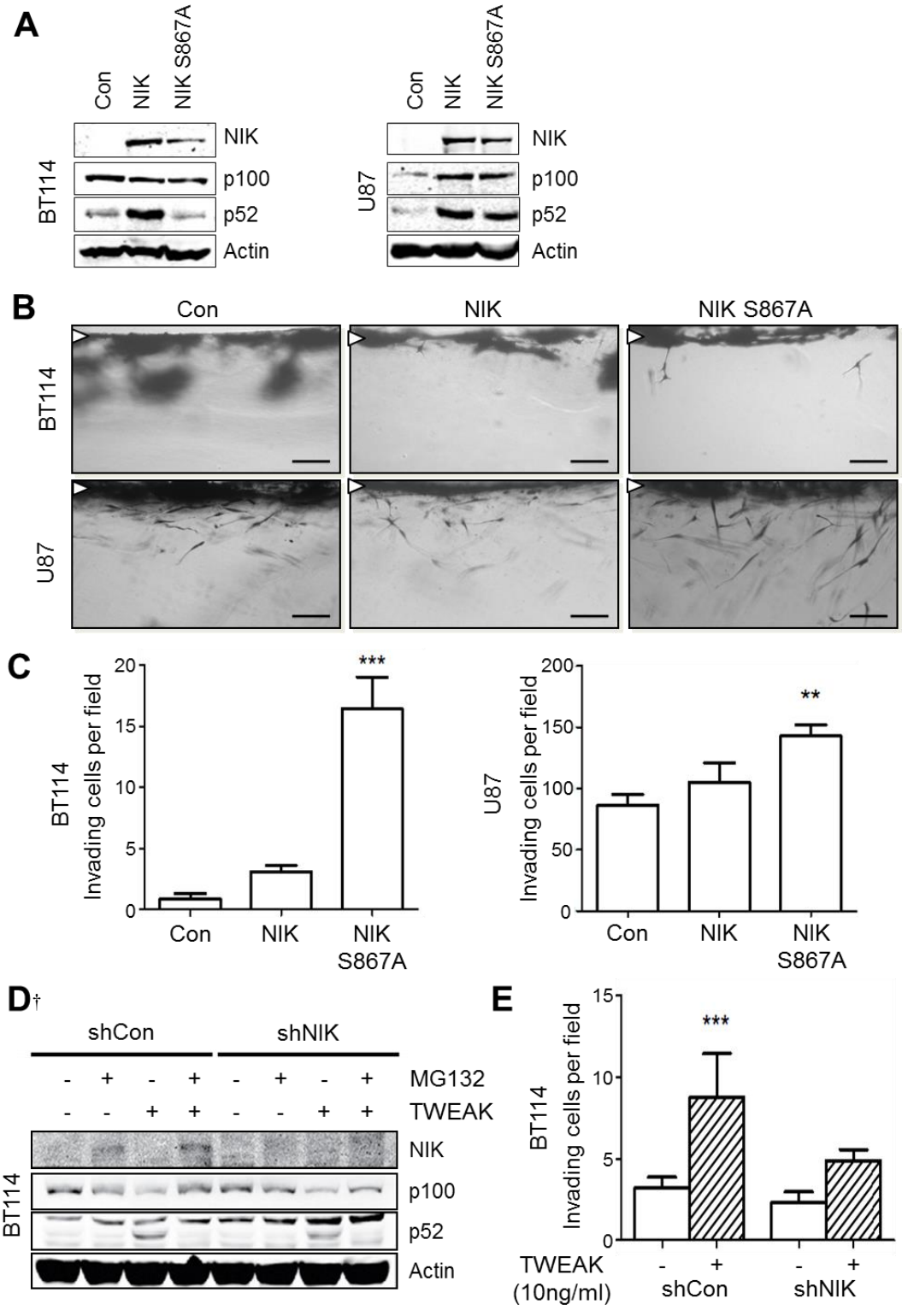

Figure 7 NIK overexpression increases invasion and NIK knockdown inhibits TWEAK-induced invasion.

protein stability through proteasome-dependent degradation [130]. We show that a low concentration of TWEAK (10 ng/ml) preferentially and potently activates the noncanonical NF-κB signaling cascade as evidenced by induction of p100 processing to p52 and nuclear accumulation of p52 and RelB (see Figure 4B). At this concentration, TWEAK failed to induce significant IκBα degradation and nuclear translocation of RelA (see Figure 4B), suggesting minimal TWEAK-induced activation of the canonical NF-κB pathway in glioma cells. Moreover, since a low concentration of TWEAK is sufficient to promote noncanonical NF-κB-mediated cell invasion, this pathway may be extremely important for initiating early, aggressive tumor dissemination.

Interestingly, we observed that TWEAK can promote noncanonical NF-κB signaling at the pre-translational level, as evidenced by accumulation of NIK mRNA in response to treatment with TWEAK. This induction of NIK mRNA was specific for TWEAK since TNFα, a potent inducer of the canonical NF-κB pathway, failed to increase NIK expression (see Figure 4D). Pre-translational regulation of NIK expression by TWEAK may be important for sustained activation of the noncanonical NF-κB pathway during the invasion process. TWEAK is synthesized in response to cellular injury and inflammation in tumor cells, as well as many cell types of the CNS, including neurons, microglia, and endothelial cells [140]. Therefore, TWEAK may function in both an autocrine and paracrine manner to robustly induce NIK expression, activate noncanonical NF-κB signaling, and increase MMP expression, thereby promoting tumor cell invasion. Overall, these data provide compelling evidence that the pathological, pro-invasive effects of TWEAK are preferentially mediated by noncanonical NF-κB signaling.

Recently, noncanonical NF-κB signaling was shown to promote glioma invasion in response to non-toxic doses of BV-6, a potential chemotherapeutic agent that promotes cancer cell death through antagonism of cellular Inhibitors of Apoptosis proteins (c-IAPs) [125]. Our data demonstrate that both basal, constitutive noncanonical NF-κB activity, as well as induction of noncanonical NF-κB signaling by an endogenous cytokine, TWEAK, play critical roles in promoting glioma invasion. According to our

findings, NIK is a critical mediator of TWEAK-induced glioma invasion. These findings demonstrate that noncanonical NF-κB signaling not only mediates therapy resistance, but also is important in the context of normal brain tumor pathogenesis.

Lastly, it was recently reported that IKK-dependent, canonical NF-κB signaling suppresses NIK activity and noncanonical NF-κB signaling [141]. In the context of those findings, our data suggest that inhibition of canonical NF-κB pathway might result in increased constitutive noncanonical NF-κB activity, thereby promoting tumor cell invasion and pathogenesis. Notably, the ability of TWEAK to induce NIK expression and promote invasion is not only observed in glioma cells expressing high levels of RelB, but also in glioma cells with low levels of endogenous RelB expression (Figure 6). Altogether, these data suggest that blocking TWEAK signaling and noncanonical NF-κB activation, alone or in combination with inhibition of canonical NF-κB signaling, will be more efficacious for attenuation of tumor cell invasion and, therefore, have therapeutic value in a broad range of glioma subtypes.

Conclusion

Here, we establish a key role for noncanonical NF-κB signaling in glioma that is independent of the canonical NF-κB pathway. Specifically, we demonstrate that RelB promotes glioma invasion in the absence of RelA, and that TWEAK preferentially regulates noncanonical NF-κB signaling in glioma through a novel, signal-specific induction of NIK expression. Moreover, NIK is sufficient to promote brain tumor growth *in vivo*. To date, therapeutic strategies targeting NF-κB have focused almost exclusively on inhibition of the canonical NF-κB pathway [142]. Our findings provide a compelling rationale for considering TWEAK/FN14 and NIK inhibition as therapeutic strategies for aggressive glioma, as well as other highly invasive cancers.

Methods

Cell culture & reagents

BT lines obtained from glioma patients (BT25, BT114, BT116, BT132) were obtained as described previously [143]. 293 T, U87-MG, and U373 cells were purchased from ATCC. Glioma cell lines were cultured in DMEM/F12 + 10% FBS (1X Glutamax, 1X Pen/Strep) or Neural Stem Cell (NSC) medium (DMEM/F12, 1X B-27 Supplement minus Vitamin A, 1X Glutamax, 50 ng/ml EGF, 50 ng/ml bFGF, 1X Pen/Strep). All cell culture reagents were from Life Technologies (Grand Island, NY). rhTNFα was obtained from Promega (Madison, WI), and rhTWEAK was obtained from PeproTech (Rocky Hill, NJ). GM6001 inhibitor, MMP Inhibitor I, and MG132 inhibitor were obtained from EMD Millipore (Temecula, CA).

3-D invasion assays

Invasion assays were performed as described previously [28, 49]. In brief, Type I collagen extracted from rat tail tendons [144] was diluted to 2 mg/ml in DMEM/F12 (1X Pen/Strep) and matrices were polymerized in half-area 96-well plates. 40,000 cells per well were seeded in 100 µl DMEM/F12 (1x Pen/Strep, 1X Glutamax) without growth factors or serum. Cells were fixed with 3% glutaraldehyde solution after 48 h of invasion and stained with 0.1% toluidine blue. Invasion density was quantified by counting cells below the plane of the monolayer by bright-field light microscopy using a 10x10 ocular grid at 10x magnification corresponding to a 1-mm^2 field. Numbers in equivalent fields were counted (n = 3 wells). Cross-sectional images were taken with an Olympus CKX41 inverted microscope and Q-Color 3 camera.

Western blots

Whole-cell lysates were prepared using RIPA buffer with 1X Halt protease and phosphatase inhibitors (Thermo Scientific, Rockford, IL). Cytoplasmic and nuclear extracts were prepared as previously described [145]. 25-40 µg of protein was separated in replicate 9% polyacrylamide (29:1 Bis) Tris gels and transferred to replicate

nitrocellulose membranes for probing proteins in parallel. After transfer, gels were stained with GelCode Coomassie (Thermo Scientific, Rockford, IL) and scanned with the IR700 channel of an Odyssey Infrared Imaging system (LI-COR Biosciences, Lincoln, NE) for first verification of even protein loading. Westerns were performed by blocking membranes in 1:1 PBS/Odyssey Blocking Buffer (LI-COR Biosciences, Lincoln, NE) prior to co-incubation with mouse and rabbit primary antibodies. Simultaneous detection was performed using with goat anti-rabbit IRDye800CW and goat anti-mouse IRDye680 secondary antibodies (LI-COR Biosciences, Lincoln NE). Membranes were probed in parallel for simultaneous detection of multiple antibodies in replicate membranes without stripping. Western blots and Coomassie-stained gels were scanned with the Odyssey Imager. Color images were scanned with a LI-COR Infrared Imaging System, converted to black and white, and analyzed using the LI-COR Image Studio software. Quantitative analysis of indicated images was performed using Image Studio or Image J software (NIH, Bethesda, MA). The following Santa Cruz Biotechnology (SC, Santa Cruz, CA) and Cell-Signaling Technology (CST, Danvers, MA) antibodies were used: RelB (CST-4922), RelA (SC- 8008), Phospho-RelA Ser536 (CST-3033), c-Rel (CST-4727), p100/p52 (CST-3017), p105/p50 (CST 13681), LaminA (SC 56137), IκBα (CST 4814), NIK (CST 4994), β-Actin (SC-69879).

Plasmids

pLenti6 overexpression constructs for RelB and NIK were generated by subcloning cDNA into pLenti6-V5-DEST (Addgene, Cambridge, MA) using the GATEWAY™ Cloning System. Luciferase (Promega, Madison, WI) or tagRFP (Evrogen, Moscow, Russia) coding sequences were subcloned into pLeni6-V5-DEST and used as controls for RelB and NIK overexpression. Mission™ Lentiviral shRNA plasmids for RelA, RelB and control were purchased from Sigma-Aldrich (St. Louis, MO). shRelB, as well as its control, was described previously as shRelB-3 [49]. shNFKB2, shNIK, and shControl oligonucleotides (Integrated DNA Technologies, Coralville, IA) were

subcloned into pLKO.1-puro (Addgene, Cambridge, MA). Exact sequences are available upon request.

Lentivirus production and transduction

293 T cells were transfected with 7 μg of lentiviral plasmids using 21 μg of polyethyleneimine (Polysciences Inc., Warrington, PA). Lentiviruses were harvested after 3 days and used to infect $2x10^5$ glioma cells. Transduced cells were selected for 72 h in DMEM/F12 NSC medium containing 0.6 μg/ml Puromycin or 3 μg/ml Blasticidin (Invivogen, San Diego, CA) to verify stable transduction. Cells were continuously selected during culture with 0.6 μg/ml Puromycin (shRNA constructs) and/or 6 μg/ml Blasticidin (overexpression constructs).

Quantitative reverse-transcriptase PCR

Total RNAs were isolated from cells using Purelink™ RNA Mini Kit (Life Technologies, Carlsbad, CA). cDNA was synthesized from 1 μg of total RNA using SuperScript® III Reverse Transcriptase (Life Technologies, Carlsbad, CA) following manufacturer's instructions. Quantitative RT-PCR was performed using SYBR® Green PCR Master Mix (Applied Biosystems, Foster City CA). Expression of mRNA was normalized to either GAPDH or RPLP0 expression levels. The following primers were used in amplifications: GAPDH 5′-AATGAAGGGGTCATTGATGG-3′, 5′-AAGGTGAAGGTCGGAGTCAA-3′; RPLP0 5′- TCGTCTTTAAACCCCTGCGTG-3′, 5′-TGTCTGCTCCCACAATGAAAC-3′; MMP-2 5′-AAGAAGTAGCTGTGACCGCC-3′ 5′-TTGCTGGAGACAAATTCTGG-3′; MMP9 5′-GCACTGCAGGATGTCATAGG-3′ 5′-ACGACGTCTTCCAGTACCGA-3′; MMP-14 5′-TGCCTACCGACAAGATTGATG-3′ 5′-ATCCCTTCCCAGACTTTGATG-3′; NIK 5′-TTCAGCCCCACCTTTTCAG-3′ 5′-ACGCTTTCCCTTCCAACAC-3′. All experiments were performed at least three times with three replicates per sample.

Orthotopic mouse xenografts

All animal experiments were done in compliance with IACUC, AAALAC and Texas A&M University Health Science Center Biosafety guidelines using an IACUC-approved Animal Use Protocol (# 2012–174). For orthotopic tumor inoculations, cells were labeled using a DiD (DiIC18(5); 1,1′-dioctadecyl-3,3,3′,3′-tetramethylindodicarbocyanine, 4-chlorobenzenesulfonate salt) cytoplasmic membrane dye; abs/em = 644/655 (Biotium, Hayward, CA) according to the manufacturer's directions. 0.5-1x10^6 cells in 3–5 μl phosphate buffered saline were injected into the right cortex of 4–6 week old CD-1 nude mice (n = 3 each). Tumor cells were imaged *in vivo* at indicated times post-injection using an IVIS Spectrum In Vivo Imaging System and Living Image Software (Perkin Elmer, Waltham, MA). Tumor volume was calculated from the formula: Volume = 0.5 x length x $width^2$. The highest and lowest numbers for calculated tumor volume in each group were excluded from analysis.

Statistical analyses

GraphPad Prism 5 software was used for all statistical analyses. Unaired student's *t*-test or one-way analysis of variance (ANOVA) with Tukey's honest significant difference (HSD) post-test was performed and an α-value of 0.05 was used as criteria for statistical significance.

CHAPTER III

META-ANALYSIS OF NCI PATIENT DATA INDICATES TWEAK AXIS EXPRESSION IS A NEGATIVE PROGNOSTIC INDICATOR

Background

Gliomas are the most common primary brain tumors in adults. High-grade gliomas, including Grade IV Glioblastoma, have an abysmal prognosis of approximately 15 months median survival [7] due to inevitable recurrence following resection, radiation, and chemotherapy [4]. High-grade gliomas can occur *de novo* or progress from lower-grade gliomas [2]. Gliomas demonstrate considerable heterogeneity of cellular origin, tumor infiltrates, differentiation status, and genomic aberrations [2, 10, 13], requiring comprehensive understanding and analysis of the multiple factors simultaneously. Additionally, clinical perspective and context are required to determine therapeutic value of basic science findings.

To address these issues, multiple initiatives to make clinical and genome-wide microarray expression data for gliomas available have been developed by the National Cancer Institute (NCI), including The Cancer Genome Atlas (TCGA) [146] and the Repository of Molecular Brain Neoplasia Data (REMBRANDT) [23]. Using expression data, the confounding heterogeneous genetics of high-grade gliomas have been addressed by principle-component analysis and hierarchical clustering to identify distinct clinically-relevant subtypes in glioblastoma [11, 24]. Hierarchical clustering of TCGA data by Verhaak et al. resulted in four distinct subtypes named by convention from the literature and gene ontology of the signatures: Classical, Mesenchymal, Neural, and Proneural [24]. These published subtype signatures have been accepted by the Broad Institute as Gene Set Enrichment Analysis signatures and made publically available (Appendix B: Table B1). From these datasets, powerful tools have become publically available to contextualize basic science research within clinical outcomes and foster translational research.

TNF-like weak inducer of apoptosis (TWEAK) is the 12th member of the TNF superfamily of cytokines with gene designation *TNSF12* [89]. TWEAK activation of its receptor FGF-inducible immediate-early response gene Number 14 (FN14, gene name *TNFRSF12A*) results in recruitment of TNF Receptor-Associated Factor 3 (TRAF3, gene name *TRAF3*) [111]. Under unstimulated conditions, TRAF3 acts as a negative regulator of constitutively active NF-κB-Inducing Kinase (NIK, gene name *MAP3K14*) and recruits an E3-ligase complex to constitutively degrade NIK [67]. NIK stabilization activates the noncanonical NF-κB pathway by IKKα activation, phosphorylation of p100 (*NFKB2*), proteolytic processing of p100 to p52, and translocation of p52-RelB heterodimers to the nucleus [97]. TRAF3 recruitment to FN14 due to TWEAK engagement eliminates TRAF3 negative regulation of NIK [96]. TWEAK is therefore a ligand that acts upon its receptor (FN14) to activate a MAP3K (NIK) by receptor-mediated engagement of a negative regulator of the MAP3K (TRAF3). We have designated this pathway the TWEAK Axis (Figure 8).

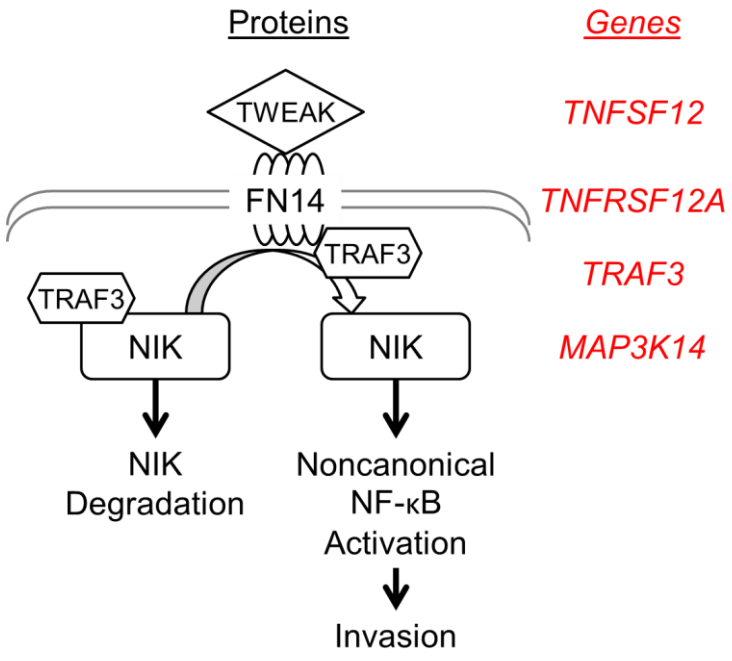

Figure 8 The TWEAK Axis. Protein names for members of the TWEAK Axis are written in black. Gene names for the corresponding genes encoding these proteins are italicized in red.

Increased TWEAK and FN14 protein levels have been recently implicated in cancer, including gliomas, though activation of NF-κB [105, 106, 116]. NF-κB is a family of evolutionarily-conserved transcription factors RelA (*RELA*), RelB (*RELB*), c-REL (*REL*), p105/p50 (*NFKB1*), and p100/p52 (*NFKB2*) that dimerize and activate gene transcription via their Rel Homology Domain (RHD). The canonical NF-κB pathway can be activated by Tumor Necrosis Factor alpha (TNFα, *TNF*) activating its receptor TNF Receptor 1 (TNFR1, *TNFSFR1A*) to activate the Inhibitor of nuclear factor Kappa-B Kinase (IKK) heteotrimeric complex (IKKα, IKKβ, IKKγ). IKKγ (*IKBKG*) acts as a scaffold for IKKα (Conserved Helix-Loop-Helix Ubiquitous Kinase *CHUK*) and IKKβ (*IKBKB*). IKKβ phosphorylates Inhibitor of Kappa-Beta alpha (IκBα, *NFKBIA*), which sequesters RelA/p50 heterodimers in the cytoplasm. Phosphorylation of IκBα triggers proteasomal-degradation of IκBα and liberation of RelA/p50 heterodimers to translocate to the nucleus and effect gene transcription. The noncanonical NF-κB pathway can be activated by TWEAK (*TNFSF12*) activating its receptor FN14 (*TNFRSF12A*), which recruits TRAF3 (*TRAF3*), (see Figure 8). Recruitment of TRAF3 to the cytoplasmic tail of FN14 removes its negative regulation of NIK (*MAP3K14*) via protein-protein interaction. Without TRAF3, NIK is able to phosphorylate and form a trimeric complex with 2 IKKα (*CHUK*) homodimers. The NIK-IKKα complex phosphorylates p100 (*NFKB2*) for partial degradation to p52. RelB (*RELB*) sequestered in the cytoplasm due to interaction with p100 is then able to form a heterodimer complex with p52, translocate to the nucleus, and effect gene transcription. c-Rel (*REL*) is able to heterodimerize with other NF-κB transcription factors, though its specific functions are poorly understood.

We have recently shown a significant biological function of TWEAK in the specific activation of noncanonical NF-κB signaling and increased invasion in high-grade glioma cells [50]. In this study, we investigate expression of TWEAK Axis genes *MAP3K14*, *TRAF3*, *TNFSF12*, and *TNFRSF12A* in patient glioma samples using a large cohort of gene expression and clinical data from NCI repositories to determine correlations with prognostic factors, NF-κB genes, and glioma subtypes.

Results

Tumor and patient clinical data is representative of glioma patients

Because of the considerable genetic and cellular complexity of gliomas as well as the dismal prognosis despite years of advances, the NCI has developed considerable initiatives to make genome-wide expression and clinical data available to basic science researchers. We sought to determine clinical relevance of the TWEAK Axis using microarray gene expression data accessed from the NCI databases TCGA and REMBRANDT [23, 146]. Probesets were background-corrected, averaged for each gene, normalized, and median-centered for each dataset. In all, 1153 samples with 883 accompanying clinical information were utilized for subsequent analysis (Appendix B: Table B2). To validate our datasets versus previous cohorts and findings, we investigated the accompanying glioma clinical data of the TCGA and REMBRANDT datasets for trends in overall survival by age, sex, grade, histologic type, and Verhaak *et al.* subtype. Median age at initial diagnosis was 56 years old, consistent with previous reports [10]. Overall survival (days to death) decreased as a function of age with the exception of poor prognosis in pediatric patients ages 10-19 (Figure 9A), which has been noted in the literature [10]. The ratio of male to female glioma patients was 1.64, consistent with previous reports [10, 147]. Overall survival was higher in female patients (Figure 9B), though this difference did not achieve statistical significance (Males: Mean 543.3, SEM 35.01, n = 329; Females: Mean 673.3, SEM 62.78, n = 202; $t(529) = 1.872$, $p = 0.062$). From one-way ANOVA with Tukey's HSD post-test, we confirmed that overall survival was significantly reduced in glioblastoma patients (Grade IV Mean 500.6, SEM 23.06, n = 562) versus lower grades (Grade II Mean 1421, SEM 153.1, n = 94, $p < 0.0001$; Grade III Mean 1251, SEM 161.3, n = 74, $p < 0.0001$), (Figure 9C). Median survival in glioblastoma was 372 days, consistent with previous reports [6]. Glioblastoma had a significantly worse overall survival (Mean 500.6, SEM 23.06, n = 562, $p < 0.0001$) versus other histological glioma types astrocytoma (Mean 1334, SEM 128, n = 111, $p < 0.0001$), oligodendroglioma (Mean 1331, SEM 227.7, n = 50, $p < 0.0001$), and mixed (Mean 1584, SEM 514.9, n = 9, $p < 0.0001$) (Figure 9D). A more

Figure 9 TCGA and REMBRANDT samples' clinical data are representative of glioma patients. (A) Overall survival stratified by age range. Data represent average overall survival in days ± SEM. **(B)** Overall survival between male and female patients. Data represent average overall survival in days ± SEM. **(C)** Overall survival stratified by tumor grade. Data represent average overall survival in days ± SEM. *$p < 0.001$ using One-way ANOVA with Tukey's HSD post-test. **(D)** Overall survival stratified by histologic type. Data represent average overall survival in days ± SEM. *$p < 0.001$ using One-way ANOVA with Tukey's HSD post-test. **(F)** Kaplan-Meier plots from microarray data, stratified by subtype. Data represent percent survival of the cohort as a function of days. C–Classical, M–Mesenchymal, N-Neural, P–Proneural. **(G)** Summary table of Kaplan-Meier survival plots by subtype. Data represent median survival in days and number of deaths per subtype. *$p < 0.05$, ***$p < 0.001$ using the Log-Rank test.

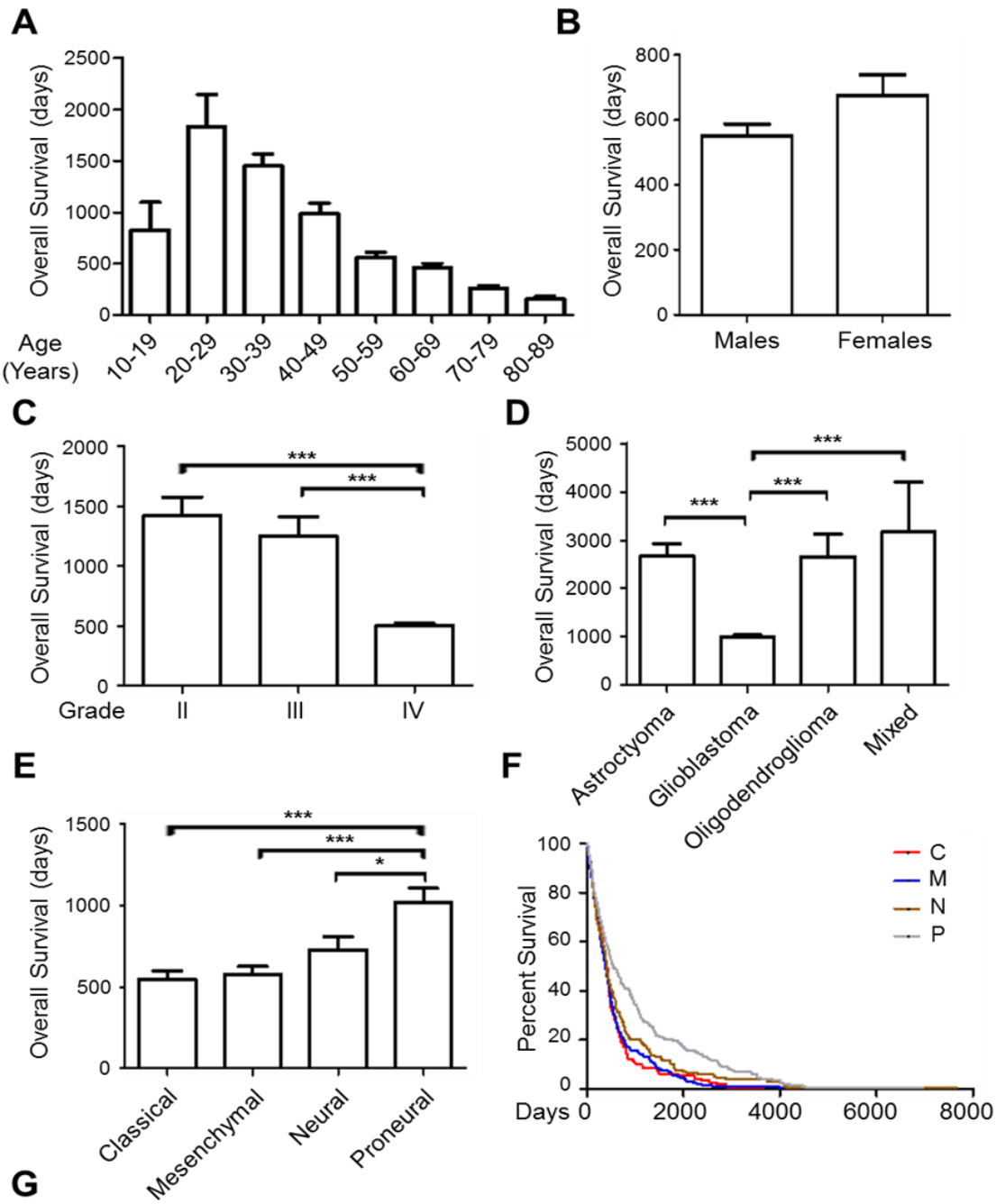

G

	Classical	Mesenchymal	Neural	Proneural	Significance
Median Survival	406 (n=147)	382 (n=228)	404 (n=154)	541 (n=179)	*N-P, ***M-P, ***C/P

Figure 9 TCGA and REMBRANDT samples' clinical data are representative of glioma patients.

favorable outcome with oligodendroglioma has been reported [10], but was not observed in our dataset. There was no significant difference in survival between glioblastoma and mixed glioma (Mean 381, SEM 537.2, n = 7).

Next, we sought to describe our dataset using recently identified glioblastoma subtypes from clustering by Verhaak *et al.* [24]. Classification of tumor samples according to Verhaak *et al.* glioblastoma subtypes was determined by calculating the percent enrichment of each subtype gene set published by Verhaak *et al.* and listed in Appendix B: Table B1. Percent enrichment was determined by counting how many of the genes in a subtype gene set were upregulated divided by the number of genes in the set. Setting the upregulation threshold at conventional 2-fold significance resulted in very low enrichment percentage scores deemed undependable. Setting the threshold to indicate any upregulation of subtype genes resulted in enrichment percentage scores determined primarily by the number of genes in the subtype classification set. Agreement in subtype classification was observed between 1.5-fold and 1.75-fold upregulation (data not shown), therefore a more-strict 1.75-fold upregulation criterion was used for calculating percent enrichment scores to classify samples by Verhaak *et al.* subtype. The classification program was verified by confirming differential expression of known subtype markers Epidermal Growth Factor Receptor (*EGFR*), Chitanse-3-Like Protein 1 (*CHI3L1*), Myelin Basic Protein (*MBP*), and Oligodendrocyte Transcription Factor 2 (*OLIG2*) (Appendix A: Figure A5). Each of the subtype markers was significantly increased in its respective subtype versus the other subtypes.

Patients in the Proneural subtype group had a significantly higher average overall survival (Mean 1021, SEM 87.1, n = 179) versus Classical subtype (Mean 549.1, SEM 51.0, n = 147, $p < 0.001$), Mesenchymal subtype (Mean 579.1, SEM 47.9, n = 228, $p < 0.001$), and Neural subtype (Mean 729.8, SEM 81.2, n = 154, $p < 0.05$) groups (Figure 9E). Further survival analysis on gliomas stratified by subtype indicated a significant difference in Kaplan-Meier survival in the Proneural subtype versus the other subtypes (Figure 9F). Median survival was greatest in the Proneural subtype group

and lowest in the Mesenchymal subtype group (Figure 9G), supporting the convention that genetic profiling of gliomas highlights different clinical entities. Together these analyses indicate that the combined TCGA and REMBRANDT dataset is representative of glioma patients and distributed equally among genetic subtypes.

The TWEAK Axis is differentially expressed in gliomas by age, grade, type, and subtype

Gender, age, grade, and histologic type have been identified as significant factors in the prognosis of gliomas [10]. Reports of stratifying tumors by subtype have proposed conflicting data whether Proneural or Mesenchymal subtypes have a poorer prognosis [11, 24]. To identify differences in TWEAK Axis expression, we compared expression of *MAP3K14*, *TRAF3*, *TNFSF12*, and *TNFRSF12A* and determined statistical relevance of TWEAK Axis expression within subsets of these prognostic indicators.

First, dataset samples were stratified by gender. There was no significant difference in expression of TWEAK Axis genes between male and female patients (data not shown).

Second, dataset samples were stratified by age at initial diagnosis (Figure 10). No significant difference in *MAP3K14* expression (Figure 10A) or *TRAF3* expression (Figure 10B) was observed between age groups. Both *TNFSF12* expression (Figure 10C) and *TNFRSF12A* expression (Figure 10D) were significantly lower in the 20-29 years and 30-39 years group versus higher age groups except for 80-89 years. *TNFSF12* and *TNFRSF12A* expression was lower in the 80-89 years group versus 40-49, 50-59, 60-69, and 70-79 years groups, though this was not significant. Sample size, average, and SEM are summarized in Figure 10E. Altogether, *MAP3K14* and *TRAF3* expression did notvary by age, but *TNFSF12* and *TNFRSF12A* expression were lowest in age ranges with the best prognosis (see Figure 9A).

Third, dataset samples were stratified by histologic grade (Figure 11). Stratification by grade indicated a significant increase in expression of *MAP3K14* (Figure 11A), *TNFSF12* (Figure 11C), and *TNFRSF12A* (Figure 11D) in glioblastomas

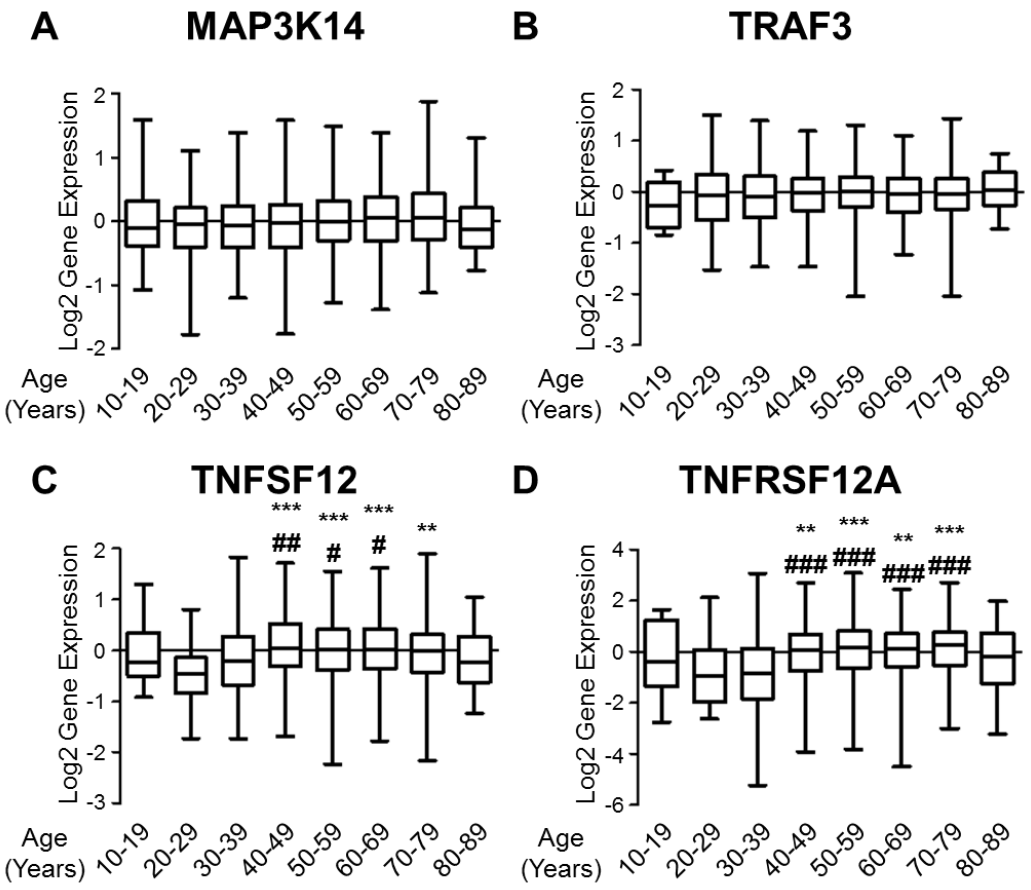

E

Age Range	Samples	MAP3K14	TRAF3	TNFSF12	TNFRSF12A
10-19	n=10	-0.012 ± 0.224	-0.220 ± 0.146	-0.074 ± 0.216	-0.276 ± 0.464
20-29	n=35	-0.108 ± 0.092	-0.054 ± 0.110	-0.462 ± 0.097	-0.871 ± 0.209
30-39	n=119	-0.054 ± 0.045	-0.109 ± 0.055	-0.218 ± 0.061	-0.855 ± 0.129
40-49	n=136	-0.022 ± 0.044	-0.062 ± 0.042	0.087 ± 0.058	-0.023 ± 0.110
50-59	n=227	0.029 ± 0.033	-0.001 ± 0.031	0.028 ± 0.040	0.062 ± 0.078
60-69	n=202	0.037 ± 0.033	-0.053 ± 0.032	0.019 ± 0.040	-0.025 ± 0.081
70-79	n=126	0.070 ± 0.045	-0.044 ± 0.046	-0.021 ± 0.055	0.128 ± 0.096
80-89	n=27	-0.056 ± 0.092	0.023 ± 0.077	-0.179 ± 0.107	-0.315 ± 0.260

Figure 10 Expression of TWEAK Axis genes stratified by age range. (A) *MAP3K14*, **(B)** *TRAF3*, **(C)** *TNFSF12*, and **(D)** *TNFRSF12A* expression values from microarray data. Data represent median log2 expression with boxes indicating upper and lower quartile and whiskers indicating range. **p < 0.01, ***p < 0.001 relative to 20-29 years; #p < 0.05, ##p < 0.01, ###p < 0.001 relative to 30-39 years using Kruskal-Wallis test with Dunn's post-test. **(E)** Summary table of TWEAK Axis expression within age groups. Data represent average log2 expression ± SEM.

(Grade IV) versus Grade II gliomas. *TRAF3* expression was not significantly different between groups (Figure 11B). A significant increase in *TNFSF12* expression was observed between Grade III gliomas and Grade IV gliomas (Figure 11C). *TNFRSF12A* expression in Grade III gliomas was significantly increased versus Grade II gliomas (Figure 11D). Sample size, average, and SEM are summarized in Figure 11E. Together these data indicate a progressive increase in *TNFSF12* and *TNFRSF12A* expression with increasing glioma grade.

Fourth, samples were stratified by histologic type (Figure 12). Stratification by histologic type indicated a significant increase in expression of *MAP3K14* (Figure 12A), *TNFSF12* (Figure 12C), and *TNFRSF12A* (Figure 12D) in glioblastomas (Grade IV) versus oligodendrogliomas. *TNFSF12* expression was also significantly different between astrocytomas and oligodendrogliomas (Figure 12C). No significant difference in *TRAF3* expression was observed between histologic types (Figure 12B). *TNFSF12* and *TNFRSF12A* expression was significantly increased in glioblastomas versus astrocytomas (Figure 12C, D). Additionally, there was a significant increase in *TNFRSF12A* expression in oligodendrogliomas versus mixed gliomas (Figure 12D). Sample size, average, and SEM are summarized in Figure 12E. Together, these data indicate increased expression of TWEAK Axis Genes in astrocytic-lineage cancers versus pure oligodendrogliomas.

Finally, samples were stratified into the four glioblastoma subtypes proposed by Verhaak *et al.* 2010 [24] (Figure 13). Stratification by Verhaak *et al.* subtype demonstrated considerable variability in expression of the TWEAK Axis genes. *MAP3K14* was comparable between Classical and Mesenchymal subtypes as well as between Neural and Proneural subtypes (Figure 13A). *MAP3K14* expression was significantly higher in both Classical and Mesenchymal versus Neural and Proneural subtypes (Figure 13A). *TRAF3* expression was highest in the Neural subtype, with median expression indicating slight upregulation of *TRAF3* (Figure 13A). Surprisingly, *TRAF3* expression was significantly different between all subtypes except for Classical and Proneural subtypes (Figure 13B). *TNFSF12* expression was the most variable of the

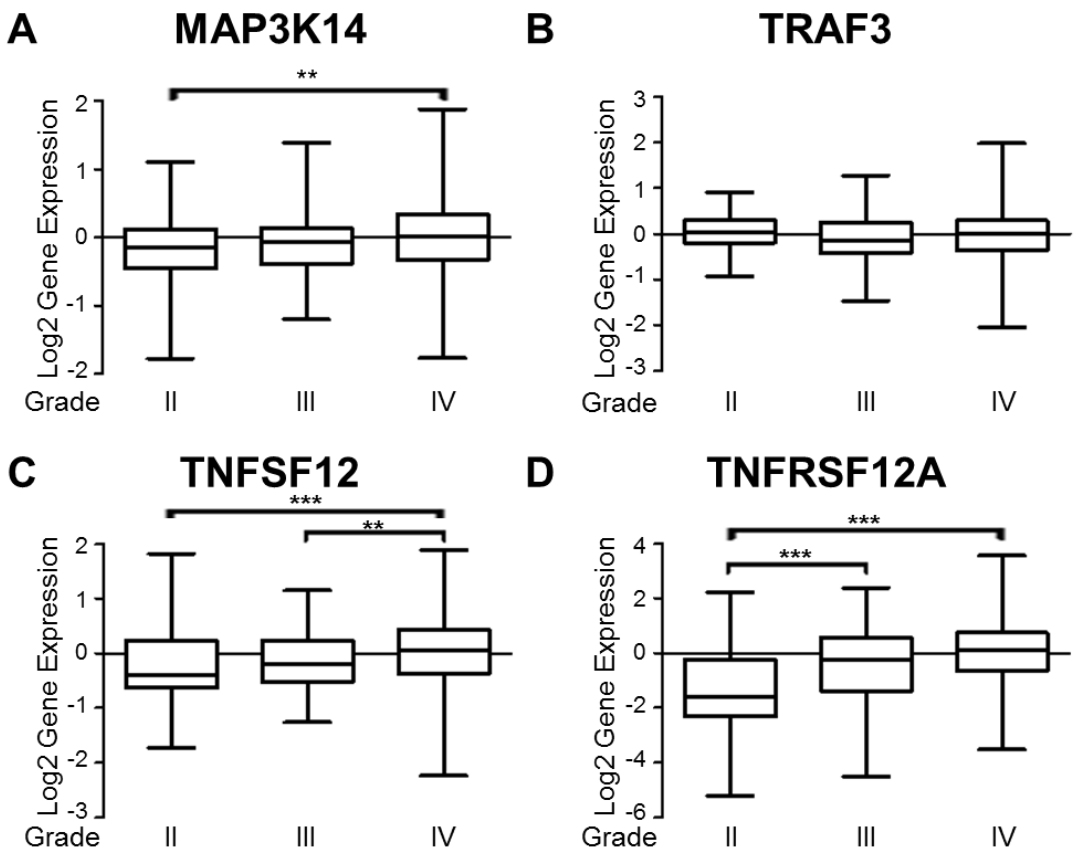

E

Grade	Samples	MAP3K14	TRAF3	TNFSF12	TNFRSF12A
II	n=98	-0.163 ± 0.045	0.029 ± 0.040	-0.152 ± 0.074	-1.349 ± 0.154
III	n=88	-0.059 ± 0.049	-0.089 ± 0.054	-0.148 ± 0.060	-0.3785 ± 0.161
IV	n=768	0.024 ± 0.018	-0.026 ± 0.019	0.037 ± 0.022	0.033 ± 0.041

Figure 11 Expression of TWEAK Axis genes stratified by tumor grade. (A) *MAP3K14*, **(B)** *TRAF3*, **(C)** *TNFSF12*, and **(D)** *TNFRSF12A* expression values from microarray data. Data represent median log2 expression with boxes indicating upper and lower quartile and whiskers indicating range. **p < 0.01, ***p < 0.001 using Kruskal-Wallis test with Dunn's post-test. **(E)** Summary table of TWEAK Axis expression within tumor grade. Data represent average log2 expression ± SEM.

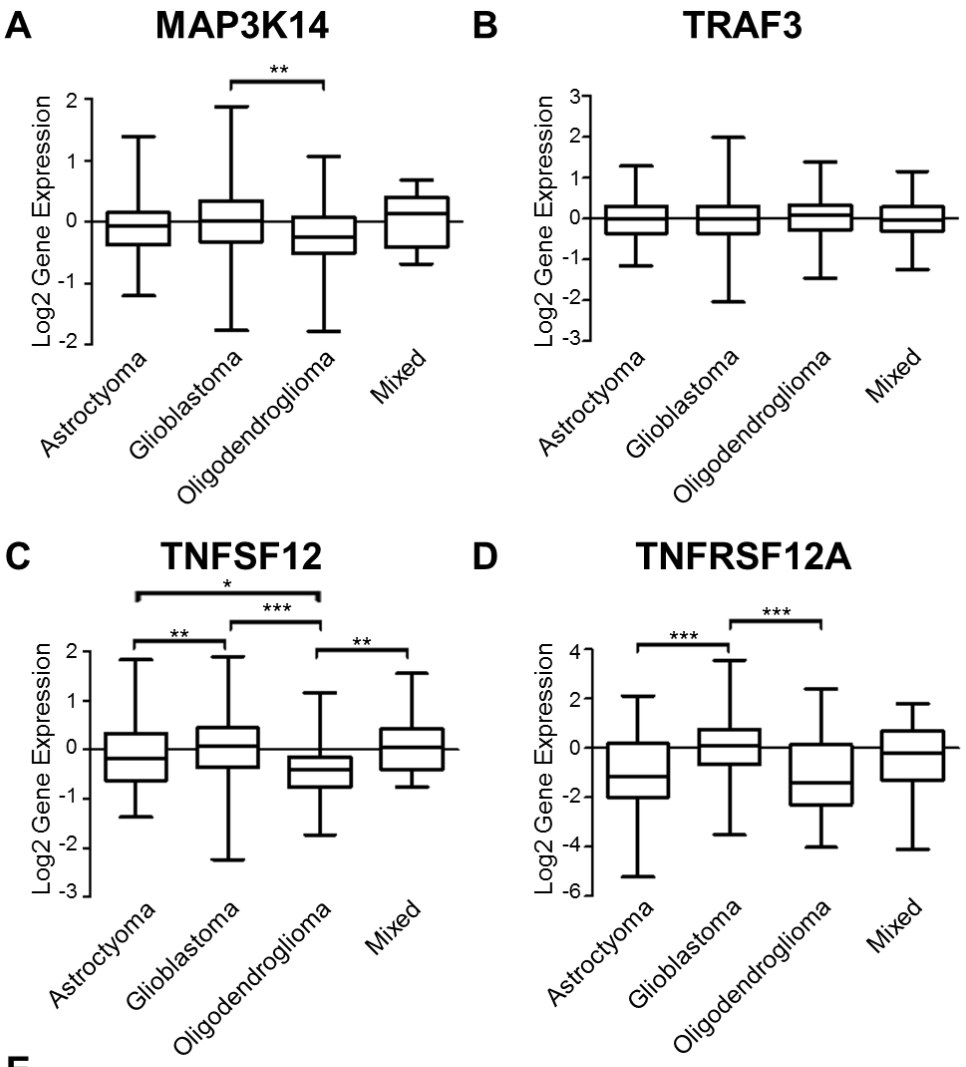

E

Type	Samples	MAP3K14	TRAF3	TNFSF12	TNFRSF12A
Astrocytoma	n=141	-0.069 ± 0.038	-0.006 ± 0.038	-0.098 ± 0.056	-0.962 ± 0.128
Glioblastoma	n=768	0.024 ± 0.018	-0.026 ± 0.019	0.037 ± 0.022	0.033 ± 0.041
Oligodendroglioma	n=65	-0.210 ± 0.059	0.042 ± 0.064	-0.397 ± 0.070	-1.135 ± 0.201
Mixed	n=20	0.041 ± 0.097	-0.011 ± 0.117	0.122 ± 0.134	-0.375 ± 0.339

Figure 12 Expression of TWEAK Axis genes stratified by histologic type. (A) *MAP3K14*, **(B)** *TRAF3*, **(C)** *TNFSF12*, and **(D)** *TNFRSF12A* expression values from microarray data. Data represent median log2 expression with boxes indicating upper and lower quartile and whiskers indicating range. *$p < 0.05$, **$p < 0.01$, ***$p < 0.001$ using Kruskal-Wallis test with Dunn's post-test. **(E)** Summary table of TWEAK Axis expression within histologic type. Data represent average log2 expression ± SEM.

TWEAK Axis and statistically significant different between all subtypes (Figure 13C). *TNFSF12* expression was highest in the Mesenchymal subtype, decreasing in the Neural, Classical, and Proneural subtypes. Similar to the trend seen in *MAP3K14* expression, *TNFRSF12A* expression was significantly higher in both Classical and Mesenchymal versus Neural and Proneural subtypes (Figure 13D). Sample size, average, and SEM are summarized in Figure 13E. Overall, gene expression levels of the TWEAK Axis were highest in the Mesenchymal subtype, comparable between the Mesenchymal and Classical subtypes, and lowest in the Proneural subtype.

Expression of the TWEAK Axis correlates with canonical and noncanonical NF-κB expression

Aberrant NF-κB signaling has been widely implicated in glioma, though the majority of studies focus on the canonical NF-κB pathway. Our lab has shown that noncanonical NF-κB signaling contributes to glioma proliferation, differentiation, and invasion [49]. It has become apparent that both NF-κB pathways must be considered in glioma. To elucidate roles of both pathways in TWEAK Axis signaling, gene expression values for *MAP3K14*, *TRAF3*, *TNFSF12*, and *TNFRSF12A* were correlated with gene expression values of NF-κB genes from both pathways (Table 1). Most comparisons indicated significant but very weak or weak correlations between TWEAK Axis genes and NF-κB genes. *TRAF3* was only very weakly correlated with NF-κB genes. All four TWEAK Axis genes were more positively correlated with *RELB* expression than *RELA* expression. Expression of *MAP3K14* and *TNFSF12* only weakly correlated with *RELB* expression, whereas *TNFRSF12A* expression moderately correlated with *RELB* expression. Additionally, expression of the four TWEAK Axis genes correlated more positively with expression of *IKBKB* and *NFKB1* than *CHUK* and *NFKB2* expression. *MAP3K14* and *TNFRSF12A* expression had moderate correlation with *IKBKB* expression and weak correlation with *NFKB1* expression. Within the TWEAK Axis, *TNFRSF12A* expression had weak correlation with *MAP3K14* expression. *TNFSF12* and its receptor *TNFRSF12A* were weakly correlated. TWEAK Axis expression was also

Figure 13 Expression of TWEAK Axis genes stratified by glioblastoma subtype. (A) *MAP3K14,* **(B)** *TRAF3,* **(C)** *TNFSF12,* and **(D)** *TNFRSF12A* expression values from microarray data. Data represent median log2 expression with boxes indicating upper and lower quartile and whiskers indicating range. *p < 0.05, **p < 0.01, ***p < 0.001 using Kruskal-Wallis test with Dunn's post-test. **(E)** Summary table of TWEAK Axis expression within glioblastoma subtype. Data represent average log2 expression ± SEM.

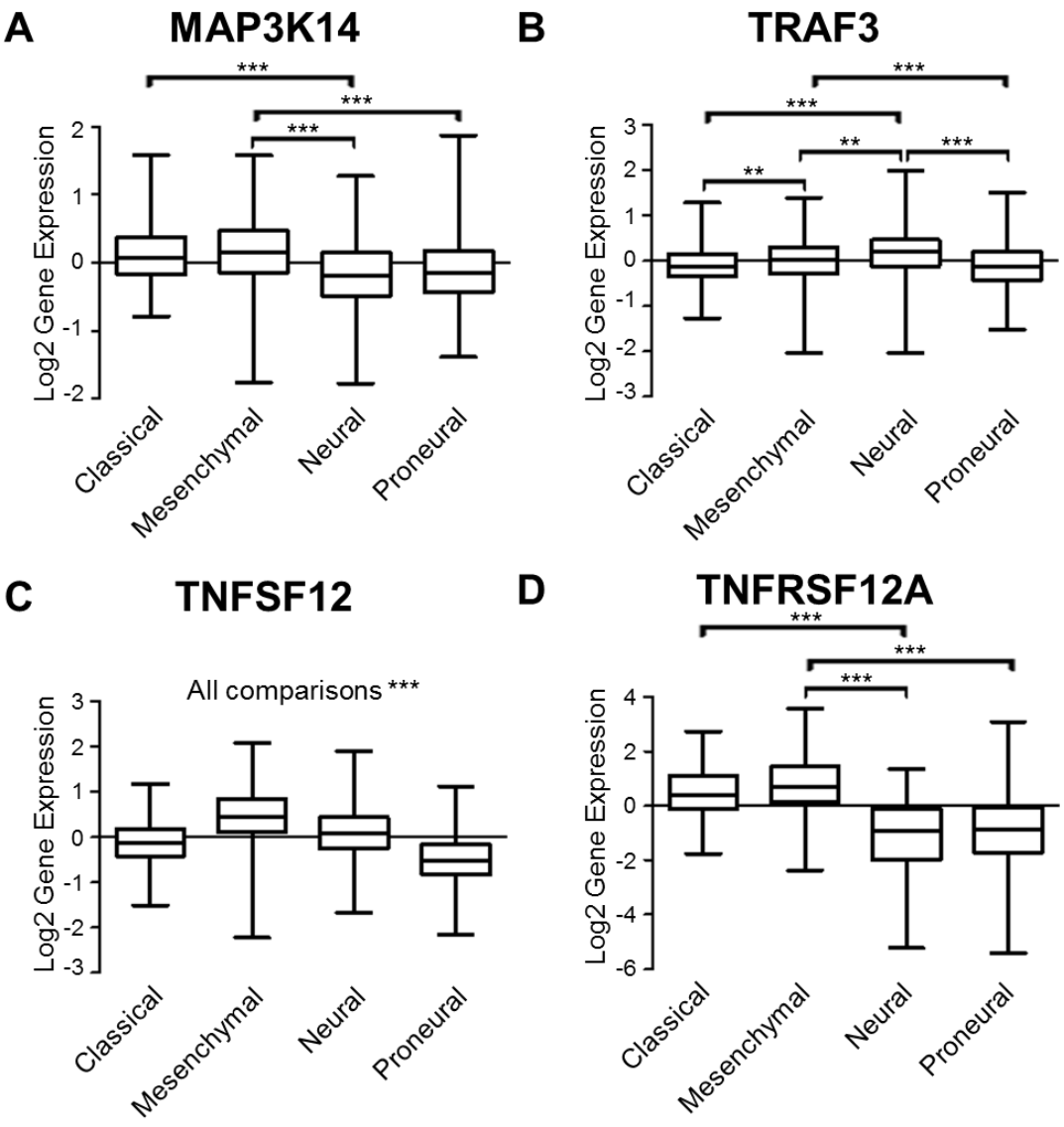

E

Subtype	Samples	MAP3K14	TRAF3	TNFSF12	TNFRSF12A
Classical	n=217	0.106 ± 0.029	-0.105 ± 0.028	-0.136 ± 0.028	0.451 ± 0.058
Mesenchymal	n=348	0.165 ± 0.026	0.022 ± 0.024	0.466 ± 0.031	0.726 ± 0.053
Neural	n=251	-0.163 ± 0.032	0.135 ± 0.034	0.096 ± 0.034	-1.052 ± 0.078
Proneural	n=306	-0.124 ± 0.026	-0.129 ± 0.029	-0.501 ± 0.029	-0.920 ± 0.073

Figure 13 Expression of TWEAK Axis genes stratified by glioblastoma subtype.

Table 1 Spearman's ρ-values for TWEAK Axis and NF-κB gene expression

NF-κB Gene	Protein (C/NC)	MAP3K14	TRAF3	TNFSF12	TNFRSF12A
REL	c-Rel	0.166***	0.120***	0.272	0.150***
RELA	RelA - C	0.266***	-0.146***	-0.010	0.238***
RELB	RelB - NC	0.376***	0.145***	0.398***	0.528***
NFKB1	p105/p50 - C	0.331***	0.136***	0.285***	0.383***
NFKB2	p100/p52 - NC	0.236***	-0.149***	0.180***	0.268***
CHUK	IKKα – C, NC	-0.081**	0.139***	-0.064*	-0.091**
IKBKB	IKKβ - C	0.410***	-0.104***	0.264	0.410***
IKBKG	IKKγ - C	0.151***	-0.019	0.150***	0.132***
NFKBIA	IκBα - C	0.245***	0.026	0.187***	0.083**
MAP3K14	NIK - NC	1.000***	-0.133	0.153***	0.318***
TNF	TNFα – C, NC	0.112***	0.085**	0.230***	-0.070*
TNFRSF1A	TNFR1 – C, NC	0.422***	-0.065*	0.487***	0.720***
TNFSF12	TWEAK – C, NC	0.153***	0.064*	1.000***	0.288***
TNFRSF12A	FN14 – C, NC	0.318***	-0.148***	0.288***	1.000***

NF-κB pathways: C–Canonical NF-κB, NC–Noncanonical NF-κB; *p < 0.05, **p < 0.01, ***p < 0.001

correlated with expression of *TNF* and its receptor *TNFRSF1A*. Correlation was weak between *TNFSF12* and *TNF* expression. There was a strong correlation between *TNFSF12A* and *TNFSF1A* expression, consistent with reports that FN14 and TWEAK are induced by tissue damage [102]. Together, these data indicate a complex relationship in the expression and regulation of NF-κB genes and the TWEAK Axis.

Expression of the TWEAK Axis correlates with mesenchymal GBM subtype

We have demonstrated that TWEAK signaling activates of the noncanonical NF-κB pathway [50] (see Figure 4) and that noncanonical NF-κB transcriptional activity control expression of Mesenchymal subtype gene *CHI3L1* and Proneural subtype gene *OLIG2* in high-grade gliomas [49]. To explore context of TWEAK signaling in glioma subtypes, gene expression values for *MAP3K14*, *TRAF3*, *TNFSF12*, and *TNFRSF12A* were correlated with gene expression values for major markers identified within Classical, Mesenchymal, Neural, and Proneural subtype genes (Table 2) categorized by Phillips *et al.* and Verhaak *et al.* [11, 24]. TWEAK Axis genes were only very weakly correlated with Classical subtype marker *EGFR*. *MAP3K14*, *TRAF3*, and *TNFSF12* had a very week correlation with Neural subtype maker *MBP*. *TNFRSF12A* correlation with *MBP* was negative and weak. Of the genes selected for correlation, *MAP3K14*, *TNFSF12*, and *TNFRSF12A* were most positively correlated with expression of the Mesenchymal subtype gene *CHI3L1*. *MAP3K14* was weakly correlated with *CHI3L1* and Collagen Type 1 α1 (*COL1A1*) and only very weakly correlated with other Mesenchymal subtype genes. *TRAF3* was only very weakly correlated with glioma genes from the subgroups except for a weak negative correlation with Sex-determining-region Y-Box 2 (*SOX2)*. Of the four TWEAK Axis genes, *TNFRSF12A* expression was most positively correlated with Mesenchymal subtype genes *MET*, *CHI3L1*, and *COL1A1* as well as pro-invasive marker *MMP9*. Both *TNFSF12* and *TNFRSF12A* had a low correlation with *MET*. Expression of *TNFRSF12A* was moderately correlated with *RELB* and strongly correlated with *TNFRSF1A* (see Table 1), both of which have been identified as upregulated in the Mesenchymal subtype [24]. *TNFSF12* had a moderate negative correlation with *OLIG2* and a weak negative correlation with *SOX2*, both of which are Proneural subtype markers. Together, these data indicate that TWEAK Axis expression correlate more positively with expression of Mesenchymal subtype genes than Classical, Neural, or Proneural subtype genes.

Table 2 Spearman's ρ-values for TWEAK Axis and subtype expression

Gene	Protein (C/M/N/P)	MAP3K14	TRAF3	TNFSF12	TNFRSF12A
EGFR	EGFR - C	0.151***	-0.115***	-0.052	0.035
MET	c-MET (HGFR) - M	-0.016	0.084**	0.305***	0.315***
CHI3L1	CHI3L1/YKL40 - M	0.331***	--0.058	0.473***	0.688***
MBP	MBP - N	-0.153***	0.195***	0.145***	-0.295***
SOX2	SOX2 - P	0.107***	-0.297***	-0.432***	-0.116***
OLIG2	OLIG2 - P	-0.164***	-0.085**	-0.378***	-0.305***
COL1A1	Collagen Type 1 α1 - M	0.236***	0.055	0.292***	0.535***
MMP9	MMP9 - Invasion	0.138***	-0.021	0.135***	0.423***

Markers for: C-Classical, M-Mesenchymal, N-Neural, P-Proneural; *p < 0.05, **p < 0.01, ***p < 0.001

Increased MAP3K14, TNFSF12, and TNFRSF12A expression negatively impacts survival

We have demonstrated that overexpression of NIK is sufficient to increase tumor volume in mice (See Figure 6). Additionally, previous data have shown high FN14 levels are a negative prognostic factor [105]. We therefore investigated whether expression of *MAP3K14*, *TRAF3, TNFSF12,* or *TNFRSF12A* in the NCI datasets correlated with patient outcome. Patient samples with accompanying clinical information including overall survival (n = 879 samples) were ranked by gene expression of the TWEAK Axis genes. For each gene, samples were divided into quartiles (n = 220 per group) and overall survival values within each quartile were graphed using Kaplan-Meier survival curves (Figure 14). Overall survival was significantly improved in *MAP3K14* between the lowest and highest quartile (Figure 14A). Although survival and *TRAF3* trended more positively by increased quartile (Figure 14B), there was no significant difference between quartiles. The lowest quartile

of *TNFSF12* expression had a significantly better overall survival versus each of the other quartiles (Figure 14C). Similarly, the lowest quartile of *TNFRSF12A* expression had a significantly better overall survival versus each of the other quartiles (Figure 14D), as well as significantly better overall survival between the second and fourth quartile. In general, increased expression of TWEAK Axis genes by quartile reflected a decrease in median survival (Figure 14E). From these data, patients with higher expression of *MAP3K14*, *TNFSF12*, and *TNFRSF12A* had a worse overall survival than patients with lower expression, suggesting a negative prognostic role for TWEAK Axis in the clinical outcome of glioma patients.

Discussion

Increased expression and activation of the noncanonical NF-κB has been identified in high-grade gliomas and shown to increase proliferation and invasion. However, noncanonical NF-κB-specific extracellular signals in autocrine, juxtacrine, or paracrine signaling within a brain tumor are not well-understood. We have shown that extracellular TWEAK can activate the noncanonical NF-κB pathway and increase invasion [50]. Whether this significant biological response is relevant in a clinical context is not clear. We show that clinical and microarray data in NCI-curated databases TCGA and REMBRANDT are representative of patient demographics and prognosis (Figure 9) and represent a *bona fide* clinical cohort for our analysis of the TWEAK AXIS at the gene and clinical levels.

Interestingly, we observed that of the TWEAK Axis genes, the ligand TWEAK (*TNFSF12)* and its receptor FN14 (*TNFRSF12A)* are the most differentially expressed among tumor samples and were expressed lowest in groups with better prognoses. *TNFSF12* and *TNFRSF12A* expression was lowest in the younger non-pediatric age groups with better prognosis (Figure 10C, D). *TNFSF12* and *TNFRSF12A* expression increased with progressive tumor grade (Figure 11C, D). In addition to increasing with grade, *TNFSF12* and *TNFRSF12A* expression was higher in glioblastoma versus lower-grade gliomas (Figure 11C,D, Figure 12C,D), indicating that expression of *TNFSF12*

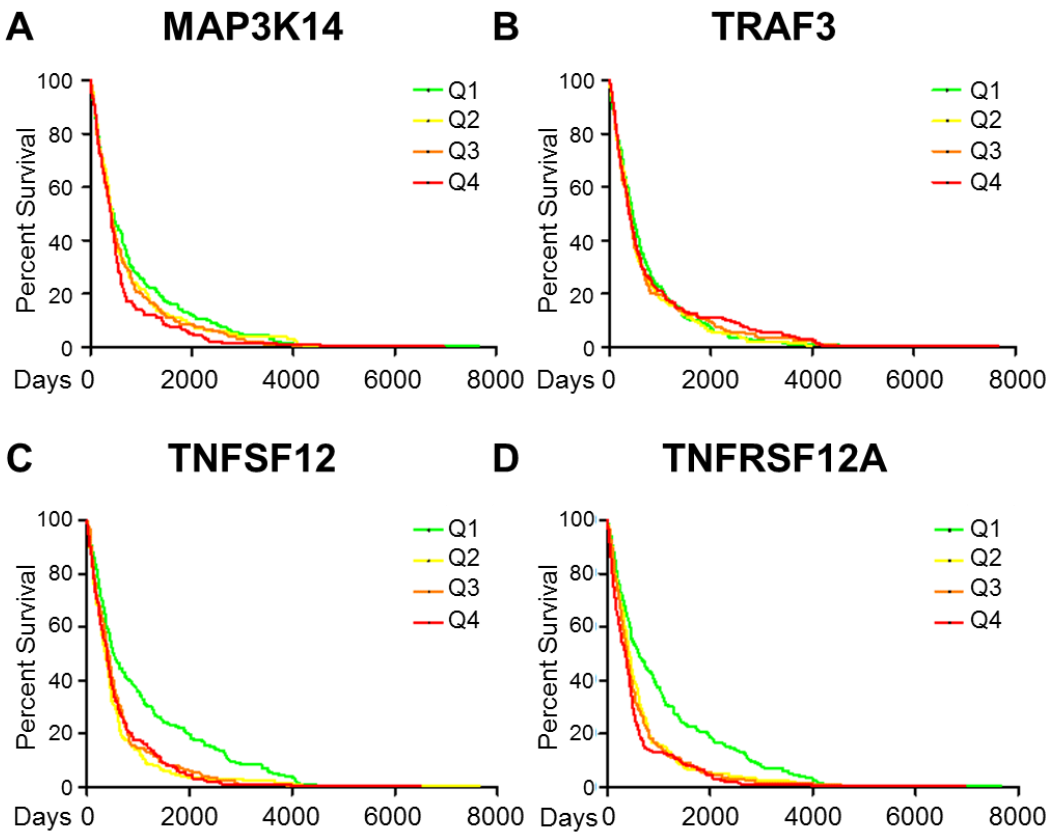

E

Gene	Q1 Median	Q2 Median	Q3 Median	Q4 Median	Significance
MAP3K14	454 (n=175)	438 (n=185)	411.5 (n=174)	406 (n=174)	**Q1-Q4
TRAF3	458 (n=186)	406 (n=176)	410 (n=178)	393 (n=168)	
TNFSF12	517 (n=176)	369 (n=171)	430 (n=179)	401 (n=182)	***Q1-Q2, Q1-Q3, Q1-Q4
TNFRSF12A	611(n=177)	427 (n=178)	383 (n=168)	346 (n=184)	***Q1-Q2, Q1-Q3, Q1-Q4 *Q2-Q4

Figure 14 Overall survivals within quartiles of TWEAK Axis gene expression. (A) *MAP3K14*, **(B)** *TRAF3*, **(C)** *TNFSF12*, and **(D)** *TNFRSF12A* Kaplan-Meier plots from microarray data, stratified by quartile. Data represent percent survival of the cohort as a function of days. **(E)** Summary table of TWEAK Axis Kaplan-Meier survival plots by quartile. Data represent median survival in days and number of deaths per quartile. *$p < 0.05$, **$p < 0.01$, ***$p < 0.001$ using the Log-Rank test.

and *TNFRSF12A* may be closely related to gliomagenesis and tumor progression. High-grade gliomas have higher incidence at later age groups, which may account for some of the prognostic indications between *TNFSF12* and *TNFRSF12A* expression in patient age and tumor grade. In contrast, *MAP3K14* expression was only differentially expressed in Grade IV Mesenchymal subtype gliomas (Figure 11A, Figure 13A). While overexpression of *MAP3K14* may be rarely observed in early pathogenesis of gliomas, normal levels of NIK mRNA for constitutive translation may still be important in later progression of gliomas as reflected by a significantly poorer survival in the highest quartile of *MAP3K14* expression (Figure 14A). Extrinsic dependence on TWEAK to activate cell signaling may therefore be an earlier or more significant event than increased intrinsic activity of the cells by overexpressing NIK. Taken together, this highlights therapeutic potential for targeting interactions of TWEAK and FN14.

Both the canonical and noncanonical NF-κB pathways can be activated by TWEAK depending on whether TWEAK is membrane-bound or soluble at high or low concentrations [94]. We show that *MAP3K14*, *TNFSF12*, and *TNFRSF12A* correlate with both canonical and noncanonical NF-κB genes (Table 1), though their biological significance is unclear. Expression of *MAP3K14*, *TNFSF12*, and *TNFRSF12A* was more strongly correlated with noncanonical NF-κB transcription factor *RELB* than either *REL* or canonical NF-κB transcription factor *RELA*. *RELB* expression has been shown as enriched in the invasive Mesenchymal subtype [24] and increased protein levels increase glioma invasion [49, 50]. The strongest correlation was between *TNFRSF1* and *TNFRSF12A* expression ($\rho = 0.720$). The interaction between TWEAK and TNF signaling and their receptors has been recently studied in induction of keratinocyte apoptosis [148], though induction of *TNFRSF1* and *TNFRSF12A* expression by their ligands has not been demonstrated in glioma. More direct analysis will be required to determine whether this correlation is through biologic signaling of TWEAK and TNFα or due to differential expression of *TNFRSF1* and *TNFRSF12A* within enrichment of mesenchymal genes.

Finally, correlation of TWEAK Axis genes with Verhaak *et al*. subtype genes and stratification of tumor samples by subtype provided key insight into differential expression of the TWEAK Axis. Prominent genes *EGFR* from the Classical subtype and *OLIG2* from the Neural subtype correlated only weakly with TWEAK Axis expression (see Table 2). *TNFSF12* and *TNFRSF12A* correlated negatively with Proneural markers *OLIG2* and *SOX2*, indicating that TWEAK signaling is distinctly downregulated in the Proneural subtype. In comparison to *EGFR*, *OLIG2*, and *SOX2*, *TNFSF12* and *TNFRSF12A* were more positively correlated with the Mesenchymal subtype gene *MET*, an oncogene often amplified in glioblastoma and associated with invasion [11, 149]. Moderate gene expression correlations between mesenchymal genes and *TNFSF12* and *TNFRSF12A* indicate that TWEAK and its receptor are differentially expressed in the mesenchymal subtype. Moderate to strong correlation was observed between *TNFSF12* and *TNFRSF12A* and the well-studied mesenchymal marker *CHI3L1*, which we have shown is regulated by RelB in glioma [49]. The aggressive invasive and recurrent natures of the Mesenchymal glioma subtype present considerable obstacles in improving outcome for glioma patients. *TNFSFR12* was moderately correlated with expression of *MMP9*, a well-studied marker for invasion and poor prognosis in cancer [39]. TWEAK has been shown to induce *MMP9* expression, and this may be primarily dependent on expression and activation of its receptor [95]. Additionally, *TNFRSF12A* expression moderately correlated with expression of *COL1A1*, a pathological substrate in brain tumors that facilitates invasion in the brain [47].

Subtype analysis revealed that *MAP3K14* and *TNFRSF12A* expression were comparable between Classical and Mesenchymal subtypes and between Neural and Proneural subtypes, though interestingly expression was significantly different than each subtype in the other pair (see Figure 13). These “tiers” may represent increasing *MAP3K14* and *TNFRSF12A* expression in less differentiated tumors. *TNFSF12* expression was highest in the Mesenchymal subtype group and significantly differentially-expressed between all subtype groups. This could reflect either a role for TWEAK signaling in maintaining distinct subtypes or that the subtype genetic landscape

of tumors predisposes the tumors to TWEAK signaling. In contrast to Mesenchymal subtype tumors, Proneural subtype tumors reflected the greatest survival (see Figure 9), which may indicate initial tumors versus recurrent tumors that relapse as mesenchymal [11]. Additionally, Proneural subtype tumors had the lowest *TNFSF12* and *TNFRSF12A* expression of the four subtypes, the second-lowest *MAP3K14* expression, and the highest expression of *TRAF3* (see Figure 13). These data are consistent with increased survival in the low quartiles of *MAP3K14*, *TNFSF12*, and *TNFRSF12A* and the highest quartiles of *TRAF3* (see Figure 14). Altogether, these data suggest that the TWEAK Axis is differentially expressed and most relevant in a subset of more-fatal tumors, supporting anti-TWEAK therapy as a more viable strategy in the treatment of high-grade gliomas than low-grade gliomas.

Conclusion

Here, we report a modest but statistically significant increase in TWEAK Axis gene expression within subsets of tumors with poorer prognosis. Specifically, we demonstrate that statistical analysis of *MAP3K14*, *TRAF3*, *TNFSF12*, and *TNFRSF12A* in a validated dataset indicated differential expression of *MAP3K14*, *TNFSF12*, and *TNFRSF12A* in groups stratified by prognostic indicators including age at diagnosis, tumor grade, tumor histologic type, and glioma subtype. *MAP3K14*, *TNFSF12*, and *TNFRSF12A* were more highly expressed in groups of these factors associated with poorer prognosis. Moreover, Kaplan-Meier survival analysis determined that groups with increased expression of these genes had significantly decreased survival. *MAP3K14*, *TNFSF12*, and *TNFRSF12A* expression correlated most positively with NF-κB signaling genes *IKBKB*, *RELB*, and *TNFRSF1A* as well as mesenchymal subtype genes *CHI3L1* and *COL1A1*. The TWEAK Axis was differentially expressed in glioma subtypes and most enriched in the Mesenchymal subtype. Our findings provide a compelling rationale for investigating inhibition of the TWEAK Axis as a viable therapeutic strategy in the treatment of high-grade invasive gliomas, particularly in the Mesenchymal subtype.

Methods

Datasets

Raw and processed samples files were downloaded from the TCGA Data Portal and ArrayExpress Archive. Dataset sources, glioma grade, numbers of samples, sample platforms, and normalization/scaling methods are summarized in Appendix B: Table B2. All files were loaded into GeneSpring GX software (Agilent Technologies, Santa Clara CA) for analysis. Data from each platform were normalized and centered separately. Probesets for the Affymetrix platform were normalized using Robust Multichip Analysis (RMA) [150]. Probesets for the Agilent two-color platform were normalized using Locally Weighted Scatterpoint Smoothing (LOWESS) [151]. Probesets were averaged for each gene. Gene-level expression values were transformed to 2-based logarithm scale and baseline transformed around the median for each dataset using GeneSpring GX software. Gene expression values for replicate patient samples within a technology were averaged. Entrez Gene ID was used to match genes between microarray technologies. Entrez Gene IDs are listed in Appendix B: Table B3.

Determination of Verhaak subtype for glioma samples

Samples were classified by GSEA according to Classical-Mesenchymal-Neural-Proneural glioblastoma subtype genes published by Verhaak *et al.* [24] and listed in Appendix B: Table B1 using an R script (available on request). In short, each gene in the subtype list that was expressed above a threshold of log2-base value of 0.807 (1.75-fold upregulated) was counted. Each patient sample was assigned an enrichment percentage score for each subtype based on the percentage of genes in each subtype list that were upregulated. Samples were designated as Classical, Mesenchymal, Neural, or Proneural determined by the highest subtype percentage score.

Statistical analysis for gene expression and overall survival

GraphPad Prism 5 software was used for all statistical analyses. Mann-Whitney U or Kruskal-Wallis with Dunn's post-test was used to assess statistical significance between

log2-base gene expression data. Survival data in months was converted to days by multiplying by 30.4, the average number of days per month. Unpaired student's *t*-test or One-way analysis of variance (ANOVA) with Tukey's Honest Significant Difference (HSD) post-test was performed to establish statistical significance for days to death survival analysis. An α-value of 0.05 was used as criteria for statistical significance.

Correlation for gene expression

Correlation values between genes were determined using Spearman's rank correlation coefficient (ρ). Correlations were described using the Evans convention [152]: very weak ($0 \leq \rho < 0.2$), weak ($0.2 \leq \rho < 0.4$), moderate ($0.4 \leq \rho < 0.6$), strong ($0.6 \leq \rho < 0.8$), or very strong ($0.8 \leq \rho \leq 1$). An α-value of 0.05 was used as criteria for statistical significance.

Kaplan-Meier survival analysis

Gene expression values for samples with clinical data were ranked and grouped by quartile (n = 220 per group). Patient mortality events within each quartile were used to generate Kaplan-Meier curves were generated in GraphPad Prism 5. Statistical significance between curves was determined using the Log-Rank (Mantel-Cox) Test. An α-value of 0.05 was used as criteria for statistical significance.

CHAPTER IV

CONCLUSIONS AND RECOMMENDATIONS

Due to our limitations of understanding the complex nature of high-grade gliomas, the prognosis with current aggressive conventional therapy of maximal resection, high-dose radiation, and chemotherapy is still an abysmal 15 months median survival. Improvements in temozolomide chemotherapy and radiation have meagerly improved the prognosis by a few months [6]. Thus, high-grade gliomas are one of the most deadly incurable forms of cancers. Sophisticated gene-array and statistical analyses aiming to account for and understand clinically-relevant mutations and differential expression have increased rather than decreased the perceived complexity of high-grade gliomas [11, 13, 22, 24]. To this end, we believe pathways identified to be clinically relevant to high-grade gliomagenesis must be evaluated biologically to understand molecular contributions of these genes and proteins in the phenotype of glioma. From the greater scope of research that precedes it, we have focused our efforts on advancing a molecular-biology understanding of the noncanonical NF-κB pathway and its activation by TWEAK in glioma invasion. Although understanding of NF-κB in the pathogenesis of high-grade gliomas has been developed following decades of insight into canonical-NF-κB signaling, we show in this work that noncanonical NF-κB is differentially expressed in invasive glioma cells and can be specifically activated by extracellular signals to promote invasion. From this, we provide a rationale for considering both the canonical and noncanonical NF-κB pathways in determining targets for new glioma therapy. We then expanded on this molecular knowledge by evaluating the clinical correlations with genes in the expression and receptor-mediated induction of TWEAK to show that expression of TWEAK, FN14, and NIK are increased in gliomas with poorer prognosis. The questions addressed in this dissertation are:

- How does upstream and extracellular activation of the noncanonical NF-κB pathway affect glioma invasion and tumorigenesis?
- What is the clinical context for expression of TWEAK-Axis genes?

This dissertation contributes new findings for glioma:

- The noncanonical NF-κB pathway is differentially expressed in gliomas and drives invasion and tumorigenesis independently of the canonical NF-κB pathway.
- Low-dose TWEAK is capable of exclusively activating the noncanonical NF-κB pathway and promoting invasion in multiple glioma lines.
- Expression of genes encoding TWEAK, its receptor FN14, and NIK correlate positively with poor prognostic factors and the Mesenchymal glioma subtype.

Overall, our findings suggest that noncanonical NF-κB potentially contributes more to the invasive phenotype of glioma than canonical NF-κB signaling, especially in the Mesenchymal subtype. Canonical NF-κB proteins are expressed in glioma and can be activated by TNFα through induction of IκBα degradation, RelA phosphorylation, RelA translocation to the nucleus, and delayed induction of noncanonical NF-κB signaling, as we also have shown in this work. Thus, the canonical NF-κB pathway is intact in all cells we studied and is more-often-studied in glioma because it is consistently present and better-understood rather than biologically relevant in glioma. A significant discovery in our work was that TWEAK was able to induce invasion in the glioma cells with complete absence of canonical NF-κB activation. Noncanonical NF-κB signaling alone is sufficient to increase invasion, highlighting a substantial gap in our understanding of both pathways in gliomagenesis and progression. We therefore propose that it is the acquisition of the noncanonical NF-κB pathway, rather than increased activity of an ubiquitous canonical NF-κB pathway, that is more relevant to glioma pathogenesis. Whereas other studies have shown high-dose TWEAK increases glioma migration in a canonical-NF-κB-dependent manner [105, 116], our work demonstrated a noncanonical-NF-κB-specific response to low-dose TWEAK in invasion. This agrees with previous reports of differential canonical or noncanonical NF-κB responses from different concentrations of soluble TWEAK [94], which has been primarily advancing in the field of mesenchymal tissue development such as myoblast maturation [153]. To that end, increased expression of TWEAK Axis genes *MAP3K14*, *TRAF3*, *TNFSF12*, and

TNFRSF12A and noncanonical NF-κB in glioma may indicate acquisition of an intact pathway of mesenchymal differentiation and invasion in glioma. There is value in validating molecular findings in mesenchymal developmental biology in glioma to determine which natural pathways are intact. Accounting for which genes and proteins are shared between mesenchymal development in mesenchymal cells and mesenchymal phenotype development in glioma would allow for a more complete understanding of signaling in glioma and potentially identify additional targets for therapy. Therefore, the studies of mesenchymal development and Mesenchymal subtype glioma could complement each other in the development of mesenchymal-specific therapies.

We utilized BT lines from patient samples from Mayo Clinic as well as ATCC-derived lines widely used in glioma research. We demonstrated that TWEAK significantly increased invasion in all cell lines, even the non-invasive BT114 line with minimal basal protein levels of RelB. We showed for the first time in reported literature that TWEAK is capable of inducing NIK mRNA expression. The current understanding of NIK regulation emphasizes post-transcriptional regulation as the primary mechanism to control NIK activity [68]. Interestingly, increased mRNA expression was mild in the 2-3 fold range which, combined with only rare incidences of NIK expression greater than 2 fold in NCI array data, suggests that NIK upregulation is likely not a major contributor to glioma pathogenesis. This is further supported by our observation that ectopic wild-type NIK increased invasion but not significantly. Rather, NIK may be an instrumental component of transmitting TWEAK/FN14 activation rather than an independent driver of the noncanonical NF-κB invasive phenotype. *TRAF3* expression has little significant relevance to prognostic factors, which further suggests that NIK overexpression or decreased negative regulation are not major mechanisms of glioma pathogenesis. Significantly improved survival in the highest and lowest quartiles of *MAP3K14* expression supports NIK expression is nonetheless important in glioma, presumably by propagating TWEAK and other extracellular activators of NF-κB. Not investigated in this study were effects of TWEAK on the expression of other noncanonical NF-κB genes, which would provide insight into a role of TWEAK in the

induction of the mesenchymal phenotype in glioma cells. Although the Mesenchymal subtype can be inferred from the elongated mesenchymal-like invading phenotype in BT116 and U87 cells as well as the MMP-dependent invasion response, we cannot definitively categorize the BT or ATCC lines without sophisticated analysis of comprehensive gene expression data. We report that TWEAK seems to specifically induce MMP9 mRNA expression, but not the other gelatinase MMP2 or inducible membrane-type collagenase MMP14. A complete panel of MMP induction by TWEAK may show additional MMP induction or activity worth evaluating in glioma invasion and clinical outcome. Taken together with pan-inhibition, there appears to be a functional rather than reporting role for MMP9 in glioma cell invasion in type 1 collagen, which is unusual given that MMP9 is usually considered a gelatinase. This does not rule out the possibility of MMP9 activating cell-surface proteins to induce invasion. This could be more directly measured by MMP9 activity following TWEAK treatment with an enzymatic assay. The purpose of this study was to evaluate activation and regulation of MMP9 expression of the noncanonical NF-κB pathway by NIK stabilization and p100 processing using TWEAK as a noncanonical NF-κB-specific ligand. It would therefore be useful to perform a microarray or sequencing experiment on our glioma cell lines to stratify them into glioblastoma subtypes and ratify our molecular biology findings and gene expression data from the NCI dataset with the cell lines used.

Nuclear translocation of RelA and RelB following treatment TWEAK versus TNFα indicate that activation of either pathway in glioma is specific rather than redundant. We posit that both pathways must be addressed in context when evaluating potential NF-κB-targeted therapies. A considerable challenge in the development of therapeutics towards NF-κB constituents in glioma or other cancers is the poor drugability of transcription factors. A molecular basis for selective RelA or RelB binding to a specific promotor is an active but unresolved area of research [51], which makes specific inhibition of DNA-protein interaction for RelA versus RelB currently impossible. Pharmacologic inhibition of upstream kinases and extracellular ligand/receptor interactions provide a more promising approach. A recent study by

Zanotto-Filho *et al.* has shown that *in vitro* anti-NF-κB therapy selectively decreased proliferation in a panel of glioma lines versus normal astrocyte lines [154]. Anti-NF-κB therapy also increased sensitization to cisplatin and doxorubicin [154]. The specific anti-NF-κB compounds were anti-inflammatories, proteasome inhibitors, and an IKKβ inhibitor. Considerable attention is dedicated to IKKβ inhibitors as the catalytic subunit of the trimeric IKK complex that phosphorylates IκBα for degradation, but selectivity versus IKKα components is poor [155]. Ubiquitously-expressed canonical NF-κB has a wide variety of cellular functions in different tissues throughout the body, making systemic side-effects a concern. Because of poor IKKα/IKKβ selectivity, NIK is the most promising choice for kinase inhibition of the noncanonical NF-κB pathway. NIK inhibitor design *in silico* is an active area of research [156, 157], and pre-clinical studies *in vitro* have shown inhibition of cell viability and p100 processing in multiple myeloma [158]. Given these results in multiple myeloma and our data showing that NIK can drive glioma tumor development, evaluation of NIK inhibitors in glioma is of considerable interest. Our work offers NIK and TWEAK as promising therapeutic targets that specifically activate the noncanonical NF-κB pathway and increase invasion in glioma, which is a particularly deadly and concerning characteristic of high-grade gliomas that makes surgical resection difficult, high-dose chemotherapy and radiation necessary, and recurrence inevitable. A new hypothesis generated from our work would be how inhibition of NIK, TWEAK, or FN14 affects noncanonical NF-κB activation and glioma invasion. Anti-TNFα antibodies (adalimumab) and decoy receptors (etanercept) are already in clinical use as anti-inflammatory agents [159, 160], indicating proof-of-principle for the development of anti-TWEAK antibodies or decoy receptors. Decoy FN14-Fc receptors of TWEAK have been shown to inhibit TWEAK-stimulated glioma migration [105]. Recent work in developing blood-brain barrier-penetrant TNFα decoy receptors for stroke highlights the possibility of developing brain-penetrating anti-TWEAK decoy receptors [161]. An FN14-ligand fusion protein has been shown to induce HCC apoptosis and reduce tumor volume in mice models [115]. Ostensibly, these receptors would inhibit TWEAK and its extracellular activation of noncanonical NF-κB

and subsequent invasion. A small-molecule inhibitor of TWEAK/FN14 would provide an additional tool to assess the drugability of the TWEAK axis in the treatment of glioma. Very recently, an abstract at the 2014 Annual Scientific Meeting of the Society for Neuro-Oncology described a cell-based screening for inhibitors of TWEAK-induced migration in glioma and identified aurintricarboxylic acid (ATA) as an inhibitor of TWEAK/FN14 signaling. We summarize our model of TWEAK-activated noncanonical NF-κB signaling in glioma and its potential therapeutic strategies in Figure 15.

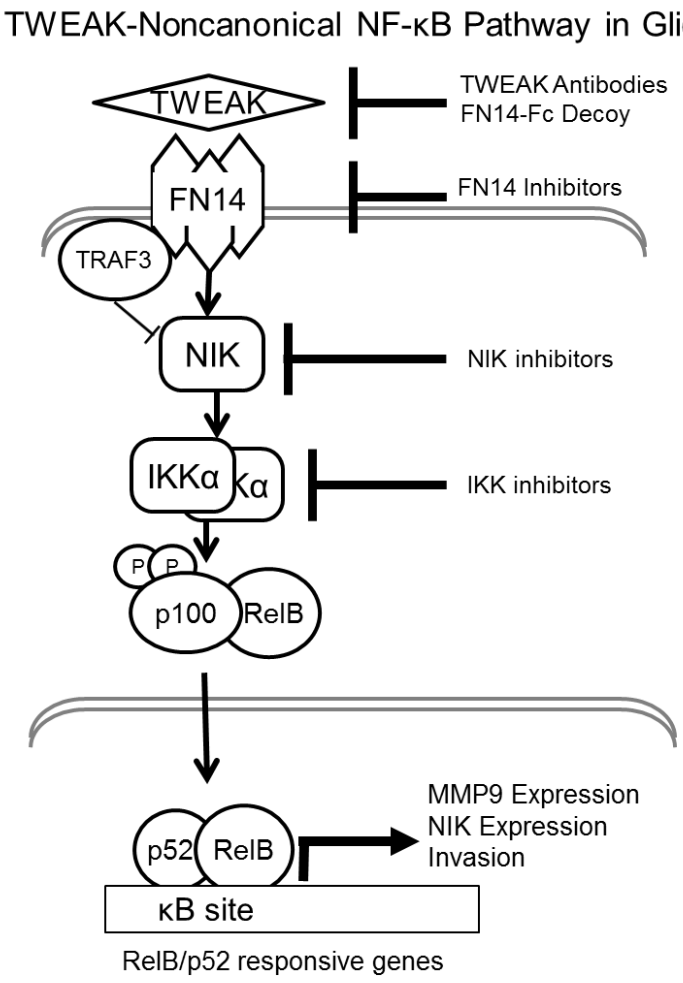

Figure 15 Proposed model for TWEAK/FN14 activation of noncanonical NF-κB in glioma invasion.

Our study provides initial rationale for targeting the TWEAK Axis and subsequent activation of noncanonical NF-κB clinically in the treatment of high-grade glioma, but evaluation of TWEAK inhibition *in vitro* and *in vivo* is required as a pre-clinical study.

Although our work clearly demonstrates a pro-invasive effect of TWEAK and the noncanonical NF-κB pathway in glioma invasion and clinical outcome, there are limitations to address. First, our loss-of-function studies for RelA, RelB, NFKB2, and NIK utilized a traditional shRNA approach. Individual shRNA constructs were selected from a panel of confirmed knockdowns for robustness and to reduce the likelihood of off-target effects. However, knockdown efficiency is a limitation in the robustness and therefore power of shRNA to determine significant effects of knockdown of the protein of interest. Incomplete RNA interference is particularly challenging in proteins with constitutive activity such as NIK, where incomplete interference may be insufficient to demonstrate a significant effect. Clustered Regularly Interspaced Short Palindromic Repeat (CRISPR) interference is an advanced technique that inhibits transcription of the gene of interest with improved efficiency and specificity versus RNA interference [162]. Utilization of CRISPR as a more powerful interference technique should further validate the significance of reduced NF-κB expression in glioma invasion.

Second, we observed significant increases in invasion despite less p100 processing in the NIK S867A mutant versus the wild-type NIK construct. These results suggest that the mutant exerts its effects beyond inherent constitutive activity of stabilized NIK, a concern not addressed in this work. Addressing the relevance of the TRAF3-binding domain, kinase domain, and other regulatory domains is the subject of a mutational analysis of NIK currently being investigated by another student in our lab. From this analysis we hope to further a fundamental understanding of NIK regulation and its function in glioma.

Third, our differential gene analysis was descriptive and requires caution in the interpretation. Because the cohort was large, the significance of the Spearman correlation ρ-values indicates they are dependable, but significance does not indicate whether these weak and moderate correlations are descriptive biologically. Biological

significance of each of these correlations would have to be investigated directly to account for complex and indirect interactions between genes that may have a functionally significant biological effect. Analysis of Covariance (ANCOVA) is a sophisticated technique to merge correlation between multiple gene expression values and linear regression of their contributions to a biological effect [163, 164]. ANCOVA utilizes Gene Ontology from known biological interactions reported in literature to score and group correlations between genes statistically as well as functionally. We have set up a framework for additional and more-sophisticated analysis of our combined NCI dataset with experienced bioinformaticists.

Fourth, gene expression analysis using DNA microarray has well-known limitations. Fortunately, batch effects and data quality were verified by TCGA and REMBRANDT requirements as well as externally validated [13, 23, 146]. Probe design is *a priori* and does not account for specific abnormal or noncoding RNA unless specifically designated. The NCI databases utilized human genome chips to assay the maximum number of wild-type human genes and were not specifically tailored to assess molecular events clinically relevant to such as mutations, alternative splicing, or promoter methylation status known to high-grade gliomas. RNAseq data is available in the TCGA, but because many of the RNAseq datasets contain the same tumor samples as the microarray sets we did not utilize RNAseq data due to the increased computing power, additional software, and complexity in interpreting quality and meaning of results. RNAseq data has promising applications in identifying clinically-relevant gene expression, mutations, and single nucleotide polymorphisms throughout the glioma genome rather than determined *a priori* like gene arrays. Determining agreement between microarray technology and next-generation sequencing and evaluating the comparative utility of the two is a worthwhile endeavor, but is well beyond the scope of this project and would best be conducted in collaboration with an experienced bioinformaticist.

Finally, all data available from the TCGA and REMBRANDT were from primary and not recurrent tumors. Our analysis would be informative in evaluating

noncanonical NF-κB and TWEAK Axis expression in recurrent tumors. Although samples from recurrent tumors for some of the TCGA patients are indicated in the clinical manifests, expression data from these samples is not accessible. It has been proposed by Phillips *et al.* that recurrent tumors are mesenchymal regardless of the subtype of the initial tumor [11]. If this is true, the relevance of TWEAK and noncanonical NF-κB would have to be evaluated in context of both the initial tumor subtype and whether TWEAK correlates with prognosis of recurrent tumors that are ultimately fatal. Therapeutic regimes and recurrence status are inconsistently annotated in the TCGA and REMBRANDT databases. Therefore, additional focused clinical studies are required to correlate TWEAK Axis expression with clinical outcome in the context of clinical strategies at initial diagnosis and recurrence.

In this work we combined a molecular & cellular biology approach as well as descriptive statistics to gene expression data for biological functional significance of TWEAK and NIK as well as clinical statistical significance of TWEAK, NIK, FN14, and TRAF3 gene expression. We therefore propose TWEAK signaling contributes to advanced glioma pathogenesis. Collectively, our work addresses a gap in knowledge of noncanonical NF-κB signaling in glioma invasion and tumorigenesis. We show that the TWEAK-noncanonical NF-κB pathway is clinically relevant and mandates additional study to advance fundamental and translational opportunities to improve outcome in a large cohort of patients with a devastating disease.

REFERENCES

1. Ostrom QT, Gittleman H, Liao P, Rouse C, Chen Y, Dowling J, Wolinsky Y, Kruchko C, Barnholtz-Sloan J: **CBTRUS statistical report: primary brain and central nervous system tumors diagnosed in the United States in 2007-2011.** *Neuro Oncol* 2014, **16 Suppl 4:**iv1-63.
2. von Deimling A, von Ammon K, Schoenfeld D, Wiestler OD, Seizinger BR, Louis DN: **Subsets of glioblastoma multiforme defined by molecular genetic analysis.** *Brain Pathol* 1993, **3:**19-26.
3. Corsa P, Parisi S, Raguso A, Troiano M, Perrone A, Cossa S, Munafo T, Piombino M, Spagnoletti G, Borgia F: **Temozolomide and radiotherapy as first-line treatment of high-grade gliomas.** *Tumori* 2006, **92:**299-305.
4. Erpolat OP, Akmansu M, Goksel F, Bora H, Yaman E, Buyukberber S: **Outcome of newly diagnosed glioblastoma patients treated by radiotherapy plus concomitant and adjuvant temozolomide: a long-term analysis.** *Tumori* 2009, **95:**191-197.
5. Wang Y, Chen X, Zhang Z, Li S, Chen B, Wu C, Wang L, Zhang X, Wang J, Chen L, Jiang T: **Comparison of the clinical efficacy of temozolomide (TMZ) versus nimustine (ACNU)-based chemotherapy in newly diagnosed glioblastoma.** *Neurosurg Rev* 2014, **37:**73-78.
6. Johnson DR, O'Neill BP: **Glioblastoma survival in the United States before and during the temozolomide era.** *J Neurooncol* 2012, **107:**359-364.
7. Wen PY, Kesari S: **Malignant gliomas in adults.** *N Engl J Med* 2008, **359:**492-507.
8. Lamborn KR, Chang SM, Prados MD: **Prognostic factors for survival of patients with glioblastoma: recursive partitioning analysis.** *Neuro Oncol* 2004, **6:**227-235.
9. Surawicz TS, McCarthy BJ, Kupelian V, Jukich PJ, Bruner JM, Davis FG: **Descriptive epidemiology of primary brain and CNS tumors: results from**

the Central Brain Tumor Registry of the United States, 1990-1994. *Neuro Oncol* 1999, **1:**14-25.

10. Wrensch M, Minn Y, Chew T, Bondy M, Berger MS: **Epidemiology of primary brain tumors: current concepts and review of the literature.** *Neuro Oncol* 2002, **4:**278-299.
11. Phillips HS, Kharbanda S, Chen R, Forrest WF, Soriano RH, Wu TD, Misra A, Nigro JM, Colman H, Soroceanu L, et al: **Molecular subclasses of high-grade glioma predict prognosis, delineate a pattern of disease progression, and resemble stages in neurogenesis.** *Cancer Cell* 2006, **9:**157-173.
12. Ducray F, Idbaih A, Wang XW, Cheneau C, Labussiere M, Sanson M: **Predictive and prognostic factors for gliomas.** *Expert Rev Anticancer Ther* 2011, **11:**781-789.
13. Brennan CW, Verhaak RG, McKenna A, Campos B, Noushmehr H, Salama SR, Zheng S, Chakravarty D, Sanborn JZ, Berman SH, et al: **The somatic genomic landscape of glioblastoma.** *Cell* 2013, **155:**462-477.
14. Johnson DR, Galanis E: **Incorporation of prognostic and predictive factors into glioma clinical trials.** *Curr Oncol Rep* 2013, **15:**56-63.
15. Sanai N, Polley MY, McDermott MW, Parsa AT, Berger MS: **An extent of resection threshold for newly diagnosed glioblastomas.** *J Neurosurg* 2011, **115:**3-8.
16. Eyupoglu IY, Buchfelder M, Savaskan NE: **Surgical resection of malignant gliomas-role in optimizing patient outcome.** *Nat Rev Neurol* 2013, **9:**141-151.
17. Stupp R, Hegi ME, Mason WP, van den Bent MJ, Taphoorn MJ, Janzer RC, Ludwin SK, Allgeier A, Fisher B, Belanger K, et al: **Effects of radiotherapy with concomitant and adjuvant temozolomide versus radiotherapy alone on survival in glioblastoma in a randomised phase III study: 5-year analysis of the EORTC-NCIC trial.** *Lancet Oncol* 2009, **10:**459-466.

18. Park JK, Hodges T, Arko L, Shen M, Dello Iacono D, McNabb A, Olsen Bailey N, Kreisl TN, Iwamoto FM, Sul J, et al: **Scale to predict survival after surgery for recurrent glioblastoma multiforme.** *J Clin Oncol* 2010, **28:**3838-3843.
19. Holland EC: **A mouse model for glioma: biology, pathology, and therapeutic opportunities.** *Toxicol Pathol* 2000, **28:**171-177.
20. Karpel-Massler G, Schmidt U, Unterberg A, Halatsch ME: **Therapeutic inhibition of the epidermal growth factor receptor in high-grade gliomas: where do we stand?** *Mol Cancer Res* 2009, **7:**1000-1012.
21. Lo HW: **EGFR-targeted therapy in malignant glioma: novel aspects and mechanisms of drug resistance.** *Curr Mol Pharmacol* 2010, **3:**37-52.
22. Cancer Genome Atlas Research N: **Comprehensive genomic characterization defines human glioblastoma genes and core pathways.** *Nature* 2008, **455:**1061-1068.
23. Madhavan S, Zenklusen JC, Kotliarov Y, Sahni H, Fine HA, Buetow K: **Rembrandt: helping personalized medicine become a reality through integrative translational research.** *Mol Cancer Res* 2009, **7:**157-167.
24. Verhaak RG, Hoadley KA, Purdom E, Wang V, Qi Y, Wilkerson MD, Miller CR, Ding L, Golub T, Mesirov JP, et al: **Integrated genomic analysis identifies clinically relevant subtypes of glioblastoma characterized by abnormalities in PDGFRA, IDH1, EGFR, and NF1.** *Cancer Cell* 2010, **17:**98-110.
25. Brown LF, Lanir N, McDonagh J, Tognazzi K, Dvorak AM, Dvorak HF: **Fibroblast migration in fibrin gel matrices.** *Am J Pathol* 1993, **142:**273-283.
26. Fishman RB, Hatten ME: **Multiple receptor systems promote CNS neural migration.** *J Neurosci* 1993, **13:**3485-3495.
27. Nicosia RF, Ottinetti A: **Modulation of microvascular growth and morphogenesis by reconstituted basement membrane gel in three-dimensional cultures of rat aorta: a comparative study of angiogenesis in matrigel, collagen, fibrin, and plasma clot.** *In Vitro Cell Dev Biol* 1990, **26:**119-128.

28. Bayless KJ, Kwak HI, Su SC: **Investigating endothelial invasion and sprouting behavior in three-dimensional collagen matrices.** *Nat Protoc* 2009, **4:**1888-1898.
29. Chen WT: **Proteolytic activity of specialized surface protrusions formed at rosette contact sites of transformed cells.** *J Exp Zool* 1989, **251:**167-185.
30. Mizutani K, Miki H, He H, Maruta H, Takenawa T: **Essential role of neural Wiskott-Aldrich syndrome protein in podosome formation and degradation of extracellular matrix in src-transformed fibroblasts.** *Cancer Res* 2002, **62:**669-674.
31. Yamaguchi H, Lorenz M, Kempiak S, Sarmiento C, Coniglio S, Symons M, Segall J, Eddy R, Miki H, Takenawa T, Condeelis J: **Molecular mechanisms of invadopodium formation: the role of the N-WASP-Arp2/3 complex pathway and cofilin.** *J Cell Biol* 2005, **168:**441-452.
32. Martin KH, Hayes KE, Walk EL, Ammer AG, Markwell SM, Weed SA: **Quantitative measurement of invadopodia-mediated extracellular matrix proteolysis in single and multicellular contexts.** *J Vis Exp* 2012**:**e4119.
33. Wang W, Goswami S, Lapidus K, Wells AL, Wyckoff JB, Sahai E, Singer RH, Segall JE, Condeelis JS: **Identification and testing of a gene expression signature of invasive carcinoma cells within primary mammary tumors.** *Cancer Res* 2004, **64:**8585-8594.
34. Laser-Azogui A, Diamant-Levi T, Israeli S, Roytman Y, Tsarfaty I: **Met-induced membrane blebbing leads to amoeboid cell motility and invasion.** *Oncogene* 2014, **33:**1788-1798.
35. Tournaviti S, Hannemann S, Terjung S, Kitzing TM, Stegmayer C, Ritzerfeld J, Walther P, Grosse R, Nickel W, Fackler OT: **SH4-domain-induced plasma membrane dynamization promotes bleb-associated cell motility.** *J Cell Sci* 2007, **120:**3820-3829.
36. Ratnikov BI, Cieplak P, Gramatikoff K, Pierce J, Eroshkin A, Igarashi Y, Kazanov M, Sun Q, Godzik A, Osterman A, et al: **Basis for substrate**

recognition and distinction by matrix metalloproteinases. *Proc Natl Acad Sci U S A* 2014, **111:**E4148-4155.

37. Rodriguez D, Morrison CJ, Overall CM: **Matrix metalloproteinases: what do they not do? New substrates and biological roles identified by murine models and proteomics.** *Biochim Biophys Acta* 2010, **1803:**39-54.
38. Puzovic V, Brcic I, Ranogajec I, Jakic-Razumovic J: **Prognostic values of ETS-1, MMP-2 and MMP-9 expression and co-expression in breast cancer patients.** *Neoplasma* 2014, **61:**439-446.
39. Farina AR, Mackay AR: **Gelatinase B/MMP-9 in Tumour Pathogenesis and Progression.** *Cancers (Basel)* 2014, **6:**240-296.
40. Liu Z, Li L, Yang Z, Luo W, Li X, Yang H, Yao K, Wu B, Fang W: **Increased expression of MMP9 is correlated with poor prognosis of nasopharyngeal carcinoma.** *BMC Cancer* 2010, **10:**270.
41. Zhao J, Li G, Zhao Z, Wang J, Gao G, He S: **Matrix metalloproteinase-9 expression is increased in astrocytic glioma and associated with prognosis of patients.** *Jpn J Clin Oncol* 2012, **42:**1060-1065.
42. Chu D, Zhao Z, Zhou Y, Li Y, Li J, Zheng J, Zhao Q, Wang W: **Matrix metalloproteinase-9 is associated with relapse and prognosis of patients with colorectal cancer.** *Ann Surg Oncol* 2012, **19:**318-325.
43. Sun C, Wang Q, Zhou H, Yu S, Simard AR, Kang C, Li Y, Kong Y, An T, Wen Y, et al: **Antisense MMP-9 RNA inhibits malignant glioma cell growth in vitro and in vivo.** *Neurosci Bull* 2013, **29:**83-93.
44. Kass L, Erler JT, Dembo M, Weaver VM: **Mammary epithelial cell: influence of extracellular matrix composition and organization during development and tumorigenesis.** *Int J Biochem Cell Biol* 2007, **39:**1987-1994.
45. Levental KR, Yu H, Kass L, Lakins JN, Egeblad M, Erler JT, Fong SF, Csiszar K, Giaccia A, Weninger W, et al: **Matrix crosslinking forces tumor progression by enhancing integrin signaling.** *Cell* 2009, **139:**891-906.

46. Huijbers IJ, Iravani M, Popov S, Robertson D, Al-Sarraj S, Jones C, Isacke CM: **A role for fibrillar collagen deposition and the collagen internalization receptor endo180 in glioma invasion.** *PLoS One* 2010, **5:**e9808.

47. Payne LS, Huang PH: **The pathobiology of collagens in glioma.** *Mol Cancer Res* 2013, **11:**1129-1140.

48. Ram R, Lorente G, Nikolich K, Urfer R, Foehr E, Nagavarapu U: **Discoidin domain receptor-1a (DDR1a) promotes glioma cell invasion and adhesion in association with matrix metalloproteinase-2.** *J Neurooncol* 2006, **76:**239-248.

49. Lee DW, Ramakrishnan D, Valenta J, Parney IF, Bayless KJ, Sitcheran R: **The NF-kappaB RelB protein is an oncogenic driver of mesenchymal glioma.** *PLoS One* 2013, **8:**e57489.

50. Cherry EM, Lee DW, Jung JU, Sitcheran R: **Tumor necrosis factor-like weak inducer of apoptosis (TWEAK) promotes glioma cell invasion through induction of NF-kappaB-inducing kinase (NIK) and noncanonical NF-kappaB signaling.** *Mol Cancer* 2015, **14:**9.

51. Wong D, Teixeira A, Oikonomopoulos S, Humburg P, Lone IN, Saliba D, Siggers T, Bulyk M, Angelov D, Dimitrov S, et al: **Extensive characterization of NF-kappaB binding uncovers non-canonical motifs and advances the interpretation of genetic functional traits.** *Genome Biol* 2011, **12:**R70.

52. Hayden MS, Ghosh S: **NF-kappaB, the first quarter-century: remarkable progress and outstanding questions.** *Genes Dev* 2012, **26:**203-234.

53. Nagai S, Washiyama K, Kurimoto M, Takaku A, Endo S, Kumanishi T: **Aberrant nuclear factor-kappaB activity and its participation in the growth of human malignant astrocytoma.** *J Neurosurg* 2002, **96:**909-917.

54. Perkins ND: **The diverse and complex roles of NF-kappaB subunits in cancer.** *Nat Rev Cancer* 2012, **12:**121-132.

55. Raychaudhuri B, Han Y, Lu T, Vogelbaum MA: **Aberrant constitutive activation of nuclear factor kappaB in glioblastoma multiforme drives invasive phenotype.** *J Neurooncol* 2007, **85:**39-47.

56. Bhat KP, Balasubramaniyan V, Vaillant B, Ezhilarasan R, Hummelink K, Hollingsworth F, Wani K, Heathcock L, James JD, Goodman LD, et al: **Mesenchymal differentiation mediated by NF-kappaB promotes radiation resistance in glioblastoma.** *Cancer Cell* 2013, **24:**331-346.

57. Mercurio F, Zhu H, Murray BW, Shevchenko A, Bennett BL, Li J, Young DB, Barbosa M, Mann M, Manning A, Rao A: **IKK-1 and IKK-2: cytokine-activated IkappaB kinases essential for NF-kappaB activation.** *Science* 1997, **278:**860-866.

58. Zandi E, Rothwarf DM, Delhase M, Hayakawa M, Karin M: **The IkappaB kinase complex (IKK) contains two kinase subunits, IKKalpha and IKKbeta, necessary for IkappaB phosphorylation and NF-kappaB activation.** *Cell* 1997, **91:**243-252.

59. Ganchi PA, Sun SC, Greene WC, Ballard DW: **I kappa B/MAD-3 masks the nuclear localization signal of NF-kappa B p65 and requires the transactivation domain to inhibit NF-kappa B p65 DNA binding.** *Mol Biol Cell* 1992, **3:**1339-1352.

60. Latimer M, Ernst MK, Dunn LL, Drutskaya M, Rice NR: **The N-terminal domain of IkappaB alpha masks the nuclear localization signal(s) of p50 and c-Rel homodimers.** *Mol Cell Biol* 1998, **18:**2640-2649.

61. Brown K, Gerstberger S, Carlson L, Franzoso G, Siebenlist U: **Control of I kappa B-alpha proteolysis by site-specific, signal-induced phosphorylation.** *Science* 1995, **267:**1485-1488.

62. Sasaki CY, Barberi TJ, Ghosh P, Longo DL: **Phosphorylation of RelA/p65 on serine 536 defines an I{kappa}B{alpha}-independent NF-{kappa}B pathway.** *J Biol Chem* 2005, **280:**34538-34547.

63. Arenzana-Seisdedos F, Thompson J, Rodriguez MS, Bachelerie F, Thomas D, Hay RT: **Inducible nuclear expression of newly synthesized I kappa B alpha negatively regulates DNA-binding and transcriptional activities of NF-kappa B.** *Mol Cell Biol* 1995, **15:**2689-2696.

64. Pahl HL: **Activators and target genes of Rel/NF-kappaB transcription factors.** *Oncogene* 1999, **18:**6853-6866.

65. Xiao G, Harhaj EW, Sun SC: **NF-kappaB-inducing kinase regulates the processing of NF-kappaB2 p100.** *Mol Cell* 2001, **7:**401-409.

66. Qing G, Qu Z, Xiao G: **Stabilization of basally translated NF-kappaB-inducing kinase (NIK) protein functions as a molecular switch of processing of NF-kappaB2 p100.** *J Biol Chem* 2005, **280:**40578-40582.

67. Liao G, Zhang M, Harhaj EW, Sun SC: **Regulation of the NF-kappaB-inducing kinase by tumor necrosis factor receptor-associated factor 3-induced degradation.** *J Biol Chem* 2004, **279:**26243-26250.

68. Vallabhapurapu S, Matsuzawa A, Zhang W, Tseng PH, Keats JJ, Wang H, Vignali DA, Bergsagel PL, Karin M: **Nonredundant and complementary functions of TRAF2 and TRAF3 in a ubiquitination cascade that activates NIK-dependent alternative NF-kappaB signaling.** *Nat Immunol* 2008, **9:**1364-1370.

69. Xiao G, Fong A, Sun SC: **Induction of p100 processing by NF-kappaB-inducing kinase involves docking IkappaB kinase alpha (IKKalpha) to p100 and IKKalpha-mediated phosphorylation.** *J Biol Chem* 2004, **279:**30099-30105.

70. Betts JC, Nabel GJ: **Differential regulation of NF-kappaB2(p100) processing and control by amino-terminal sequences.** *Mol Cell Biol* 1996, **16:**6363-6371.

71. Solan NJ, Miyoshi H, Carmona EM, Bren GD, Paya CV: **RelB cellular regulation and transcriptional activity are regulated by p100.** *J Biol Chem* 2002, **277:**1405-1418.

72. Hohmann HP, Remy R, Scheidereit C, van Loon AP: **Maintenance of NF-kappa B activity is dependent on protein synthesis and the continuous presence of external stimuli.** *Mol Cell Biol* 1991, **11:**259-266.

73. Savinova OV, Hoffmann A, Ghosh G: **The Nfkb1 and Nfkb2 proteins p105 and p100 function as the core of high-molecular-weight heterogeneous complexes.** *Mol Cell* 2009, **34:**591-602.

74. Razani B, Zarnegar B, Ytterberg AJ, Shiba T, Dempsey PW, Ware CF, Loo JA, Cheng G: **Negative feedback in noncanonical NF-kappaB signaling modulates NIK stability through IKKalpha-mediated phosphorylation.** *Sci Signal* 2010, **3:**ra41.

75. Shih VF, Davis-Turak J, Macal M, Huang JQ, Ponomarenko J, Kearns JD, Yu T, Fagerlund R, Asagiri M, Zuniga EI, Hoffmann A: **Control of RelB during dendritic cell activation integrates canonical and noncanonical NF-kappaB pathways.** *Nat Immunol* 2012, **13:**1162-1170.

76. Burkly L, Hession C, Ogata L, Reilly C, Marconi LA, Olson D, Tizard R, Cate R, Lo D: **Expression of relB is required for the development of thymic medulla and dendritic cells.** *Nature* 1995, **373:**531-536.

77. Senftleben U, Cao Y, Xiao G, Greten FR, Krahn G, Bonizzi G, Chen Y, Hu Y, Fong A, Sun SC, Karin M: **Activation by IKKalpha of a second, evolutionary conserved, NF-kappa B signaling pathway.** *Science* 2001, **293:**1495-1499.

78. Beg AA, Baltimore D: **An essential role for NF-kappaB in preventing TNF-alpha-induced cell death.** *Science* 1996, **274:**782-784.

79. Franzoso G, Carlson L, Poljak L, Shores EW, Epstein S, Leonardi A, Grinberg A, Tran T, Scharton-Kersten T, Anver M, et al: **Mice deficient in nuclear factor (NF)-kappa B/p52 present with defects in humoral responses, germinal center reactions, and splenic microarchitecture.** *J Exp Med* 1998, **187:**147-159.

80. Weih F, Carrasco D, Durham SK, Barton DS, Rizzo CA, Ryseck RP, Lira SA, Bravo R: **Multiorgan inflammation and hematopoietic abnormalities in mice with a targeted disruption of RelB, a member of the NF-kappa B/Rel family.** *Cell* 1995, **80:**331-340.

81. Yin L, Wu L, Wesche H, Arthur CD, White JM, Goeddel DV, Schreiber RD: **Defective lymphotoxin-beta receptor-induced NF-kappaB transcriptional activity in NIK-deficient mice.** *Science* 2001, **291:**2162-2165.

82. Shinkura R, Kitada K, Matsuda F, Tashiro K, Ikuta K, Suzuki M, Kogishi K, Serikawa T, Honjo T: **Alymphoplasia is caused by a point mutation in the mouse gene encoding Nf-kappa b-inducing kinase.** *Nat Genet* 1999, **22:**74-77.

83. Zarnegar B, Yamazaki S, He JQ, Cheng G: **Control of canonical NF-kappaB activation through the NIK-IKK complex pathway.** *Proc Natl Acad Sci U S A* 2008, **105:**3503-3508.

84. Bren GD, Solan NJ, Miyoshi H, Pennington KN, Pobst LJ, Paya CV: **Transcription of the RelB gene is regulated by NF-kappaB.** *Oncogene* 2001, **20:**7722-7733.

85. Derudder E, Dejardin E, Pritchard LL, Green DR, Korner M, Baud V: **RelB/p50 dimers are differentially regulated by tumor necrosis factor-alpha and lymphotoxin-beta receptor activation: critical roles for p100.** *J Biol Chem* 2003, **278:**23278-23284.

86. Jacque E, Tchenio T, Piton G, Romeo PH, Baud V: **RelA repression of RelB activity induces selective gene activation downstream of TNF receptors.** *Proc Natl Acad Sci U S A* 2005, **102:**14635-14640.

87. Wang H, Wang H, Zhang W, Huang HJ, Liao WS, Fuller GN: **Analysis of the activation status of Akt, NFkappaB, and Stat3 in human diffuse gliomas.** *Lab Invest* 2004, **84:**941-951.

88. Claudio E, Brown K, Park S, Wang H, Siebenlist U: **BAFF-induced NEMO-independent processing of NF-kappa B2 in maturing B cells.** *Nat Immunol* 2002, **3:**958-965.

89. Chicheportiche Y, Bourdon PR, Xu H, Hsu YM, Scott H, Hession C, Garcia I, Browning JL: **TWEAK, a new secreted ligand in the tumor necrosis factor family that weakly induces apoptosis.** *J Biol Chem* 1997, **272:**32401-32410.

90. Donohue PJ, Richards CM, Brown SA, Hanscom HN, Buschman J, Thangada S, Hla T, Williams MS, Winkles JA: **TWEAK is an endothelial cell growth and chemotactic factor that also potentiates FGF-2 and VEGF-A mitogenic activity.** *Arterioscler Thromb Vasc Biol* 2003, **23:**594-600.

91. Chicheportiche Y, Chicheportiche R, Sizing I, Thompson J, Benjamin CB, Ambrose C, Dayer JM: **Proinflammatory activity of TWEAK on human dermal fibroblasts and synoviocytes: blocking and enhancing effects of anti-TWEAK monoclonal antibodies.** *Arthritis Res* 2002, **4:**126-133.

92. Desplat-Jego S, Varriale S, Creidy R, Terra R, Bernard D, Khrestchatisky M, Izui S, Chicheportiche Y, Boucraut J: **TWEAK is expressed by glial cells, induces astrocyte proliferation and increases EAE severity.** *J Neuroimmunol* 2002, **133:**116-123.

93. Jakubowski A, Ambrose C, Parr M, Lincecum JM, Wang MZ, Zheng TS, Browning B, Michaelson JS, Baetscher M, Wang B, et al: **TWEAK induces liver progenitor cell proliferation.** *J Clin Invest* 2005, **115:**2330-2340.

94. Roos C, Wicovsky A, Muller N, Salzmann S, Rosenthal T, Kalthoff H, Trauzold A, Seher A, Henkler F, Kneitz C, Wajant H: **Soluble and transmembrane TNF-like weak inducer of apoptosis differentially activate the classical and noncanonical NF-kappa B pathway.** *J Immunol* 2010, **185:**1593-1605.

95. Li H, Mittal A, Paul PK, Kumar M, Srivastava DS, Tyagi SC, Kumar A: **Tumor necrosis factor-related weak inducer of apoptosis augments matrix metalloproteinase 9 (MMP-9) production in skeletal muscle through the activation of nuclear factor-kappaB-inducing kinase and p38 mitogen-activated protein kinase: a potential role of MMP-9 in myopathy.** *J Biol Chem* 2009, **284:**4439-4450.

96. Vince JE, Chau D, Callus B, Wong WW, Hawkins CJ, Schneider P, McKinlay M, Benetatos CA, Condon SM, Chunduru SK, et al: **TWEAK-FN14 signaling induces lysosomal degradation of a cIAP1-TRAF2 complex to sensitize tumor cells to TNFalpha.** *J Cell Biol* 2008, **182:**171-184.

97. Saitoh T, Nakayama M, Nakano H, Yagita H, Yamamoto N, Yamaoka S: **TWEAK induces NF-kappaB2 p100 processing and long lasting NF-kappaB activation.** *J Biol Chem* 2003, **278:**36005-36012.

98. Rousselet E, Traver S, Monnet Y, Perrin A, Mandjee N, Hild A, Hirsch EC, Zheng TS, Hunot S: **Tumor necrosis factor-like weak inducer of apoptosis induces astrocyte proliferation through the activation of transforming-growth factor-alpha/epidermal growth factor receptor signaling pathway.** *Mol Pharmacol* 2012, **82:**948-957.

99. Potrovita I, Zhang W, Burkly L, Hahm K, Lincecum J, Wang MZ, Maurer MH, Rossner M, Schneider A, Schwaninger M: **Tumor necrosis factor-like weak inducer of apoptosis-induced neurodegeneration.** *J Neurosci* 2004, **24:**8237-8244.

100. Polavarapu R, Gongora MC, Winkles JA, Yepes M: **Tumor necrosis factor-like weak inducer of apoptosis increases the permeability of the neurovascular unit through nuclear factor-kappa B pathway activation.** *J Neurosci* 2005, **25:**10094-10100.

101. Desplat-Jego S, Creidy R, Varriale S, Allaire N, Luo Y, Bernard D, Hahm K, Burkly L, Boucraut J: **Anti-TWEAK monoclonal antibodies reduce immune cell infiltration in the central nervous system and severity of experimental autoimmune encephalomyelitis.** *Clin Immunol* 2005, **117:**15-23.

102. Iocca HA, Plant SR, Wang Y, Runkel L, O'Connor BP, Lundsmith ET, Hahm K, van Deventer HW, Burkly LC, Ting JP: **TNF superfamily member TWEAK exacerbates inflammation and demyelination in the cuprizone-induced model.** *J Neuroimmunol* 2008, **194:**97-106.

103. Dai L, Gu L, Ding C, Qiu L, Di W: **TWEAK promotes ovarian cancer cell metastasis via NF-kappaB pathway activation and VEGF expression.** *Cancer Lett* 2009, **283:**159-167.

104. Pettersen I, Baryawno N, Abel F, Bakkelund WH, Zykova SN, Winberg JO, Moens U, Rasmuson A, Kogner P, Johnsen JI, Sveinbjornsson B: **Expression of**

TWEAK/Fn14 in neuroblastoma: implications in tumorigenesis. *Int J Oncol* 2013, **42:**1239-1248.

105. Tran NL, McDonough WS, Savitch BA, Fortin SP, Winkles JA, Symons M, Nakada M, Cunliffe HE, Hostetter G, Hoelzinger DB, et al: **Increased fibroblast growth factor-inducible 14 expression levels promote glioma cell invasion via Rac1 and nuclear factor-kappaB and correlate with poor patient outcome.** *Cancer Res* 2006, **66:**9535-9542.
106. Dhruv HD, Whitsett TG, Jameson NM, Patel F, Winkles JA, Berens ME, Tran NL: **Tumor necrosis factor-like weak inducer of apoptosis (TWEAK) promotes glioblastoma cell chemotaxis via Lyn activation.** *Carcinogenesis* 2014, **35:**218-226.
107. Wiley SR, Cassiano L, Lofton T, Davis-Smith T, Winkles JA, Lindner V, Liu H, Daniel TO, Smith CA, Fanslow WC: **A novel TNF receptor family member binds TWEAK and is implicated in angiogenesis.** *Immunity* 2001, **15:**837-846.
108. Feng SL, Guo Y, Factor VM, Thorgeirsson SS, Bell DW, Testa JR, Peifley KA, Winkles JA: **The Fn14 immediate-early response gene is induced during liver regeneration and highly expressed in both human and murine hepatocellular carcinomas.** *Am J Pathol* 2000, **156:**1253-1261.
109. Meighan-Mantha RL, Hsu DK, Guo Y, Brown SA, Feng SL, Peifley KA, Alberts GF, Copeland NG, Gilbert DJ, Jenkins NA, et al: **The mitogen-inducible Fn14 gene encodes a type I transmembrane protein that modulates fibroblast adhesion and migration.** *J Biol Chem* 1999, **274:**33166-33176.
110. Girgenrath M, Weng S, Kostek CA, Browning B, Wang M, Brown SA, Winkles JA, Michaelson JS, Allaire N, Schneider P, et al: **TWEAK, via its receptor Fn14, is a novel regulator of mesenchymal progenitor cells and skeletal muscle regeneration.** *EMBO J* 2006, **25:**5826-5839.
111. Brown SA, Richards CM, Hanscom HN, Feng SL, Winkles JA: **The Fn14 cytoplasmic tail binds tumour-necrosis-factor-receptor-associated factors 1,**

2, 3 and 5 and mediates nuclear factor-kappaB activation. *Biochem J* 2003, **371:**395-403.

112. Huang M, Narita S, Tsuchiya N, Ma Z, Numakura K, Obara T, Tsuruta H, Saito M, Inoue T, Horikawa Y, et al: **Overexpression of Fn14 promotes androgen-independent prostate cancer progression through MMP-9 and correlates with poor treatment outcome.** *Carcinogenesis* 2011, **32:**1589-1596.
113. Asrani K, Keri RA, Galisteo R, Brown SA, Morgan SJ, Ghosh A, Tran NL, Winkles JA: **The HER2- and heregulin beta1 (HRG)-inducible TNFR superfamily member Fn14 promotes HRG-driven breast cancer cell migration, invasion, and MMP9 expression.** *Mol Cancer Res* 2013, **11:**393-404.
114. Whitsett TG, Cheng E, Inge L, Asrani K, Jameson NM, Hostetter G, Weiss GJ, Kingsley CB, Loftus JC, Bremner R, et al: **Elevated expression of Fn14 in non-small cell lung cancer correlates with activated EGFR and promotes tumor cell migration and invasion.** *Am J Pathol* 2012, **181:**111-120.
115. Aronin A, Amsili S, Prigozhina TB, Tzdaka K, Rachmilewitz J, Shani N, Tykocinski ML, Dranitzki Elhalel M: **Fn14*TRAIL effectively inhibits hepatocellular carcinoma growth.** *PLoS One* 2013, **8:**e77050.
116. Tran NL, McDonough WS, Savitch BA, Sawyer TF, Winkles JA, Berens ME: **The tumor necrosis factor-like weak inducer of apoptosis (TWEAK)-fibroblast growth factor-inducible 14 (Fn14) signaling system regulates glioma cell survival via NFkappaB pathway activation and BCL-XL/BCL-W expression.** *J Biol Chem* 2005, **280:**3483-3492.
117. Malinin NL, Boldin MP, Kovalenko AV, Wallach D: **MAP3K-related kinase involved in NF-kappaB induction by TNF, CD95 and IL-1.** *Nature* 1997, **385:**540-544.
118. Coope HJ, Atkinson PG, Huhse B, Belich M, Janzen J, Holman MJ, Klaus GG, Johnston LH, Ley SC: **CD40 regulates the processing of NF-kappaB2 p100 to p52.** *EMBO J* 2002, **21:**5375-5385.

119. Ranuncolo SM, Pittaluga S, Evbuomwan MO, Jaffe ES, Lewis BA: **Hodgkin lymphoma requires stabilized NIK and constitutive RelB expression for survival.** *Blood* 2012, **120:**3756-3763.

120. Uno M, Saitoh Y, Mochida K, Tsuruyama E, Kiyono T, Imoto I, Inazawa J, Yuasa Y, Kubota T, Yamaoka S: **NF-kappaB inducing kinase, a central signaling component of the non-canonical pathway of NF-kappaB, contributes to ovarian cancer progression.** *PLoS One* 2014, **9:**e88347.

121. Keats JJ, Fonseca R, Chesi M, Schop R, Baker A, Chng WJ, Van Wier S, Tiedemann R, Shi CX, Sebag M, et al: **Promiscuous mutations activate the noncanonical NF-kappaB pathway in multiple myeloma.** *Cancer Cell* 2007, **12:**131-144.

122. Annunziata CM, Davis RE, Demchenko Y, Bellamy W, Gabrea A, Zhan F, Lenz G, Hanamura I, Wright G, Xiao W, et al: **Frequent engagement of the classical and alternative NF-kappaB pathways by diverse genetic abnormalities in multiple myeloma.** *Cancer Cell* 2007, **12:**115-130.

123. Sasaki Y, Calado DP, Derudder E, Zhang B, Shimizu Y, Mackay F, Nishikawa S, Rajewsky K, Schmidt-Supprian M: **NIK overexpression amplifies, whereas ablation of its TRAF3-binding domain replaces BAFF:BAFF-R-mediated survival signals in B cells.** *Proc Natl Acad Sci U S A* 2008, **105:**10883-10888.

124. Kaur N, Ranjan A, Tiwari V, Aneja R, Tandon V: **DMA, a bisbenzimidazole, offers radioprotection by promoting NFkappaB transactivation through NIK/IKK in human glioma cells.** *PLoS One* 2012, **7:**e39426.

125. Tchoghandjian A, Jennewein C, Eckhardt I, Rajalingam K, Fulda S: **Identification of non-canonical NF-kappaB signaling as a critical mediator of Smac mimetic-stimulated migration and invasion of glioblastoma cells.** *Cell Death Dis* 2013, **4:**e564.

126. Hoesel B, Schmid JA: **The complexity of NF-kappaB signaling in inflammation and cancer.** *Mol Cancer* 2013, **12:**86.

127. DiDonato JA, Mercurio F, Karin M: **NF-kappaB and the link between inflammation and cancer.** *Immunol Rev* 2012, **246:**379-400.

128. Bredel M, Scholtens DM, Yadav AK, Alvarez AA, Renfrow JJ, Chandler JP, Yu IL, Carro MS, Dai F, Tagge MJ, et al: **NFKBIA deletion in glioblastomas.** *N Engl J Med* 2011, **364:**627-637.

129. Sun SC: **Non-canonical NF-kappaB signaling pathway.** *Cell Res* 2011, **21:**71-85.

130. Sun SC: **Controlling the fate of NIK: a central stage in noncanonical NF-kappaB signaling.** *Sci Signal* 2010, **3:**pe18.

131. Fusco AJ, Savinova OV, Talwar R, Kearns JD, Hoffmann A, Ghosh G: **Stabilization of RelB requires multidomain interactions with p100/p52.** *J Biol Chem* 2008, **283:**12324-12332.

132. Takeiri M, Horie K, Takahashi D, Watanabe M, Horie R, Simizu S, Umezawa K: **Involvement of DNA binding domain in the cellular stability and importin affinity of NF-kappaB component RelB.** *Org Biomol Chem* 2012, **10:**3053-3059.

133. Watts GS, Tran NL, Berens ME, Bhattacharyya AK, Nelson MA, Montgomery EA, Sampliner RE: **Identification of Fn14/TWEAK receptor as a potential therapeutic target in esophageal adenocarcinoma.** *Int J Cancer* 2007, **121:**2132-2139.

134. Nyga A, Cheema U, Loizidou M: **3D tumour models: novel in vitro approaches to cancer studies.** *J Cell Commun Signal* 2011, **5:**239-248.

135. Buss H, Dorrie A, Schmitz ML, Hoffmann E, Resch K, Kracht M: **Constitutive and interleukin-1-inducible phosphorylation of p65 NF-{kappa}B at serine 536 is mediated by multiple protein kinases including I{kappa}B kinase (IKK)-{alpha}, IKK{beta}, IKK{epsilon}, TRAF family member-associated (TANK)-binding kinase 1 (TBK1), and an unknown kinase and couples p65 to TATA-binding protein-associated factor II31-mediated interleukin-8 transcription.** *J Biol Chem* 2004, **279:**55633-55643.

136. Sizemore N, Leung S, Stark GR: **Activation of phosphatidylinositol 3-kinase in response to interleukin-1 leads to phosphorylation and activation of the NF-kappaB p65/RelA subunit.** *Mol Cell Biol* 1999, **19:**4798-4805.

137. Burkly LC, Michaelson JS, Zheng TS: **TWEAK/Fn14 pathway: an immunological switch for shaping tissue responses.** *Immunol Rev* 2011, **244:**99-114.

138. Varfolomeev E, Goncharov T, Maecker H, Zobel K, Komuves LG, Deshayes K, Vucic D: **Cellular inhibitors of apoptosis are global regulators of NF-kappaB and MAPK activation by members of the TNF family of receptors.** *Sci Signal* 2012, **5:**ra22.

139. Jin J, Xiao Y, Chang JH, Yu J, Hu H, Starr R, Brittain GC, Chang M, Cheng X, Sun SC: **The kinase TBK1 controls IgA class switching by negatively regulating noncanonical NF-kappaB signaling.** *Nat Immunol* 2012, **13:**1101-1109.

140. Yepes M: **TWEAK and the central nervous system.** *Mol Neurobiol* 2007, **35:**255-265.

141. Gray CM, Remouchamps C, McCorkell KA, Solt LA, Dejardin E, Orange JS, May MJ: **Noncanonical NF-kappaB signaling is limited by classical NF-kappaB activity.** *Sci Signal* 2014, **7:**ra13.

142. Erstad DJ, Cusack JC, Jr.: **Targeting the NF-kappaB pathway in cancer therapy.** *Surg Oncol Clin N Am* 2013, **22:**705-746.

143. Kelly JJ, Stechishin O, Chojnacki A, Lun X, Sun B, Senger DL, Forsyth P, Auer RN, Dunn JF, Cairncross JG, et al: **Proliferation of human glioblastoma stem cells occurs independently of exogenous mitogens.** *Stem Cells* 2009, **27:**1722-1733.

144. Rajan N, Habermehl J, Cote MF, Doillon CJ, Mantovani D: **Preparation of ready-to-use, storable and reconstituted type I collagen from rat tail tendon for tissue engineering applications.** *Nat Protoc* 2006, **1:**2753-2758.

145. Sitcheran R, Comb WC, Cogswell PC, Baldwin AS: **Essential role for epidermal growth factor receptor in glutamate receptor signaling to NF-kappaB.** *Mol Cell Biol* 2008, **28:**5061-5070.

146. Cancer Genome Atlas Research N, Weinstein JN, Collisson EA, Mills GB, Shaw KR, Ozenberger BA, Ellrott K, Shmulevich I, Sander C, Stuart JM: **The Cancer Genome Atlas Pan-Cancer analysis project.** *Nat Genet* 2013, **45:**1113-1120.

147. Inskip PD, Linet MS, Heineman EF: **Etiology of brain tumors in adults.** *Epidemiol Rev* 1995, **17:**382-414.

148. Zimmermann M, Koreck A, Meyer N, Basinski T, Meiler F, Simone B, Woehrl S, Moritz K, Eiwegger T, Schmid-Grendelmeier P, et al: **TNF-like weak inducer of apoptosis (TWEAK) and TNF-alpha cooperate in the induction of keratinocyte apoptosis.** *J Allergy Clin Immunol* 2011, **127:**200-207, 207 e201-210.

149. De Bacco F, Casanova E, Medico E, Pellegatta S, Orzan F, Albano R, Luraghi P, Reato G, D'Ambrosio A, Porrati P, et al: **The MET oncogene is a functional marker of a glioblastoma stem cell subtype.** *Cancer Res* 2012, **72:**4537-4550.

150. Irizarry RA, Bolstad BM, Collin F, Cope LM, Hobbs B, Speed TP: **Summaries of Affymetrix GeneChip probe level data.** *Nucleic Acids Res* 2003, **31:**e15.

151. Cleveland WS: **Robust Locally Weighted Regression and Smoothing Scatterplots.** *Journal of the American Statistical Association* 1979, **74:**829-836.

152. Evans JD: *Straightforward statistics for the behavioral sciences.* Pacific Grove: Brooks/Cole Pub. Co.; 1996.

153. Enwere EK, Holbrook J, Lejmi-Mrad R, Vineham J, Timusk K, Sivaraj B, Isaac M, Uehling D, Al-awar R, LaCasse E, Korneluk RG: **TWEAK and cIAP1 regulate myoblast fusion through the noncanonical NF-kappaB signaling pathway.** *Sci Signal* 2012, **5:**ra75.

154. Zanotto-Filho A, Braganhol E, Schroder R, de Souza LH, Dalmolin RJ, Pasquali MA, Gelain DP, Battastini AM, Moreira JC: **NFkappaB inhibitors induce cell death in glioblastomas.** *Biochem Pharmacol* 2011, **81:**412-424.

155. Tian F, Zhou P, Kang W, Luo L, Fan X, Yan J, Liang H: **The small-molecule inhibitor selectivity between IKKalpha and IKKbeta kinases in NF-kappaB signaling pathway.** *J Recept Signal Transduct Res* 2014**:**1-12.

156. Li K, McGee LR, Fisher B, Sudom A, Liu J, Rubenstein SM, Anwer MK, Cushing TD, Shin Y, Ayres M, et al: **Inhibiting NF-kappaB-inducing kinase (NIK): discovery, structure-based design, synthesis, structure-activity relationship, and co-crystal structures.** *Bioorg Med Chem Lett* 2013, **23:**1238-1244.

157. Mortier J, Masereel B, Remouchamps C, Ganeff C, Piette J, Frederick R: **NF-kappaB inducing kinase (NIK) inhibitors: identification of new scaffolds using virtual screening.** *Bioorg Med Chem Lett* 2010, **20:**4515-4520.

158. Demchenko YN, Brents LA, Li Z, Bergsagel LP, McGee LR, Kuehl MW: **Novel inhibitors are cytotoxic for myeloma cells with NFkB inducing kinase-dependent activation of NFkB.** *Oncotarget* 2014, **5:**4554-4566.

159. van Luijn JC, Danz M, Bijlsma JW, Gribnau FW, Leufkens HG: **Post-approval trials of new medicines: widening use or deepening knowledge? Analysis of 10 years of etanercept.** *Scand J Rheumatol* 2011, **40:**183-191.

160. Burmester GR, Matucci-Cerinic M, Mariette X, Navarro-Blasco F, Kary S, Unnebrink K, Kupper H: **Safety and effectiveness of adalimumab in patients with rheumatoid arthritis over 5 years of therapy in a phase 3b and subsequent postmarketing observational study.** *Arthritis Res Ther* 2014, **16:**R24.

161. Sumbria RK, Boado RJ, Pardridge WM: **Brain protection from stroke with intravenous TNFalpha decoy receptor-Trojan horse fusion protein.** *J Cereb Blood Flow Metab* 2012, **32:**1933-1938.

162. Mali P, Esvelt KM, Church GM: **Cas9 as a versatile tool for engineering biology.** *Nat Methods* 2013, **10:**957-963.

163. Mansmann U, Meister R: **Testing differential gene expression in functional groups. Goeman's global test versus an ANCOVA approach.** *Methods Inf Med* 2005, **44:**449-453.

164. Hummel M, Meister R, Mansmann U: **GlobalANCOVA: exploration and assessment of gene group effects.** *Bioinformatics* 2008, **24:**78-85.

APPENDIX A

SUPPLEMENTAL FIGURES

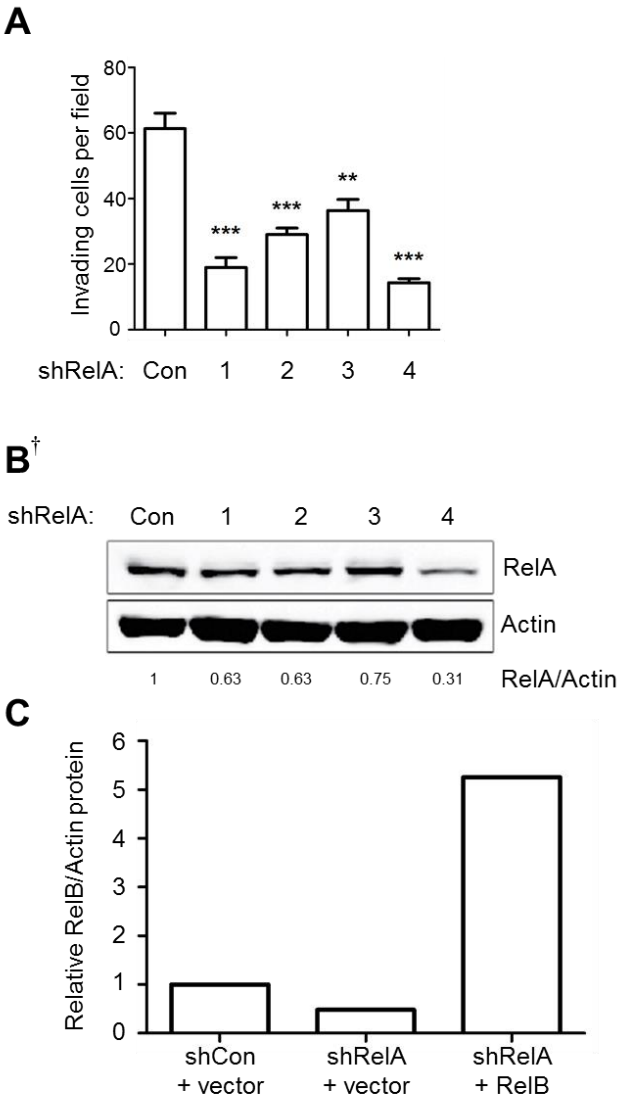

Figure A1 Efficiency of RelA knockdown among multiple shRNA constructs and quantification of RelB overexpression. (A) Quantification of invasion density at 48 h for U87 RelA knockdown cell lines 1-4. Data represent average numbers of invading cells per 1-mm^2 field (n = 3 wells) ± SEM. **p < 0.01 ***p < 0.001 relative to shCon using One-way ANOVA with Tukey's HSD post-test. **(B)** Western blot of whole-cell lysates from U87 shRelA glioma lines using the indicated antibodies. Numbers indicate semi-quantitative measurements of RelA protein levels relative to actin protein levels and normalized to shCon. (C) Semi-quantitative measurement RelB protein levels relative to actin protein levels for western blot of whole-cell lysates from U87 shCon and shRelA cells transduced with RFP cDNA (+Vector) or RelB cDNA (+RelB) from Figure 2D. Data are normalized to shCon. †Data contributed by DW Lee.

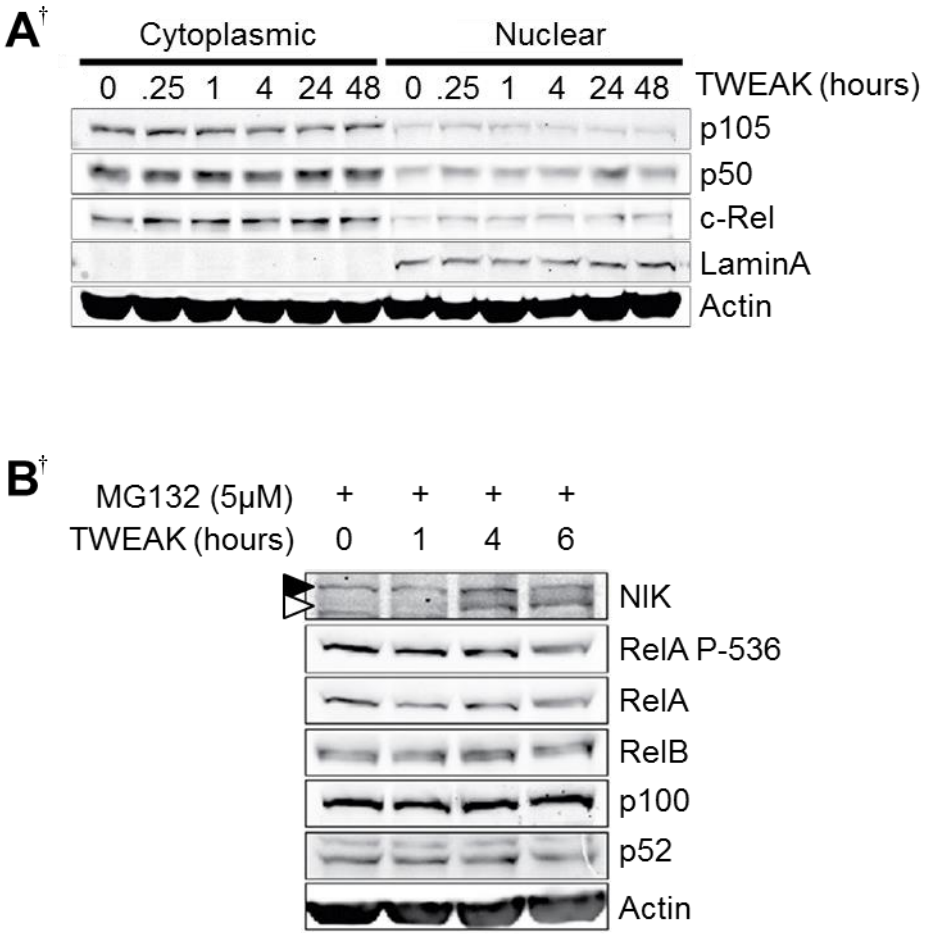

Figure A2 TWEAK specifically induces noncanonical NF-κB activation in glioma cells via NIK protein accumulation. (A) Western blot analysis of proteins from cytoplasmic and nuclear fractions of BT116 cells stimulated with 10 ng/ml TWEAK at indicated times using the indicated antibodies. **(B)** Western blot analysis of BT116 glioma cell lysates at indicated time post-treatment with 10 ng/ml TWEAK and 5μM proteasome inhibitor MG132 using the indicated antibodies. White arrowhead indicates NIK band. Black arrowhead indicates non-specific band. †Data contributed by DW Lee.

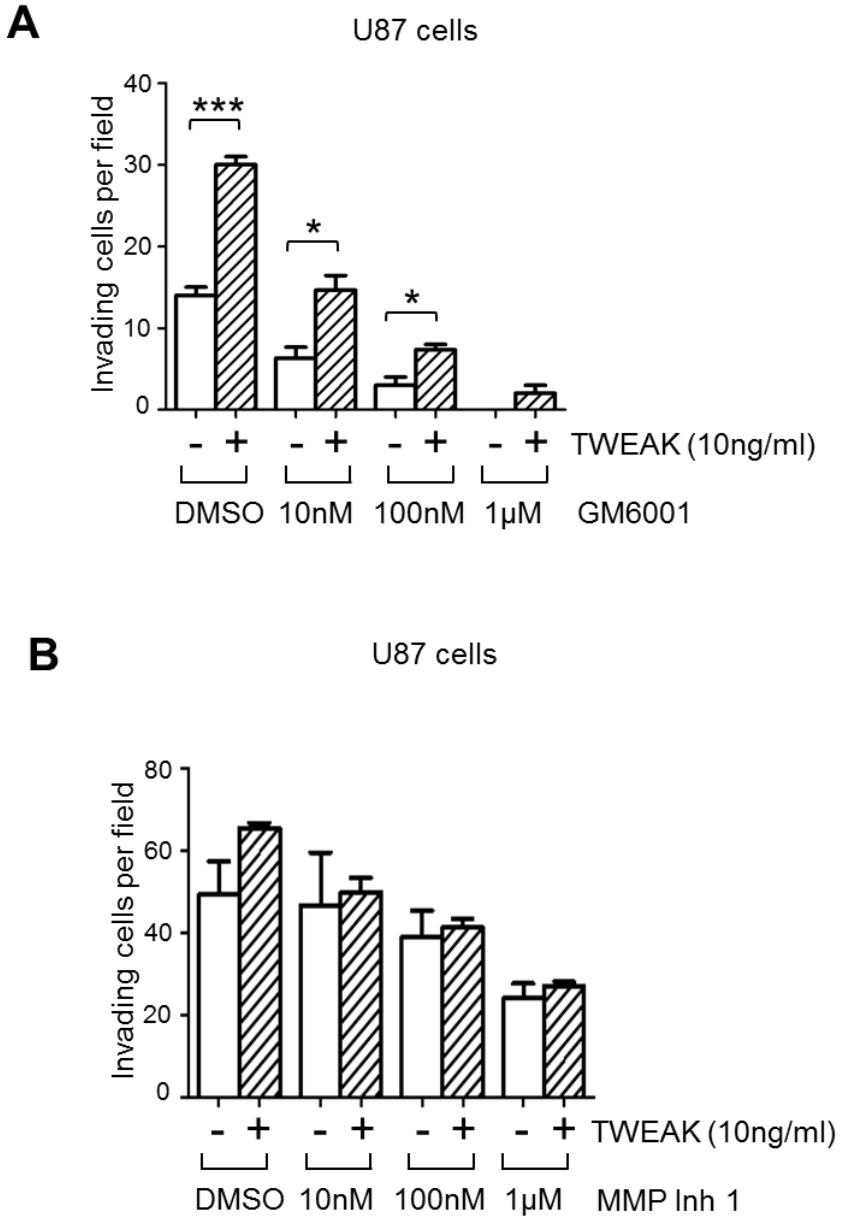

Figure A3 TWEAK-enhanced invasion is attenuated by broad-spectrum MMP and MMP9-selective inhibition. (A) Quantification of invasion density at 48 h for U87 cells with or without 10 ng/ml TWEAK in the collagen matrix. Cells were treated during the 48 h invasion assay with broad-spectrum MMP inhibitor GM6001 at indicated concentrations. Data represent average numbers of invading cells per 1-mm^2 field (n = 3 wells) ± SEM. *p < 0.05 ***p < 0.001 between indicated groups using unpaired Student's t-test. **(B)** Quantification of invasion density at 48 h for U87 cells with or without 10 ng/ml TWEAK in the collagen matrix. Cells were treated during the 48 h invasion assay with MMP9-specific Inhibitor I at indicated concentrations. Data represent average numbers of invading cells per 1-mm^2 field (n = 3 wells) ± SEM. *p < 0.05 **p < 0.01 ***p < 0.001 between indicated groups using unpaired Student's t-test.

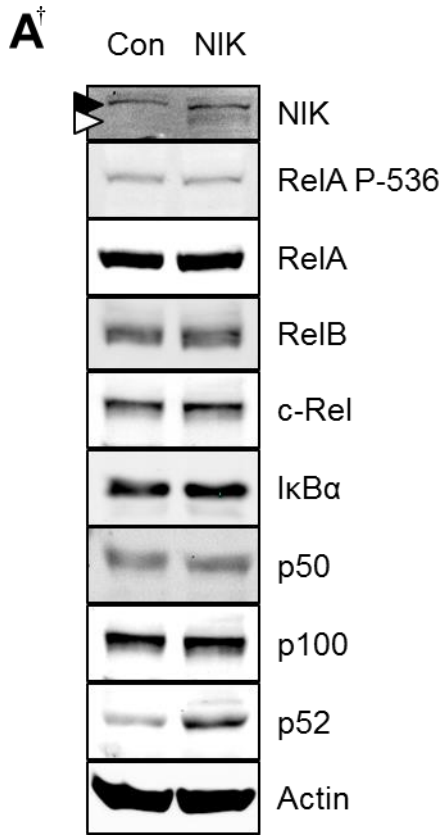

Figure A4 NIK overexpression specifically induces p100 processing in glioma cells. (A) Western blot analysis of BT114 glioma cells transduced with lentivirus containing NIK cDNA or luciferase cDNA (Con) using the indicated antibodies. White arrowhead indicates NIK band. Black arrowhead indicates non-specific band. †Data contributed by DW Lee.

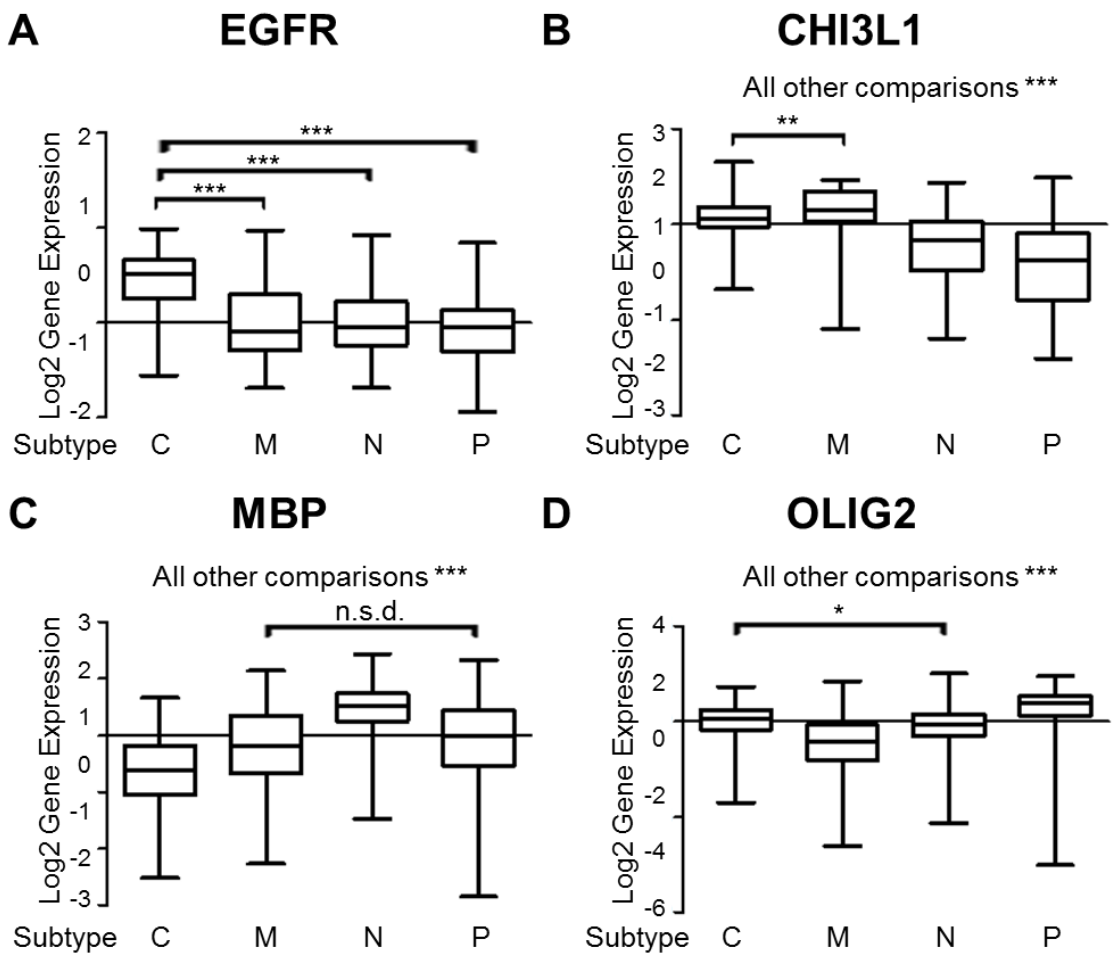

E

Subtype	Samples	EGFR	CHI3L1	MBP	OLIG2
Classical	n=217	2.076 ± 0.114	0.357 ± 0.067	-1.270 ± 0.093	0.050 ± 0.061
Mesenchymal	n=348	-0.110 ± 0.095	0.718 ± 0.062	-0.420 ± 0.081	-1.262 ± 0.076
Neural	n=251	-0.006 ± 0.108	-1.152 ± 0.106	0.910 ± 0.057	-0.262 ± 0.064
Proneural	n=306	-0.426 ± 0.094	-2.113 ± 0.117	-0.225 ± 0.084	0.665 ± 0.069

Figure A5 Expression of subtype marker genes stratified by glioblastoma subtype. (A) *EGFR*, **(B)** *CHI3L1*, **(C)** *MBP*, and **(D)** *OLIG2* expression values from microarray data. Data represent median log2 expression with boxes indicating upper and lower quartile and whiskers indicating range. *$p < 0.05$, **$p < 0.01$, ***$p < 0.001$, n.s.d. no significant difference using Kruskal-Wallis test with Dunn's post-test. **(E)** Summary table of subtype marker gene expression within glioblastoma subtype. Data represent average log2 expression ± SEM.

APPENDIX B

SUPPLEMENTAL TABLES

Table B1 GSEA genes correlated with Verhaak *et al.* subtypes

Classical	Mesenchymal	Neural	Proneural
ABCD2	*ACPP*	*ACSL4*	*ABAT*
ACSBG1	*ACSL1*	*ACYP2*	*ACTR1A*
ACSL3	*ADAM12*	*ADD3*	*ALCAM*
ACSS3	*AIM1*	*AGTPBP1*	*AMOTL2*
ADAM19	*ALDH3B1*	*AGXT2L1*	*ARHGAP33*
AKT2	*ALOX5*	*AKR7A3*	*ARHGEF9*
ANXA5	*AMPD3*	*ANKRD46*	*ASCL1*
APBA3	*ANXA1*	*ANKS1B*	*ATAD5*
ARAP2	*ANXA2*	*ANXA3*	*ATAT1*
ARAP3	*ANXA4*	*ANXA7*	*ATP1A3*
ARNTL	*ARHGAP29*	*ARRB1*	*BAI3*
B3GALT1	*ARPC1B*	*ATP5F1*	*BCAN*
BLM	*ARSJ*	*ATP5L*	*BCL7A*
BTBD2	*ASL*	*ATRNL1*	*BCOR*
C19orf22	*BATF*	*BASP1*	*BEX1*
C19orf66	*BDKRB2*	*BCAS1*	*C1orf106*
CALM1	*BLVRB*	*BEST1*	*C1orf61*
CAMK2B	*BNC2*	*C17orf108*	*C1QL1*
CC2D1A	*C1orf38*	*CA4*	*CA10*
CD151	*C1orf54*	*CALM2*	*CAMSAP2*

Classical	Mesenchymal	Neural	Proneural
CD3EAP	*C5AR1*	*CAMK2G*	*CASK*
CD97	*CASP1*	*CASQ1*	*CBX1*
CDH2	*CASP4*	*CCDC121*	*CDC25A*
CDH4	*CASP5*	*CCK*	*CDC7*
CDH6	*CASP8*	*CDC42*	*CDK5R1*
CDK6	*CAST*	*CDR1*	*CDKN1B*
CLIP2	*CCDC109B*	*CHN1*	*CELF3*
CREB5	*CCR5*	*CLCA4*	*CHD7*
DAG1	*CD14*	*COX5B*	*CKB*
DENND2A	*CD2AP*	*CPNE6*	*CLASP2*
DLC1	*CD4*	*CRBN*	*CLGN*
DMWD	*CDCP1*	*CRYL1*	*CNTN1*
DOCK6	*CEBPB*	*CRYM*	*CRB1*
EGFR	*CHI3L1*	*CRYZL1*	*CRMP1*
ELOVL2	*CLCF1*	*CUTC*	*CSNK1E*
EPHB4	*CLEC2B*	*CYTH1*	*CSPG5*
ERCC2	*CLIC1*	*DHRS9*	*CXXC4*
EXTL3	*CNN2*	*DYNC1I1*	*DBN1*
EYA2	*COL1A1*	*EDIL3*	*DCAF7*
FBXO17	*COL1A2*	*ENPP2*	*DCX*
FGFR3	*COL5A1*	*ENPP4*	*DGKI*
FZD3	*COL8A2*	*EPB41L3*	*DLL3*
FZD7	*COPZ2*	*EVI2A*	*DNM3*
GALNT4	*CSTA*	*FAM49B*	*DPF1*
GAS1	*CTSB*	*FBXO3*	*DPP6*

Classical	Mesenchymal	Neural	Proneural
GJA1	*CTSC*	*FEZF2*	*DPYSL4*
GLG1	*CTSZ*	*FHIT*	*DUSP26*
GLI2	*CYBRD1*	*FUT9*	*E2F3*
GNAS	*CYTH4*	*FXYD1*	*EPB41*
GNG7	*CYTIP*	*GABARAPL2*	*EPHB1*
GPR56	*DAB2*	*GABRB2*	*ERBB3*
GRIK1	*DCBLD2*	*GNAI1*	*FAM110B*
GRIK5	*DOK3*	*GPR22*	*FAM125B*
GSTK1	*DRAM1*	*GRM1*	*FBXO21*
HMG20B	*DSC2*	*GRM3*	*FERMT1*
HS3ST3B1	*DSE*	*GUK1*	*FGF9*
HSPBP1	*EFEMP2*	*HPCA*	*FHOD3*
ILK	*EHD2*	*HPCAL4*	*FLRT1*
IRF3	*ELF4*	*HPRT1*	*FXYD6*
IRS2	*EMP3*	*IMPA1*	*GABRA3*
ITGA7	*ENG*	*KCNJ3*	*GADD45G*
ITGB8	*FCGR2A*	*KCNK1*	*GNG4*
JAG1	*FCGR2B*	*KIAA1598*	*GPM6A*
JUND	*FES*	*LYRM1*	*GPR17*
KCNF1	*FHL2*	*MAGEH1*	*GRIA2*
KEAP1	*FHOD1*	*MAT2B*	*GRID2*
KIAA0355	*FMNL1*	*MBP*	*GSK3B*
KLHDC8A	*FNDC3B*	*MDH1*	*GSTA4*
KLHL25	*FOLR2*	*MGC72080*	*HDAC2*
KLHL4	*FPR3*	*MGST3*	*HMGB3*

Classical	Mesenchymal	Neural	Proneural
LAMB2	*FURIN*	*MMD*	*HN1*
LFNG	*FXYD5*	*MORF4L2*	*HOXD3*
LHFP	*GCNT1*	*MRPL49*	*HRASLS*
LMO2	*GLT25D1*	*MSRB2*	*ICK*
LRFN3	*GNA15*	*MYBPC1*	*IL1RAPL1*
LRP10	*GRN*	*NANOS1*	*KAT7*
LRP5	*HEXA*	*NDRG2*	*KDM1A*
LRRC16A	*HEXB*	*NDUFS3*	*KIF21B*
MAB21L1	*HFE*	*NSL1*	*KLRC3*
MCC	*HK3*	*NTSR2*	*KLRC4*
MEGF8	*ICAM3*	*ORC4*	*KLRK1*
MEIS1	*IFI30*	*PARP8*	*LOC81691*
MEOX2	*IGFBP6*	*PDE6D*	*LPAR4*
MGC2752	*IL15RA*	*PEX11B*	*LPHN3*
MLC1	*IL1R1*	*PEX19*	*LRP6*
MYO5C	*IL4R*	*PGBD5*	*LRRTM4*
NDP	*IQGAP1*	*PLCL1*	*MAP2*
NES	*ITGA4*	*POPDC3*	*MAPT*
NOS2	*ITGA5*	*PPA1*	*MARCKS*
NPAS3	*ITGAM*	*PPFIA2*	*MARCKSL1*
NPEPL1	*ITGB2*	*PPP1R1A*	*MAST1*
NR2E1	*KYNU*	*PPP2R5A*	*MATR3*
NR2F6	*LAIR1*	*PRPSAP2*	*MCM10*
OSBPL3	*LAMB1*	*REPS2*	*MLLT11*
PCSK5	*LAPTM5*	*RERGL*	*MMP15*

Classical	Mesenchymal	Neural	Proneural
PDGFA	*LCP1*	*RND1*	*MMP16*
PEPD	*LCP2*	*ROGDI*	*MPPED2*
PIPOX	*LGALS1*	*S1PR1*	*MTSS1*
PLA2G5	*LGALS3*	*SAR1A*	*MYB*
PLIN3	*LHFPL2*	*SCHIP1*	*MYO10*
PMP22	*LILRB2*	*SEPP1*	*MYT1*
POFUT1	*LILRB3*	*SEPW1*	*NCALD*
POMT2	*LOX*	*SERPINI1*	*NCAM1*
PRKD2	*LRRFIP1*	*SGK3*	*NKAIN1*
PRPF31	*LTBP1*	*SH3GL2*	*NKX2-2*
PTPN14	*LTBP2*	*SH3GL3*	*NLGN3*
PTPRA	*LY75*	*SIRT5*	*NOL4*
QTRT1	*LY96*	*SLC16A7*	*NR0B1*
RASGRP1	*MAFB*	*SLC30A10*	*NRXN1*
RBCK1	*MAN1A1*	*SLC31A2*	*NRXN2*
RBM42	*MAN2A1*	*SLCO1A2*	*OLIG2*
RFX2	*MAN2B1*	*SNCG*	*P2RX7*
RFXANK	*MAPK13*	*SNX11*	*PAFAH1B3*
RGS12	*MFSD1*	*SPAST*	*PAK3*
RGS6	*MGAT1*	*TCEAL1*	*PAK7*
RIN1	*MGST2*	*TCEAL2*	*PCDH11X*
SARS2	*MRC2*	*THTPA*	*PCDH11Y*
SCAMP4	*MS4A4A*	*TMEM144*	*PDE10A*
SEMA6A	*MSR1*	*TPM3*	*PELI1*
SEMA6D	*MVP*	*TSNAX*	*PFN2*

Classical	Mesenchymal	Neural	Proneural
SEPT11	*MYH9*	*TTC1*	*PHF16*
SHOX2	*MYO1F*	*TTPA*	*PHLPP1*
SIPA1L1	*MYOF*	*UGT8*	*PLCB4*
SLC12A4	*NCF2*	*UROS*	*PODXL2*
SLC2A10	*NCF4*	*USP33*	*PPM1D*
SLC4A4	*NOD2*	*VIP*	*PPM1E*
SLC6A11	*NPC2*	*VSX1*	*PURG*
SLC6A9	*NR4A3*	*YPEL5*	*RAB33A*
SMO	*NRP1*	*ZNF323*	*RAD21*
SNTA1	*P4HA2*		*RALGPS1*
SOCS2	*PDPN*		*RALGPS2*
SOX9	*PGCP*		*RAP2A*
SPRY2	*PHF11*		*RBPJ*
SSH3	*PIGP*		*REEP1*
TBX2	*PLA2G15*		*RNFT2*
TEAD3	*PLAU*		*RUFY3*
TGFB3	*PLAUR*		*SATB1*
TGIF2	*PLBD1*		*SCG3*
TLE2	*PLK3*		*SCN3A*
TMED1	*PLS3*		*SEC61A2*
TMEM147	*POLD4*		*SEZ6L*
TMEM161A	*PROCR*		*SLC1A1*
TRIB2	*PTGER4*		*SLCO5A1*
TRIP6	*PTPN22*		*SORCS3*
VAV3	*PTPN6*		*SOX10*

Classical	Mesenchymal	Neural	Proneural
VPS16	*PTPRC*		*SOX11*
WSCD1	*PTRF*		*SOX2*
ZFHX4	*PYGL*		*SOX4*
ZFP112	*RAB11FIP1*		*SPTBN2*
ZNF134	*RAB27A*		*SRGAP3*
ZNF20	*RAB32*		*STMN1*
ZNF211	*RABGAP1L*		*STMN4*
ZNF227	*RAC2*		*TAF5*
ZNF235	*RBKS*		*TMCC1*
ZNF264	*RBM47*		*TMEFF1*
ZNF304	*RBMS1*		*TMEM35*
ZNF419	*RELB*		*TMSB15A*
ZNF446	*RHOG*		*TOP2B*
ZNF45	*RRAS*		*TOPBP1*
ZNF606	*RUNX2*		*TOX3*
ZNF671	*S100A11*		*TSPAN3*
ZNF8	*S100A13*		*TTC3*
	S100A4		*TTYH1*
	SAT1		*VAX2*
	SCPEP1		*VEZF1*
	SEC24D		*WASF1*
	SERPINA1		*YPEL1*
	SERPINE1		*ZC4H2*
	SFT2D2		*ZEB2*
	SH2B3		*ZNF184*

Classical	Mesenchymal	Neural	Proneural
	SHC1		*ZNF248*
	SIGLEC7		*ZNF286A*
	SIGLEC9		*ZNF510*
	SLAMF8		*ZNF643*
	SLC10A3		*ZNF711*
	SLC11A1		*ZNF804A*
	SLC16A3		*ZNF821*
	SP100		
	SQRDL		
	SRPX2		
	ST14		
	STAB1		
	STAT6		
	STXBP2		
	SWAP70		
	SYNGR2		
	SYPL1		
	TCIRG1		
	TES		
	TGFBI		
	TGFBR2		
	TGOLN2		
	THBD		
	THBS1		
	TIMP1		

Classical	Mesenchymal	Neural	Proneural
	TLR2		
	TLR4		
	TMBIM1		
	TNFAIP3		
	TNFAIP8		
	TNFRSF11A		
	TNFRSF1A		
	TNFRSF1B		
	TRADD		
	TRIM22		
	TRIM38		
	TRPM2		
	TYMP		
	UAP1		
	UCP2		
	VAMP5		
	VDR		
	WIPF1		
	WWTR1		
	YAP1		
	ZNF217		

Table B2 NCI Dataset Summaries

Source	Sample Types	Dataset	Clinical Data/ Total Samples	Platform
REMBRANDT (ArrayExpress)	LGG GBM	E-MTAB-3073^	287/522	Affymetrix HG_U133_Plus_2
TCGA	GBM	UNC__AgilentGF4502A_07_1#	102/122	Agilent GF4502A_07
TCGA	GBM	UNC__AgilentGF4502A_07_2#	467/483	Agilent GF4502A_07
TCGA	LGG	UNC__AgilentGF4502A_07_3#	27/27	Agilent GF4502A_07
Total	LGG GBM		883/1153	

GBM Glioblastoma, LGG Lower Grade Glioma; ^RMA/Quantile-normalized, #LOWESS-normalized

Table B3 Entrez Gene IDs for probesets

Gene Name	Entrez Gene ID	Protein	Category
MAP3K14	9020	NIK	TWEAK Axis, NF-κB (Noncanonical)
TRAF3	7187	TRAF3	TWEAK Axis, NF-κB
TNFSF12	8742	TWEAK	TWEAK Axis, NF-κB
TNFRSF12A	51330	FN14 (TWEAKR)	TWEAK Axis, NF-κB
EGFR	1956	EGFR	Classical
MBP	4155	MBP	Neural
COL1A1	1277	Collagen Type 1 α1	Invasion, Mesenchymal
MMP9	4318	MMP9	Invasion
MET	4233	c-MET (HGFR)	Mesenchymal
CHI3L1	1116	CHI3L1	Mesenchymal
SOX2	6657	SOX2	Proneural
OLIG2	10215	OLIG2	Proneural
REL	5966	c-Rel	NF-κB
RELA	5970	RelA	NF-κB (Canonical)
RELB	5971	RelB	NF-κB (Noncanonical)
CHUK	1147	IKKα	NF-κB (Canonical & Noncanonical)
IKBKB	3551	IKKβ	NF-κB (Canonical)
IKBKG	8517	IKKγ (NEMO)	NF-κB (Canonical)
NFKB1	4790	p105/p50	NF-κB (Canonical)
NFKB2	4791	p100/p52	NF-κB (Noncanonical)
NFKBIA	4792	IκBα	NF-κB (Canonical)
TNF	7124	TNFα	NF-κB (Canonical & Noncanonical)
TNFRSF1A	7132	TNFR1	NF-κB (Canonical & Noncanonical)